CRANFIELD UNIVERSITY

SCHOOL OF MECHANICAL ENGINEERING

MPhil THESIS

Academic years 1994 - 6

CHRISTOS E. PAPADOPOULOS

Flow measurement and monitoring using orifice plates

Supervisor: Dr Hoi Yeung

March 1996

This thesis is submitted in partial fulfilment for the degree of
Master of Philosophy

ABSTRACT

The orifice meter is still commonly used for natural gas measurement despite its many limitations. Considerable efforts in recent years have resulted in improved knowledge of factors such as installation effects and the value of discharge coefficient but a serious problem still remains with the measurement of differential pressure since, when line static pressures are as high as 200 bar, differential pressures of 500mbar have to be measured. Furthermore, the flow is never absolutely steady and the performance of the pressure transducers under such conditions is not yet fully understood. This thesis demonstrates the need to apply modern signal processing and analysis techniques to enhance the performance of process instrumentation systems. The use of two static pressure transducers of resonance type upstream and downstream the orifice meter, with a high frequency response, can offer the ability, by using spectral analysis and spectrum estimation methods, to extract additional information regarding the meter's performance as well as diagnostic information about the whole process plant. It also demonstrates a method to check and, at the same time, to safeguard the flow information obtained from an orifice meter with the use of a third pressure transducer upstream of a Mitsubishi flow conditioner. Furthemore, information about the performance of the package orifice - conditioner using the discharge coefficient (Cd) and the amplitude spectrum from the three pressure transducers can be obtained.

ACNOWLEDGEMENTS

I would like first of all to give my warmest thanks to Dr Hoi Yeung whose scientific guidance and his excellent spirit of cooperation were invaluable for the duration of this project. Special thanks to Mr Chris Evans whose tireless willingness to help during all the stages of this project could not be described by common words. Many thanks as well to Mrs Janet Dare for her boundless kindness as well as to Dr Vivien Morris, Dr Gary Oddie, Mr Will Rawes, Mr David Crow and to Mr Duncan MacLeod for their valuable recommendations during this project.

I would like as well to express many thanks to the State Scholarships Foundation in Greece for its financial support since without their help the fulfilment of this project would not have been possible.

Lastly, I would like to send my greatest thanks to my parents for their understanding and support and especially to my fiancee, Miss Vasso Panou, whose moral support and patience were inexhaustible, so unavoidably this thesis is devoted to her.

"Εν οἶδα ὅτ,ι οὐδὲν οἶδα

(Σωκράτης)

" Only of one thing I am fully aware,
that I know nothing."

(Sokrates)

LIST OF CONTENTS

LIST OF FIGURES

LIST OF TABLES

NOTATION

Cd	Orifice discharge Coefficient
Cc	Contraction coefficient
f	Friction factor
D	Pipe diameter
d	Orifice diameter
b, β	Beta ratio
P	Wall static pressure
$\mathbf{V_1}$	Mean velocity upstream of the orifice
$\mathbf{V_2}$	Mean velocity downstream of the orifice
dP, ΔP	Differential pressure across the orifice
ρ	Density
$\mathbf{A_2}$	Pipe area
$\mathbf{A_1}$	Orifice area
m	Area ratio
Q	Volumetric flow rate
E	Velocity of approach factor
Ex	Expansibility factor
k	Ratio of specific heats
$\mathbf{P_r}$	Ratio of static pressure downstream to that upstream the orifice plate.
K	Flow coefficient
C_∞	Discharge coefficient at infinite Reynolds number
Re	Reynolds number
$\mathbf{K_o}$	Loss coefficient of the orifice plate
$\mathbf{K_{co}}$	Loss coefficient of Mitsubishi conditioner

$\mathbf{K_R}$	Resistance coefficient
$\mathbf{K_m}$	Turbine meter factor
L	Pipe length
U	Mean pipe velocity
u	Local axial velocity at radius r
w	Tangential velocity
κ	Pipe roughness
$\Delta P(\mathbf{2,1})$	Differential pressure across the Mitsubishi conditioner and the upstream tapping of the orifice
$\Delta P(\mathbf{2,0})$	Differential pressure across the Mitsubishi conditioner and the downstream tapping of the orifice
$\Delta P(\mathbf{1,0})$	Differential pressure across the orifice
K(2,1)	K proportionality factor between point 2 and 1
K(2,0)	K proportionality factor between point 2 and 0
K(1,0)	K proportionality factor between point 1 and 0
$\mathbf{C_{dk}}$	Correction factor of K proportionality factor
$\mathbf{a_1,a_2}$	Kinetic energy coefficients upstream the orifice and to the throat respectively.
R	Pipe radius
r	Radial distance measured from the center of the pipe
S	Swirl number
$\mathbf{f_t(i)}$	Output frequencies of the turbine meter
$F(j\omega)$	Fourier integral or Fourier Transform
$\lvert F(j\omega)\rvert$	Amplitude spectral density
$\varphi(\omega)$	Phase angle
N	Number of samples
Ω	First harmonic frequency

X(k)	Fast Fourier transform components
T	Sampling interval

ABBREVIATION

ADC	Analogue - digital converter
DMA	Direct memory access
ESD	Electronic system design
DFT	Discrete Fourier transform
FFT	Fast Fourier transform
cdf	Cumulative distribution function
pdf	Probability distribution function

1. INTRODUCTION

The recent advances in flow metrology and especially the great power of the new electronic and computational techniques require an improved approach to what we generally call flow measurement and particularly flow metering.

In order to give an enhanced definition in flow meter it is necessary to reassess some basic definitions in flow metrology. Thus, we should define that:

A ***Flowmeter*** is a device that measures the rate of flow or quantity of a moving fluid in an open or closed conduit. It usually consists of both a primary and secondary device. **(Miller, 1983).**

Subsequently, the flowmeter ***primary device*** is the device mounted internally or externally to the fluid conduit that produces a signal with a defined relationship to the fluid flow in accordance with known physical laws relating the interaction of the fluid to the presence of the primary device. The primary device may consist of one or more elements necessary to produce the primary device signal.

The flowmeter ***secondary device*** is a device that responds to a signal from the primary device and converts it to a display or to an output signal that can be translated relative to flow rate or quantity. The secondary device may consist of one or more elements as needed to translate the primary device signal into standardised or nonstandarised display or transmitted units (recorder, indicator, totalizer, etc.).

From the above definitions it can be easily understood that a flow meter cannot be considered as an isolated device, since the modern view examines it as a whole system. Exactly in the same way we have to consider the orifice meter also, despite its

simplicity of construction and the great volume of research data available for predicting its behaviour. This system sometimes includes some other devices (such as flow conditioners, control valves etc.) that should be considered as parts of the system.

In terms of the principal objective of a flow meter system, a good definition is given by **Baker (1989),** that is to deliver a signal uniquely related to the flow rate despite the influences of installation and operating environment. However, with increasing computing power, analysis of signals and especially of the frequency spectrum of the output from the improved forms of traditional flow meters, such as the orifice plate, may offer now important information regarding the instrument itself and the process operation too. Particularly, if the signal for process control purposes is separated from the ***noise*** components and the spectrum of the latter is analysed, then additional information regarding the status of the flow measurement system and the associated process plant equipment can be recovered.

Thus, the main objective of the work carried out in this project was to examine the possibility of deriving some useful information regarding the performance of the orifice meter and that of a Mitsubishi flow conditioner from the unconditioned signal of three strain gauge pressure transducers installed at D and D/2 tappings of the orifice plate and 1D upstream the Mitsubishi flow conditioner. In addition, the use of the pressure difference across the Mitsubishi conditioner - orifice package, that under normal conditions would be proportional to velocity squared, as a check of the performance of the orifice meter itself, was examined. Also, a simple pipe configuration that could be characterised as a "damper", was used to replace the Mitsubishi conditioner and was tested under similar conditions. In order to meet the above objectives, an extensive literature survey was carried out regarding the monitoring capabilities of unconditioned static pressure signals across an orifice plate as well as to the flow conditioning aspects upstream an orifice plate and is presented in Chapter 2.

Chapter 3 deals with the theoretical estimations of the factors that could affect the performance of the orifice meter as well as some equations that could describe the pressure differences across the Mitsubishi conditioner and the orifice plate. At the end of this chapter, there are some useful theoretical considerations in terms of pulsation effects on the performance of the orifice meter and a new approach regarding the role of wall static pressures.

In Chapter 4 the whole nature of the experiments is described and how they were carried out and in Chapter 5 the results of the relative measurements are presented. Chapter 6 is devoted to a general discussion of the results and in Chapter 7 are presented the subsequent conclusions that were drawn by the completion of this project as well as some useful recommendations for further work.

In summary, modern applications of the flow meters could be classified according to the following scheme:

1. Monitoring of processes and operations,
2. Control of processes and operations,
3. Experimental engineering analysis.

2. LITERATURE SURVEY

2.1 MONITORING USING ORIFICE PLATES.

An extensive literature survey has been undertaken in terms of monitoring using orifice plates. **Zhu, Higham and Amadi-Echendu (1992),** described how the "*noise*" components of differential pressure signals from an orifice plate measurement system can be analysed in many applications, detecting possible changes not only in the flow regime and the associated process plant, but also in the measurement system itself.

Making their studies in a flow rig that was based on 1.5 inch pvc, they used silicon strain gauge differential pressure transducers in order to have much greater detail of the flow regime and especially of the noise components. The orifice plate diameter was 0.67 and 40D, 10D lengths of straight pipe existed upstream and downstream of it respectively. All the measurements were made by D and D/2 tapping points. The main pump was a centrifugal type rated at 2,800rpm, 1.1KW. Also, a pulsator was used as a source of disturbances, perturbated sinusoidally at frequencies up to 5kHz. The low pass filter had been removed from the signal conditioning circuit in order to obtain the widest possible frequency response from the system and the analysis was adjusted to the "*noise*" components of the signal by removing its mean value using a single stage high-pass CR filter. The data acquisition system had a 12-bit A/D converter and a 2,048Hz sample rate. The spectral analysis applied in 4,096 data points of the sampled record giving a resolution of 0.5Hz.

They made measurements to monitor changes:

1. *In the status of a centrifugal pump.* As the pump was rated at approximately 2,400 rpm (40Hz) with the normal impeller they obtained the waveform and frequency spectrum of the differential pressure signal under normal conditions with a dominant peak at 40Hz. Removing the normal impeller and fitting an "L" shape bracket close to

the perimeter of one of the impeller vanes and obtaining their results they observed that the normal peak at 40Hz was just distinct but with a clear increase in its magnitude that was also obvious in the third harmonic at 120Hz. In addition the level of the "*noise*" components between 20Hz and 40Hz appeared increased.

2. *In the status of the associated plant.* Similarly by establishing the reference conditions driving the pump again at 40Hz they introduced perturbations 30 and 70 Hz and they received clear evidence of their effects from the changes in the waveform and spectra.

3. *On the signal from the effect of valve noise.* Closing the valve by rotating its shaft through 45^0 firstly and then 60^0, they observed a 9% and 66% respectively reduction in the flow rate and a distinct increase in the flow noise in the waveform and frequency spectrum.

4. *On the signal of partial blockage of the process connections.* They noticed that initial blockage of the process connections can be detected from changes in the frequency spectrum of the measurement signal.

Moreover, they made some measurements to identify the status of a bi-wing and a tri-lobe pump driven at 300 and 440 rpm respectively. They noticed that the relative magnitude of the harmonics was varying due not only to the arrangement of the drive shafts but also to the dimensional tolerances of the pump body.

In an earlier research, **Amadi-Echendu and Hurren (1990),** presented some analysis methods being used to obtain additional information from the output signals of orifice plate and turbine flowmeter. The experimental rig that they used in this study was constructed of plastic pipes and the process fluid was water. Each flowmeter was

installed so that the upstream and downstream lengths of straight pipe were at least 30 and 15 diameters, respectively.

Knowing that positive displacement equipment in a process plant induces pulsatile flow, they analysed the frequency content of the signal period data using the Fast Fourier Transform and they revealed the periodicities that were associated with the pulsatile flow. Furthermore, by examination of the resulting spectrum of the flow "*noise*" signature obtained by the orifice plate flowmeter they revealed the modulations of the flow that had been caused by the water and the turbine meter respectively.

Finally, examining the time domain signatures of the turbine flowmeter within the process plant, they proposed a way for the identification of defective blades. They introduced a special coefficient, B*i*, that describes the contribution of the *i*th blade to the expected pulse period and they maintained that if a blade had been damaged, at least two of these coefficients would have been changed significantly even at a constant flow rate. Particularly, they asserted that possibly this behaviour should be a picture of the significant change of the flow regime within the turbine rotor structure.

Fell, Ajaya and Tsiknakis (1987), using signal analysis techniques (*Sparse Fourier Transforms*) obtained the frequency spectrum of a liquid and a gas turbine flowmeter. So, they examined the effects on the turbine "*signature*" when the gas flowmeter is operated with an asymmetric flow profile. They asserted that those effects of the asymmetric velocity profile arose because each blade had a different lift characteristic, owing to the torque applying to the rotor, that was no longer constant but varied cyclically in synchronism with the rotor rotation.

They also detected a noisy flow, caused by a faulty control valve and a pulsating flow caused by a positive displacement meter connected in series with the turbine. They maintained that these kinds of flows cause variations in the rotor angular velocity that, since they were not generally synchronous with the rotor rotation, appeared as new

features in the pulse spectrum. Particularly, the signature peaks were still present, but changed in magnitude, since some of the energy formerly shared between them was, at that moment, at the flow fluctuation frequency.

Amadi-Echendu (1988), analysed the instantaneous flow signal obtained from an orifice plate/differential pressure flowmeter employed to measure the flow of water in a one-inch plastic pipe flow rig. In his experiments he obtained sample records of the flow signal and by computing the frequency response function $H(\omega) = H(z = e^{j.\omega})$ for different installation conditions and flowrates he examined how the function was changing. Particularly, he observed that as the flowrate was increased or additional pulsations were introduced in the flow via a pulsator, the bandwidth of the frequency response function was increased slightly and the slope of the response function was decreased especially at lower magnitudes.

An investigation has been carried out by **Turner, Wynne, and Tong (1993)**, who applied signal processing techniques to the time series data collected from a vortex shedding flow meter. Their objective was to examine the influence of low frequency flow pulsations and obstructions in the upstream pipework in the performance of this specific flow meter. Specifically, they applied *spectral analysis* methods, *Zero Crossing analysis* and *parametric* methods. In terms of spectral analysis they observed that low frequency flow pulsations introduced at the left and right of the single dominant peak of normal conditions, frequency components at the sum and difference of the shedding and the pulsating frequency respectively. Furthermore, examining the sideband frequencies obtained from each spectrum of a set of spectra of three volumetric flow rates with eight different pulsating frequencies at each flow rate, they observed an excellent correlation between those frequencies and the low frequency pulsations. It is important to mention that the above researchers had made no attempt to generate flow pulsations with a frequency comparable to the frequency of vortex shedding where 'lock-in' may occur.

In addition using narrow and wide obstructions in the flow upstream of the meter they observed in the frequency spectrum how the "*noise*" level increased in both cases whereas, the main component was significantly affected only by the wide obstruction.

Also some previous studies by **Hurren et al (1988),** and **Higham et al (1986),** revealed the usefulness of the analysis of flow meter signals to the time and frequency domain, in order to collect as much information as possible either for the flowmeter itself or for the associated process plant. Particularly, **Hurren et al**, applied the *Fast Fourier Transform (FFT)* method to a series of period data which were equal to the variations in flow rate about the mean flow rate having as a result a spectrum which revealed the frequency components of the flow "*noise*".

2.2 FLOW CONDITIONERS.

A literature survey has been also carried out on the *flow conditioners* and especially on the *perforated plates*, in terms of their design and their performance under different flow layouts and different flow profiles. In **B.S. 1042** there are tables and suggestions for the required lengths between primary device and different pipe fittings including flow conditioners in order to have the greatest accuracy in flow measurement. As an example consider a 28D straight length of pipe upstream an orifice plate with d=0.70D that is fitted after a single 90^0 bend and 7D of straight pipe downstream the orifice plate in order not to have additional uncertainty. The stated uncertainty for BS 1042 in this case is b%=0.7%. Using a flow conditioner half of both the above lengths are required for no additional uncertainty. In **ASME** the proposed lengths for the above example are 12D upstream and 4D downstream the orifice plate with no conditioner for a stated uncertainty 0.5% and half of them with conditioner for zero additional uncertainty respectively.

In a quite recent study **Stokes et al (1993),** investigated the porosity characteristics of perforated materials in normal flow. Presented in a logarithmic scale they revealed the manner in which the ratio of pressure drop through the perforated material to the density of fluid was varying with the velocity for two different values of the density. They observed that for high pipe Reynolds numbers, the pressure drop was varying approximately with the velocity squared and also they indicated that the most significant factor in determining the porosity characteristic of the perforated materials was the open ratio and not the hole diameter.

De Bray (1992), carried out a study into the effect of perforations upon the velocity fluctuations downstream of square plates normal to airstream with reference to their use as air brakes. His important conclusion, which particularly interested the author, was that the plates that had *uniform* perforations with holes of the same diameter had given substantial reduction in the level of velocity fluctuations.

Reader-Harris, Hutton and **Laws (1989)**, presented an extensive work on the performance of flow straighteners and flow conditioners under different flow conditions. They said that the objective of an effective flow (ideal flow) conditioner
is to produce the best approximation to the fully developed velocity and turbulent profile (appropriate to the pipe Reynolds number) regardless of upstream flow conditions. They also pointed out that the demands in terms of flow through different layouts are different too and so the selection of the proper flow conditioner is dependent on those demands. Particularly some times it may only be necessary to remove swirl for a flowmeter to achieve the best performance with the least pressure drop. On the contrary, some other times it may only be necessary to remove asymmetry in flow.

They also recommended that tests on the performance of flow conditioners to measure the changes in the discharge coefficient sometimes are necessary not only in disturbed flow conditions but also in fully developed upstream flow. It is important for

the conditioner not to disturb good flow conditions. Describing the design of the *Mitsubishi* flow conditioner and experiments of some other researchers they concluded that it is a very effective conditioner in severe asymmetry with or without swirl, simple in construction and with a low pressure loss. They primarily summarised in tables the percentage changes in the calibration of the orifice plate. Concerning the *Mitsubishi* plate their results are presented in **Table 11.** The Mitsubishi conditioner was installed 2D downstream of a single 90^0 bend and 6D upstream of an orifice plate with d=0.8D and with flange taps introduced a 2% installation error. Moreover, they noticed that the distance between the conditioner and the meter was more important than that between the disturbance and the conditioner.

In a later research, **Laws (1990),** presented some experiments concerned with the comparative performance of some tube bundles flow conditioners and perforated plates being installed downstream of double bends or partially open ball valves. She concluded that a variable resistance perforated plate device was better as a flow conditioner than the tube bundle. Particularly, for her perforated plate (Law's plate), she observed that its capability of achieving downstream flow conditions, close to fully developed within a relatively short downstream length, was due to its grading of resistance to the flow that allows more flow to pass through the central section than near the walls.

Sanderson and **Sweetland (1991)** investigated the effect of the *Mitsubishi* and Law's *perforated plates* and of two designs of tube bundle on the performance of a turbine and a vortex liquid flow meter when they are installed downstream of single and double bends. Using the 4" line of the Cranfield water calibration rig they pointed out that the *Laws plate* appeared to give the best overall performance. However, in terms of the installation of the conditioner after a single bend one could observe a slightly better performance of the *Mitsubishi plate* than that of the *Laws plate* (the relative values of the meters factors were closer to the values obtained at datum calibration), which could not be achieved after a double bend arrangment.

The superior performance of the *Laws plate* downstream of a multiple bend combination or a partially open ball valve, has also been pointed out by **Laws (1990),** in a later experimental work. Using analytical formulas of flow through screens, she estimated that for a plane screen with a pressure loss coefficient K=2.7 the downstream flow would be uniform regardless of the nature of the upstream flow. So testing her perforating plate with the above loss coefficient that is higher than that of the *Mitsubishi* (K=1.7 at $Re=10^6$ decreasing to 1.5 at $Re=2x10^5$ and to 1.35 if its holes are sharp edged at their downstream face), she obtained better comparative results saying that probably this increased loss coefficient accounts for the improved performance of "*Laws*" unit. Improved results revealed as well in already developed flows where the *Laws' plate* quickly restored the flow to very close to its upstream condition. No results were concluded in terms of a single bend.

Another significant area of flow conditioning has to do with the elimination of pulsation effects in the performance of the flow meters. A very interesting recommendation in terms of flow conditioning under pulsation is coming from a manufacturer of flow meters (Foxboro) where an addition of system capacitance usually as 'blader-type' units has been recommended if the pulsation source can not be eliminated (**Mottram and Sproston, 1989**).

So, based obviously on the above idea two companies acting as partners (Fluid Components, Inc. and Vortab Co.) have recently developed a new flow conditioner that seemed very promising under pulsating conditions. Their objective in designing this flow conditioner consisting in a number of arrays of trapezoidal shaped elements positioned around the pipe, was to combine mixing techniques by producing rapid-cross stream mixing, due to the inserted sleeves, eliminating at the same time swirl and velocity profile distortions (including pulsations). In addition, all these improvements could be achieved with a low pressure drop.

Lastly, a reference ought be made to the experiments of **Gebhart** and **Munukutla, (1992),** where they investigated the turbulence behind screens and perforated plates. They found that the turbulence values downstream the screens were fairly independent of the Reynolds number beyond a velocity of 9.1 m/sec and the reduction on the power of turbulence was independent of the screen thickness.

3. THEORETICAL APPROACH.

3.1. INTRODUCTION

The *sharp-edge orifice* is undoubtedly the most widely employed flowmetering device. Its operational principle is based on the fact that by placing a flow restriction of some type in a pipe or duct, a pressure decrease that varies with the flow rate due to velocity increase as it goes through the restriction, is caused by this restriction. Thus measurement of the pressure difference by means of a suitable differential pressure pickup allows flow-rate to be determined.

3.1.1. Applications (Advantages - Disadvantages)

We can use the orifice meter with almost any single phase Newtonian flow. Nevertheless, it is unsuitable for fluids that contain suspended solids which tend to collect behind the plate and cause irregular flow. This problem can be solved by using an "eccentric" orifice. It's also unsuitable for abrasive fluids and requires additional care when it is used in two-phase fluids.

We could say that the orifice meter's major advantages are its simplicity, its low cost, the great volume of research data available for predicting its behaviour and its calculable uncertainty. Its major disadvantage is that it is a non-linear device since flow

rate is proportional to $\sqrt{\Delta p}$. This non-linearity restricts the accurate range of flow measurement since a 10:1 change in Δp corresponds to only about a 3:1 change in flow rate (approximately). Since a differential pressure device becomes quite inaccurate below about 10% of its full scale reading, orifice meter cannot be used accurately below 30% of its maximum flow rating. However, the use of intelligent differential pressure transmitters that rely heavily on microprocessor technology can improve the low - range accuracy and increase the range to about 20:1.

3.1.2. Orifice as a billing meter in natural gas industry.

The massive amount of experience in terms of the performance of the orifice meter is the main reason of its wide use in applications where the best accuracy becomes the most important factor. Naturally it is not the most accurate device; however, it supports a confidence in occasions where much money has to change hands such as in large hydrocarbon measuring facilities. Moreover, in such applications as in large natural gas transmission ducts, where usually high pressures exist, orifice meters are almost the only applicable solution. Turbine meter should be an alternative solution. It has the advantage of linearity but unfortunately has the inclination to overestimate the total flow in fluctuated conditions. Morever, its demand for frequent maintainance because of contaminated or worn out bearings, sometimes restricts its use.

It must be pointed out here that in such large scale measurements knowing *all* the possible errors in flow measurement introduced by any factor (installation errors, recorder or computer errors, human errors etc.) is of major importance. In analysing the above concept, it should be mentioned that sometimes the minutest error could correspond to a large amount of money loss that could reach thousands of dollars. **Spitzer (1991)** presents a good example. He made his calculations for an eight inch meter tube using a 4in orifice plate and natural gas, as flowing fluid with a specific

gravity of 0.580 having a zero per cent carbon dioxide and nitrogen. A value of $4.00/Mcf was used to show the daily and yearly loss in revenue. In his calculations about a 0.22% error in differential pressure measurement corresponded to about $40,880 loss on a yearly basis. Similar results could be obtained as well by errors in temperature measurement showing how such a small error could cause a considerable revenue loss over a time period. From the above example one easily realises how important the proper maintenance, calibration and subsequently operation of the meter is in such large scale measurements.

Morever in terms of the maintenance we could say that very often tests of all metering equipment are necessary, starting by a visual inspection for any sign of improper operation and continuing to calibration of every individual element of the station such as the meter itself as well as all the parts of the secondary instrumentation.

Usually in large gas metering stations calibrated master meters are used to measure the flow and to calibrate other meters. The demand to achieve very high performance has led in the development of multiple techniques such as the calibration of the meter with the upstream pipework and a flow straightener permanently in position with two of these packages in series **(Baker, 1989)** So any deviation or malfunction of one meter will appear as a relative shift in calibration between the two meters.

In terms of proper operation the best operating range for metering systems is within the 25% to 90% range of the meter. Subsequently, if flow variations that exceed the range of the meter are impossible to be controlled, then the use of a combination of multiple meters is required, mainly in parallel, to reduce losses in high flow rates and it is followed by some type of flow switching control to put them in and out of service.

3.2 TURBULENT COMPRESSIBLE AND INCOMPRESSIBLE FLOW THROUGH ORIFICE PLATES.

3.2.1. Description.

Figure 3.1 shows the flow through an orifice plate at high Reynolds numbers (above 3.5 x 10E+3). As it can be observed, the fluid contracts to the sharp edged side of the orifice (2) separating away from the surface of the orifice and forms a fluid jet downstream the plate. Since the jet continues past the orifice supported by an annular vortex which is the major contributor to the pressure loss, it continues to contract to a minimum cross sectional area known as the " *Vena Contracta*". Between the jet and the pipe a secondary flow region is formed dominated by a circular motion.

In terms of the pressure distribution shown in **Figure 3.2**, we could claim that the flow accelerates continuously on the axis from a distance upstream the orifice until the *Vena Contracta* point while the pressure decreases. Beyond the Vena Contracta the situation could be described similarly with that of a sudden "expansion" where the velocity on the axis decreases owing to the fact that the fluid starts to fill the available flow area that has increased.

Subsequently, the pressure on the axis increases until it reaches a maximum about at the plane at which reattachment occurs. As we can observe in **Figure 3.2**, there is a nonrecoverable head loss that is proportional to the ratio of the orifice area to the total cross-sectional area and constitutes sometimes a significant factor for the selection of an orifice meter. In addition, we could say that the wall pressure increases as the corner of the upstream face of the plate is approached. Then there is a sharp decrease in pressure

across the orifice, which is used for the flow measurement, continuing to decrease gradually until the *Vena Contracta* after which it starts to increase until the recovery plane.

3.2.2. Flow Equations.

Considering the flow though the orifice plate as shown in **Figure 3.1** then by applying **Bernoulli's** equation to the upstream **(1)** and the throat **(2)** we have:

$$\frac{U_2^2 - U_1^2}{2} = \int_{\rho 2}^{\rho 1} \frac{dP}{\rho} \qquad \textbf{(1)}$$

For fluids we have $\rho_1 = \rho_2$ (incompressible). **(2)**

Defining firstly $\beta = \frac{d}{D}$ (Beta ratio) and $m = \frac{A_2}{A_1} = \beta^2$ (area ratio) we have,

$$E = \frac{1}{\sqrt{1-\beta^4}} = \frac{1}{\sqrt{1-m^2}} \text{ (Velocity of approach factor),}$$

$P_1 - P_2 = \Delta P$ (Differential Pressure)

and knowing that the volume flowrate Q is given by:

$Q = U_1 A_1 = U_2 A_2$ or similarly for the mass flow rate $\rho_1 D^2 U_1 = \rho_2 d^2 U_2 \Rightarrow U_1 = \frac{d^2}{D^2} U_2$ **(3)**

then the volume flowrate for the orifice using **(1)**, **(2)** and **(3)** is given by:

$$Q = \frac{\pi d^2}{4} Em \sqrt{\frac{2\Delta P}{\rho}} \qquad \textbf{(4)}$$

that is an analytical formula applicable to most differential pressure flowmeters.

The previous equation is applied between planes **(1)** and **(2)** in **Figure 3.1**, assuming an ideal contracting flow and it is obvious that the orifice diameter d does not give the correct answer since the more correct diameter is the *Vena Contracta.* However, it is not theoretically possible to determine this diameter, so an empirical factor, the **"Discharge Coefficient (Cd)"** is used for the correction of the diameter or else it is a Coefficient that allows for the very different flow in the orifice plate as compared with an ideal contracting flow.

Thus the true theoretical volume flow rate for the orifice plate is :

$$Q = \frac{\pi d^2}{4} ECd \sqrt{\frac{2\Delta P}{\rho}} \quad (5)$$

Equation **(5)** is applicable only to incompressible fluids since in terms of gases compressibility affects the operation of the orifice plate and particularly affects the discharge coefficient. Thus another factor introduced for compressible fluids, called *expansibility factor (Ex),* given by the following equation:

$$Ex = \frac{\sqrt{\left(\kappa^{\frac{P_r}{\kappa}}\right)\left(1-m^2\right)\left(1-P_r^{\frac{\kappa-1}{\kappa}}\right)}}{\sqrt{(\kappa-1)\left(1-m^2 P_r^{\frac{2}{\kappa}}\right)\left(1-P_r\right)}}$$

where k = ratio of specific heats and P_r is the ratio of absolute pressure at the downstream tapping to that at the upstream tapping. Actually, the expansibility factor is dependent on the isentropic exponent that is the ratio of the relative variation in pressure to the corresponding relative variation in density under elementary reversible adiabatic (isentropic) transformation conditions, **BS. 1042.**

However, the ratio of specific heats can be used in place of the isentropic exponent. Only when Pr>0.75 the simpler formula below can be applied for **Ex**,

$$Ex = 1 - \left(0.41 + 0.35\beta^4\right)\frac{\Delta P}{\kappa P_1}$$

Thus, for compressible fluids the volume flowrate for orifice plate is given by:

$$Q = \frac{\pi d^2}{4} ExCdE\sqrt{\frac{\Delta P}{\rho}} \quad \textbf{(6)}$$

In some equations the discharge coefficient is combined with the velocity of approach, E, and redefined as *flow coefficient* K where K=ECd **(Spitzer, 1991)**..

3.2.3. Discharge Coefficient (Cd).

The discharge coefficient is derived from laboratory test data of the actual flow rates and ideal theoretical flow rate. It is defined as:
Cd = (true flow rate)/(theoretical flow rate).

Thus, based on experimental data for different orifice meter sizes and Reynolds number ranges, a number of empirical equations have been developed for **Cd** that are used to determine the flow rate and most of them are refered to flange or corner tappings. Many of them could be found in **(Spitzer D.W.,1991).** For example;

The ISO - ASME equation that for D, D/2 is as follows:

$$Cd = 0.5959 + 0.0312 * b^{2.1} - 0.1840 * b^8 + 0.0390 * b^4 / (1 - b^4) - 0.01584 * b^3$$
$$+91.71 * b^{2.5} / \mathrm{Re}_D^{0.75}$$

Also, the new AGA/API equation that was just developed in 1989 by Reader-Harris & Gallagher (R-G equation), and the Cd for corner taps and for D>2.8in is given by:

$$Cd = 0.5961 + 0.0291 * b^2 - 0.2290 * b^8 + 0.000511 * (10^6 / \mathrm{Re}_D)^{0.7}$$
$$+[0.0210 + 0.0049 * (19000 * b / \mathrm{Re}_D)^{0.8}] * b^4 * (10^6 / \mathrm{Re}_D)^{0.35}$$

According to **Spitzer** the values of the discharge coefficient, Cd, predicted by each of the above equations for the same orifice meter and same flowing conditions differ, but for the typical applications of the orifice the percentage difference in the discharge coefficient between the two equations is usually less than the measurement uncertainty.

For the test orifice used in this work the discharge coefficient for D and D/2 tappings, d=68mm, D=100mm and $\beta = 0.68$ is given by the next equation:

$$\mathrm{Cd} = 0.606996 + 196.63928\mathrm{Re}^{-0.75} \quad (7)$$

for a Re that is $5.9E+04 \leq \mathrm{Re} \leq 10^8$. The discharge coefficient is around 0.621 with an uncertainty 0.68%.

Equation **(7)** is based on **BS 1042** where there is analytical reference to the discharge coefficient and some of its empirical equations. We can generally conclude that **Cd** for the most of the differential pressure primary elements in turbulent flows (Re>4000) is given as: $Cd = C_\infty + \dfrac{b}{\mathrm{Re}_D^n}$ **(8)**

where C_∞ is the discharge coefficient at infinite Reynolds number, b is a constant and n is the exponent for the pipe Reynolds number (**see 3.2.4**).

3.2.4. Factors affecting the Discharge Coefficient.

The generalised equation **(8)** for the discharge coefficient is valid for most differential pressure flow meters. We could say that the infinite Reynolds number discharge coefficient may be a constant or a function of the dimensions of the primary element or tap location. Concerning the correction of the Reynolds number, b could be a function of the flowmeter dimensions and the exponent n is a constant dependent on the primary element. Thus, we could easily assert that the discharge coefficient is affected by the following factors:

- It varies considerably with the **Reynolds number**. Deviation in linearity increases as the Reynolds number decreases due to change in the flow velocity profile with Reynolds number.

- Furthermore, Cd varies considerably with the **area ratio** since deviation in linearity increases for large area ratios and starts at a higher Reynolds number.

- The upstream **pipe roughness** has an effect on the Cd so the pipe has to be as smooth as possible.

- The upstream **edge** of the orifice has to be as **sharp** as possible because any rounding of the edge results in an increase in the Cd. The standards specify that the edge radius has to be smaller than 0.0004d.

The **position of the tappings** is also an important factor affecting Cd. Particularly, D and D/2 tappings are more close to the theoretical values since the Vena Contracta is positioned approximately half a pipe diameter downstream of the orifice. Thus, the arithmetic values of **Cd** for D and D/2 tappings are larger compared with the

respective values for corner and flange tappings for the same conditions; however, they have more difficulties in design and manufacturing.

- Finally, another factor that has already been described extensively is the **compressibility**.

The above factors could be characterised as "**design factors**" of the orifice meter itself, except for the Reynolds number and the compressibility which are factors of the flow and the fluid respectively. An other significant factor that virtually gives meaning to the above, could be in general terms the "*associated system's layout*". Particularly, the system's layout is the factor that creates the "*velocity profile*", and inevitably combined with the Reynolds number, is a virtual factor affecting the orifice meter's accuracy.

It is well known that the discharge coefficient quoted in the standards applies to normal conditions; that is, steady flow (no pulsations or transients) and fully developed turbulent profile upstream of the flow meter.

However, sometimes it is not possible to have, in actual applications, sufficient straight length of pipe upstream the orifice plate that is free from obstructions and in accordance to the standards. Thus, non ideal velocity profiles approach the meter affecting the **Cd.** In these cases the demand of a flow straightener or a conditioner that should remove all or part of the distortion, including swirl, appears and is another important factor.

There are several other effects that could be quoted and are present in real orifice flows such as the curvature of the flow etc. However they are of less significance.

3.2.5 Differential pressures across the Mitsubishi flow conditioner and the orifice - Theoretical estimations.

It is well known that any component being installed in a pipe flow change the velocity of the flowing fluid either in magnitude (e.g. expansion or contraction) or direction (bends) resulting in loss of energy. These component losses are commonly expressed in terms of velocity heads using the relationship:

$$\Delta p = Kco\frac{1}{2}\rho U^2$$

Here, Kco is the loss coefficient of the Mitsubishi conditioner, ρ is the fluid density and U is the mean velocity upstream or downstream the flow conditioner. In a straight pipe there are losses as well that due to friction and are given by the Darcy-Wiesbach equation:

$$\Delta p = f\frac{L}{D}\frac{\rho U^2}{2}$$

where L is the length of the pipe, D is the diameter, and f is the friction factor which could be taken from the following form of the Colebrook-White equation yielding similar accuracy to the original:

$$f = \frac{0.25}{\left[\log\left(\frac{k}{3.7D} + \frac{5.74}{\mathrm{Re}^4}\right)\right]^2}$$

where k is the pipe roughness. The only reason the above equation was chosen is that it includes all the possible factors that could affect the friction factor although to the author's point of view the second term of the denominator in high Reynolds number is meaningless. Calculating the pressure difference across position 2 (upstream the conditioner) and position 1 (upstream the orifice) and 0 (downstream the orifice) we simply have:

$$\Delta p(2,1) = \left(Kco + f\frac{L}{D}\right)\frac{\rho U^2}{2} \Rightarrow U = \frac{1}{\sqrt{Kco + f\frac{L}{D}}}\sqrt{\frac{2\Delta p(2,1)}{\rho}}$$

However, Q=UA, where A is the pipe area, thus we have:

$$Q = \frac{1}{\sqrt{Kco + f\frac{L}{D}}} \frac{\pi D^2}{4} \sqrt{\frac{2\Delta p(2,1)}{\rho}}$$

Finally, introducing the previous form of the Colebrook-White equation we obtain the following equation:

$$Q = \frac{1}{\sqrt{\frac{0.25L}{\left[\log\left(\frac{k}{3.7D} + \frac{5.74}{\mathrm{Re}^4}\right)\right]^2 D} + Kco}} \frac{\pi D^2}{4} \sqrt{\frac{2\Delta p(2,1)}{\rho}}$$

Similarly for positions 2 and 0 we could obtain the next equation:

$$Q = \frac{1}{\left(\sqrt{\frac{0.25L}{\left[\log\left(\frac{k}{3.7D} + \frac{5.74}{\mathrm{Re}^4}\right)\right]^2 D} + Kco + Ko}\right)} \frac{\pi D^2}{4} \sqrt{\frac{2\Delta p(2,0)}{\rho}}$$

where Ko is the loss coefficient of the orifice plate, d is the diameter of the orifice and m the area ratio of the orifice and the pipe. If in the above equations we preserve only Q and the square root of the differential pressures we simply obtain:

$$Q = K(2,1)\sqrt{\Delta p(2,1)} = K(2,0)\sqrt{\Delta p(2,0)} = K(1,0)\sqrt{\Delta p(1,0)} = \frac{\pi d^2}{4} ECd \sqrt{\frac{2\Delta p(1,0)orif.}{\rho}}$$

In the last equation we have obtained three different functions for the flow rate. Since the flow rate Q is expressed in m^3/hr then the **K factor has to be multiplied by 3.600** since the time (sec) is included in the differential pressure that is expressed in Pa ($N/m^2=kg/(m*sec^2)$). It can be easily seen that the above proportionality factor (K) is dependent on the loss coefficients of the conditioner and the orifice (Kco, Ko), the pipe and orifice diameters (D, d) and consequently the area ratio (m), the length of the pipe (L) and the pipe roughness (k). The K factor is independent on the Reynolds number, although it is included in the function of K and this could be an interesting point. It can

be easily understood after a few simple calculations with real data that the Reynolds number term inside the function has no effect on the friction factor and subsequently in the proportionality factor; otherwise, we could not expect a linear relationship between Q and $\sqrt{\Delta p}$.

Finally, the K factor must be dependent on the velocity profile just as the coefficient of discharge in the orifice. Any distorted velocity profile could create an abnormal pressure gradient and subsequently the differential pressures across the conditioner and the orifice would not follow a linear relationship with the square of flow rate. In the previous equations there is no parameter as to the effects of the velocity profile and the position of the "Vena Contracta" for the case of $\Delta p(2,0)$ and this could suggest for a correction factor similar to Cd (Cdk) having therefore the flow rate: $Q = CdkK\sqrt{\Delta p}$. The nature of this correction factor as well as of the K factor itself has to be the same as that of the Cd, affected almost by the same factors as the Cd that has been described extensively in previous sections.

It is also nessecary to mention that virtually this factor (K) indicates the resistance of every section for which it is estimated. It is related to the resistance coefficient K_R through the relation $K = \frac{1}{\sqrt[n]{K_R}}$. It is known that the loss of head between two points in a pipe line is, $H=K_R Q^n$ or the flow rate $Q = \frac{1}{\sqrt[n]{K_R}} \Delta P^{\frac{1}{n}}$ where n is some power that depends on the type of flow. For turbulent flow, n will be equal to 2 if separation losses are neglible. Subsequently, concerning the results that will be presented in Chapter 5 we have to keep in mind that a high estimated value of K factor means a low resistance coefficient and furthermore a value of power n close to 0.5 should indicate negligible separation losses.

3.3. INSTALLATION EFFECTS ON THE PERFORMANCE OF THE ORIFICE METER.

In order to explain the effects of the system's layout on the performance of the orifice meter it is primarily necessary to describe the perturbations or disturbances introduced in pipe flow by common pipe fittings or any other source. Generally, the following categories of disturbances could be quoted:

1. Axisymmetric distortions,
2. Asymmetric distortions,
3. Swirl,
4. Pulsations and transients,
5. Vibrations from external sources.

In terms of *axisymmetric* distortions we can briefly say that they are caused by extensive pipe roughness, by orifice plates in series or generally by any step change in the pipe bore. The way they affect the performance of the orifice is easily understood by looking at the next equation for the discharge coefficient, referred by **Irving (1976).**

$$Cd = Cc\left[\frac{1-m^2}{a_2 + Ko - a_1 Cc^2 m^2}\right]^{\frac{1}{2}}$$

where Cc is the *contraction coefficient*, Ko is the *loss coefficient* of the orifice, m is the area ratio of orifice and a_1, a_2 are the kinetic energy coefficients upstream and in the throat respectively. The Kinetic energy coefficients could be a measure as to the "*peakness*" of the profile since they are given by the next equation:

$$a = \frac{\int_0^R 2\pi r u \frac{u^2}{2g} dr}{\pi R^2 U \frac{U^2}{2g}}$$

where u is the local velocity at radius r and U is the mean velocity.

Considering the extensive work on the subject that has been done by **Ghazi (1962),** it could finally be stated that high core type non-standard flow profiles increase the discharge coefficient, while, on the other hand, flat or blunt shaped flow profiles decrease it. The effects are more significant in orifice meters with large area ratio than in those with small one. Furthermore, **Ghazi** by introducing a "*distortion parameter*", suggested that non-standard upstream flow conditions could be detected only by measurements of wall pressures. The location of the vena contracta seemed to be independent of upstream flow conditions.

3.3.1. Asymmetric velocity profiles and swirl through orifice meter.

All kinds of single bends produce *asymmetric* velocity profiles sometimes accompanied by *swirl.* Interaction between the pressure and centrifugal forces set up in a bend cause adverse pressure gradients to the flow and particularly on the outer wall at the inlet to a bend, and on the inner wall at the outlet from a bend. These pressure gradients result in the creation of a system of secondary flows and for bends with a radius ratio less than 1.5 can cause *flow separation* on the inside of the bend at the exit as shown in **Figure 3.3**.

Moreover, as the flow expands to refill the pipe 2 to 4 diameters downstream as **Blake (1973)** has shown, the static pressure rises, and so if the orifice is installed near this region of separated flow, the upstream pressure tappings, particularly the D tapping, will record a false low value. Thus, the measured differential pressure across the orifice plate is too low and this inevitably results in an increase in the discharge coefficient.

Blake has shown as well that the gross asymmetry in the velocity profile has disappeared after about 5D downstream of a single bend and the static pressure distribution around the pipe becomes again uniform.

Blake has shown as well that the gross asymmetry in the velocity profile has disappeared after about 5D downstream of a single bend and the static pressure distribution around the pipe becomes again uniform.

Similarly, valves are fittings that produce *asymmetric* velocity profiles. Partial closure of a valve causes the flow to contract and to re-expand downstream of the valve leading to the creation of a turbulent mixing region.

Based on the results of previous experimental work on the subject (for example of **Irving (1977)** and of **Avery & Moore (1983)),** it can be anticipated that for bends and valves the values of the discharge coefficient given in **ISO 5167** *overestimate* the mass flow rate. The only exceptions are a fully open valve as well as an orifice installed very close to a pipe fitting. For 90^0 bends the introduced error in the discharge coefficient is maximum at a radius ratio of about 1.0 and is less for mitred bends. The error is less for the smaller orifice plate area ratio and for D and D/2 tappings than for corner and flange tappings. The only exception, in terms of the position of the tappings, is only in the case where the orifice is installed close to a fitting.

According to **Ghazi,** upstream *asymmetric* flow conditions can be detected by the measurement of wall pressures and the estimation of the distortion parameter**.** The "*distortion parameter*" is a measure of *axisymmetric* conditions. This is the ratio of the wall pressure rise upstream of the orifice to the differential pressure across it and seems to correlate well with the performance of the orifice plate.

Although some axisymetric and asymmetric distorted profiles may be free from swirl, usually when swirl is present the velocity profile is also distorted. There are several fittings that could generate swirl such as inclined radial vanes, rotating impellers etc, but the best known swirl generator that is a very common pipework configuration is the two 90^0 offset bends combination. The flow accelerates on the outer side of the exit of the

first bend and enters the second bend in a different plane resulting in a swirling motion. Bulk swirl produces errors in orifice plate Cd values by two different mechanisms. Each one of these two mechanisms has opposing effects for large and small area ratio orifices respectively. **(Avery and Moore, 1983)**

In terms of the first mechanism, the produced distorted profile with the relatively high near *wall momentum* results in negative Cd errors especially in large area ratio orifice plates. On the contrary, concerning the second mechanism, the angular momentum associated with the swirl is conserved downstream the orifice throat leading to a less contraction of the flow at the vena contracta. The result is a positive Cd error for small area ratio orifice plates. The above opposite effects cancel each other in intermediate area ratio orifice plates resulting in very low Cd errors.

A good measure of swirl in a pipe except for the commonly used swirl angle is the *swirl number, S,* given by the following equation:

$$S = \int_0^{2\pi} \int_0^R \frac{uwr^2 dr d\theta}{2\pi R^3 U^2}$$

where r is the radial distance from the centre of the pipe, R the radius of the bore, u and w the axial and tangential velocities and U the mean axial velocity. A small swirl number ensures good flow conditions. Swirl can be removed at a lower cost in pressure loss than can asymmetry by using flow straighteners. Furthermore, it is quite important to remove swirl since it is extremely persistent and can be present at 100D or further downstream. However, if it is also necessary to remove asymmetry then the use of a perforated plate is required.

In addition to the effects of velocity profile and swirl, the distribution of turbulence across the pipe that varies and possibly affects the performance of the orifice

meter, may be of great importance (**Hutton and Laws, 1989**). According to the authors this factor should be regarded as very significant, since its effects have not been investigated so extensively as the others (asymmetry, swirl) and probably could provide solutions to the proper performance of many flowmeters.

3.3.2 Pulsation effects on the performance of orifice meter and wall static pressure.

It is necessary to examine pulsation alone in a separate chapter, since it can be easily stated that among all factors that have been presented until now it is the only one that is always present to some extent in all pipe flows. Turbulent flow is, by nature, an unsteady flow which consists of both deterministic and random components. It could be pointed out that is very difficult to achieve a truly pulsation free condition and the existence of severe pulsations is always possible. There are several sources of pulsating flows such as pumps, compressors, valves as well as those being generated from external imposed vibrations from the process plant.

The necessity of characterising a particular flow as a typical turbulent or pulsatile flow, steady or unsteady to the author's point of view is somewhat misleading. The virtual factors used to characterise a flow as pulsating, steady or simply turbulent are the pulsation amplitude, frequency and waveform. Bearing this in mind we could easily say that a steady turbulent flow is a flow that consists of low amplitude pulsations of various frequencies. These pulsations could be the product of rotational or irrotational flow in the region that are examined. Thus, the point is that turbulent flow is a pulsatile flow that has not exceeded some certain limits and so those small pulsations due to turbulence itself are assumed not to seriously affect the performance of the flowmeter.

In terms of the orifice meter and the description of its performance it is necessary at this point to clarify some other important aspects. As it has been described extensively in previous sections, the orifice plate is a differential pressure device. In simple words, the flow velocity information derived by it is coming from two particular points, the wall static pressures upstream (P_1) and downstream (P_0) of the orifice. In the end, this means that virtually any change in the mean velocity reading obtained from a particular orifice meter that is installed in a pipe layout is dependent only upon the change of the mean wall static pressures upstream or downstream the orifice assuming that the instrumentation used to obtain the pressure readings ensure good accuracy, repeatability etc. On the other hand any change in the mean axial velocity will cause a respective change in those two static pressures upstream and downstream the orifice.

To the author's point of view it is very important to comprehend this mechanism because it gets to the heart of the matter since all factors mentioned in previous sections affecting the orifice meter operation do not do anything else than to change, in different ways, those two pressures. Having a differential pressure sensor that is normally used in conjunction with the orifice plate, the relationship between the axial flow velocity and the pressure difference created across the orifice may be expressed as

$$\Delta p(t) = \frac{Cd * (1 - \beta^4) * u^2(t)}{2 * g}$$

The signal output from a differential pressure sensor follows the next relationship:

$y(t) = K(t) * \sqrt{\Delta p(t)} = k * V(t)$ where K(t) represents the transfer characteristics of both the transducer and the signal processor and the proportionality variable k is dependent on the d/p sensor and its mechanical construction. If the differential pressure sensor is a resonant mode sensor, such as a strain gauge with a fast response, then its resonant

frequency **fr** is a function of the square root of the differential pressure ($f_r \propto \sqrt{\Delta P}$) and subsequently its frequency output is linear with flowrate.

The axial flow velocity signal, being to the turbulent regime, may simply be expressed as:

$$u(t) = \alpha(t)\left[1 + \sum_{\kappa=0}^{\eta} X_\kappa e^{j[\kappa\omega + \varphi(t)]}\right]$$

where a(t) represents amplitude variations (trends), $\varphi(t)$ represents phase perturbations and X_k, k account for the amplitude and frequency respectively of the Fourier harmonics in the velocity wave. From the monitoring point of view it is worth examining how the velocity signal is generated. Since the flow generating mechanism is, in most of the cases, a pump (or a compressor for gases), it operates by forcing a number (N) of fluid volumes (depending on the design of its impellers) per revolution of the pump rotor. The volume per each packet of fluid may be a function of time as well as the pump speed and so u(t) may be expressed as:

$u(t) \approx N(t) * \omega_{pump}(t) * \frac{d}{2}$ where ω_{pump} is the angular velocity of the pump rotor and d is the effective diameter of the impeller. Considering this initial flow signal u(t), we could say that across the pipe layout this flow signal is continuously modified by the equipment installed in the process plant until it approaches the orifice meter, is modified by it and is sensed by the pressure transducers. Thus the velocity signal that is sensed by the flow meter, in the form of a differential pressure signal, could be characteristically affected by every piece of equipment in the path of the fluid and subsequently it will contain both deterministic and random components.

Therefore, our objective was to distinguish, by some method, those deterministic components that could be associated with some of the equipment of the pipe layout. For this purpose and after the examination of the first results, it was decided that we

concentrate our effort on the ***amplitude spectrum estimation*** of the pressure signals, that seemed to offer very useful information in terms of the operation of the whole layout. Some basic considerations of the amplitude spectrum will be explained in the next chapter. Based on all the above, some further discussion needs to be done concerning a relation between the wall static pressure and its fluctuations and the axial velocity fluctuations.

To the author's knowledge, a straightforward relation between the instantaneous values of these two variables has not yet been reported. A great effort has been made by many researchers to determine a correlation between them but the research was mostly limited in the region of the turbulent boundary layer (near wall flow) since it was the most prominent region of a relation between the two variables in question and it is as well the critical region associated with the turbulent production.

The very many papers that have been written on the subject have the common title "Wall - pressure fluctuations and pressure - velocity correlation in a turbulent boundary layer". Just one will be mentioned, that of **Haritonidis J,H, Gresko L,S and Breuer K,S, 1988** which, to the author's point of view, includes some very useful conclusions on the matter. They found that the most prominent connection between the wall pressure and the near wall flow field is through the normal component of velocity, v. Wall pressure peaks and wave trains are related to corresponding structures in the near wall field. They also concluded that no definite statement can be made about the formation of high amplitude pressure peaks, as opposed to waves, other than that pressure peaks may be associated with unusually rapid velocity fluctuations. Although it was not in the aim of this project to enlarge upon this question, it was regarded necessary to mention it at this point in order to explain the following ideas.

By all means, there is the straightforward relation between the mean values of the above variables which is coming from the simplified form of Bernoulli's equation that is used in flow measurement with Pitot - Tube: $P_0 = P_{static} + 0.5 * \rho * u^2$=const. where P_o is the total pressure, ρ is the density and P_{static} is the wall static pressure. It is the same equation that is used in the Ideal Flow theory where a fluid is assumed to have no viscosity, no boundary layers and no friction forces trying to slow it down. Bearing in mind all the above and also that the pressure measurements carried out in this project were coming from simply static pressure transducers, not differential pressure, it was decided to check first of all the possibility of deriving information on the flow field from these measurements.

Another thing that must become clear at this moment is that by definition the static pressure is said to be the result of the molecular vibration and rotation near the wall. The flow is regarded parallel to the axis of the pipe and since the velocity is a vector, the component of velocity that will act through a hole at 90° to the flow direction will be u(t)*cos90, which is zero. Depending on the hole diameter, (e.g large) and its proper construction, some elements of the dynamic pressure will affect the reading and therefore they are regarded as error expressed as pressure deviation from the true pressure for **zero** hole diameter **(Shaw, R.,1960).** Although the national standards specify that a 2mm hole diameter is usually satisfactory, this would need a lot of discussion since it seems that always some dynamic components are present in the static pressure readings.

The most apparent way to correlate the above contrasts is probably the idea of a virtually non parallel flow, that is rational if we consider the way that the flow is generated and is coming into a pipe layout (by a pump usually centrifugal) as well as the fact that flow pulsations, irrelevant of magnitude, are always present in a pipe flow.

4. EXPERIMENTAL WORK.

4.1 NATURE, PURPOSE AND SCOPE OF EXPERIMENTS.

The research objectives were multiple and could be summarised as follows:

1. To obtain the differential pressure across the upstream tapping of the flow conditioner and the upstream and dowstream tappings of the orifice plate, for different Reynolds numbers, in order to obtain the relationships between those differential pressures and the flow rate. This could have a number of benefits. Firstly, it becomes possible to have a check of the flow measured by the orifice plate under normal conditions. Secondly, the flow measurement is safeguarded in case of a failure of one of the three pressure transducers.

2. To examine the performance of the Mitsubishi conditioner installed 6D downstream of a single 90^0 bend and 5D, 12D, 14D and 34D upstream of an orifice plate having a 0.68 beta ratio. Some useful conclusions were drawn by the change of the discharge coefficient when the conditioner was installed in good flow conditions (34D upstream the orifice plate). That is a sufficient length of straight pipe according to **ISO 5167** for a fully developed flow. Furthermore, an effort was made, to examine the performance of a conditioner designed by the author, that has been named for the purposes of this project as "Damper", using the discharge coefficient and the amplitude spectrum of the pressure signals and very interesting conclusions were drawn as well.

3. To examine the possibility of deriving useful information regarding all the test equipment (orifice meter, conditioner, pump) from the unconditioned signals of the strain gauge pressure transducers. According to other researchers useful information may be derived from the so called noise of the measurement signal that has to do with the

operational status of the process plant equipment as well as the general condition of the process plant.

In order to meet the objectives, the experiments were designed as follows:

Installing a Mitsubishi flow conditioner 6D downstream of a single 90^0 bend and an orifice plate 20D downstream of the bend, in a water flow rig, measurements were carried out in terms of the absolute static pressure in three positions, where pressure tappings were fitted. Using silicon diaphragm strain gauge pressure transducers, several measurements of the static pressure 1D upstream of the conditioner, 1D upstream of the orifice plate and D/2 downstream of the orifice plate (D, D/2 tappings) were made for different Reynolds numbers. Similar measurements were made without the conditioner installed (Tests 1 & 2).

In addition, increasing the distance between the flow conditioner and the orifice plate at 34D (orifice installed 40D from the bend), the same measurements were repeated, with and without the conditioner installed (Tests 3 & 4). A few measurements were made without the orifice and the conditioner installed mainly to check the performance of the pressure transducers after a recalibration (for this reason only a few results will be presented from this test (Test 5)). Subsequently, having the conditioner permanently positioned 6D from the bend, the orifice was shifted 11D and 18D downstream of the bend and similar measurements were carried out (Test 6 & 7). During Test 7 some extra measurements were taken 1D downstream of the Mitsubishi conditioner. Finally, it was decided to remove the flow conditioner and to install at the same position a simple pipe configuration that could be characterised as a damper and could be seen in **Figure 4.8**. With this pipe layout similar measurements were carried out with the orifice positioned 11D and 13D downstream the bend (Tests 8 & 9).
All the tests are summarised in the next table:

Device	**Location (Distance from the 90^0 bend)**							
	Test 1	Test 2	Test 3	Test 4	Test 6	Test 7	Test 8	Test 9
Orifice	40D	40D	20D	20D	11D	18D	11D	13D
Conditioner	6D	Out	Out	6D	6D	6D	Damper	Damper

Table 4.1 Summary table of all Tests

Using a data acquisition board, with a 12-bit Analogue to Digital Converter (ADC), the continuous output signals of the pressure transducers were digitised. Some statistical and digital signal analysis techniques were applied in the discretised version of the signals. The effort concentrated on the estimation and subsequently on the examination of the amplitude spectra of the signals obtained from the three pressure transducers for different layouts and different flow rates. According to many other researchers, such as **Amadi-Echendu, 1991, Tingham, 1988** e.t.a, there is a lack of appreciation of the extent of the information from flow sensors, the virtual meaning of their spectrum, and the significance or not of the noise that is always removed by low pass filtering or signal averaging techniques. Sufficient measurements were made for each of the eight different pipe layouts that will be described next.

4.2 DESCRIPTION OF THE EQUIPMENT AND THE MEASUREMENTS MADE.

4.2.1 Overall description of the flow rig.

Figures 4.1, 4.2 and **4.3,** show the test loop designed for the pressure measurements mentioned in the previous section. The Fibreglass tank, 2.5m length, 1.2m height, and 1.2m width contained about $2.5m^3$ water during the experiments. The water was drawn out from one side of the tank at a low position through a bellmouth and was

returned to the opposite and above the tank. The bellmouth was positioned at sufficient depth ensuring that no air bubbles travelling from the free surface could be entrained into the pump due to vortices. Inside the tank a perforated metallic screen and a wooden board, dividing the tank in three, ensured again that no air was entrained into the suction pipe. In addition, the wooden board supported an adequate decrease of the strong turbulence coming from the outlet of the pipe, providing steady and uniform flow conditions at the pump inlet. A drain was fitted at one of the tank corners. The tank was drained, cleaned and refilled repeatedly in order to provide a sufficiently clean water supply for the measurements. The tank was topped by wooden covers to protect the clean water from contamination by dust.

The flow loop started at the bellmouth. Water left the tank through a 4" fully open gate valve and through a 3.2m, 4" ABS pipe was driven to the centrifugal pump. The pump was driven by a three phase motor, rated at 2900 rpm, 15KW. It was an 80-160/150 pump, having 34 mH_2O maximum total head and an impeller consisting of six blades. At the outlet of the pump a 3" gate valve was installed followed by 1.2 m, 3" vertical straight pipe and an ABS tee junction connected with a bypass line. This bypass line returned into the far end of the tank and was always shut off with a ball valve throughout the course of experiments. It was used only when some rearrangement of the flow loop was necessary in order to drain the water from the 3" vertical pipe into the tank.

About 26D downstream the pump outlet, a 3" turbine flow meter was installed. It was used as the reference meter for the calibration of the orifice meter. This turbine meter was calibrated versus a 4" turbine meter that had been calibrated in *QUADRINA LTD (UK).* The calibration data and curves of the two meters are shown in **Figures 4.4** and **4.5. Figure 4.4,** in dark font, also shows the range of flow rates that the 3" turbine meter operated.

The mean meter factor (K_m) was approximately 18,693 ± 15 for the flow rates used in the experiments. The flow rates were $3600f_t(i)/ K_m$ in m^3/Hr where $f_t(i)$ being the output frequencies of the turbine meter. The flowrates were maintained throughout the duration of the experiments within an accuracy of ± 1Hz that is an error almost ±0.15% of full range.

The loop continued with two 90^0 mitre bends in the same plane and the same positioning, connected together with a 3" to 4" pipe converter. The inlet to the test section started with a 90^0 bend preceded by a section of about 23D of vertical straight pipe. This arrangement helped avoid the interaction of bends that could create an unwanted level of swirl.

A *Mitsubishi* flow conditioner was installed 6D after the bend followed by the orifice plate 14D and 34D downstream. Moreover, provision had been made for other positions for installation of the orifice plate, 5D and 12D downstream the *Mitsubishi* plate between two *BS 10, Table D/E (Co:130110)* flanges. Details of the construction of the test section are given in **Section 4.2.2.**

At the end of the flow loop, a gate valve was installed. Ten different flow rates were obtained for the Tests 1 to 4 by opening slowly this valve. A steady reading of the turbine meter was definite after a period of 15 minutes. Another nine different flow rates were obtained by closing slowly the valve in order to avoid possible *"water hammer"* effects. For Tests 5 to 9 ten different flow rates were obtained in total with the same method. At the far end of the tank, where the water was returning, a dipping thermometer was located, capable of measuring temperature to within 0.5 ^0C . At the inlet and the outlet pipes of the pump two Bourdon gauges were attached in order to obtain a continuous reading of the pump head. The Reynolds number range where the experiments were carried out was 2.21E+05 to 4.54E+05 and the respective flow rate range was 71 m^3/Hr to 147. 5 m^3/Hr.

4.2.2 The Test section.

The test section, as shown in **Figure 4.6,** was constructed of ABS pipe and flanges. At the start three pairs of flanges were attached 6D, 20D and 40D after the single 90^0 bend ready to receive the orifice plate or the Mitsubishi conditioner. However, other preconstructed pipe components of different lengths, shown in **Figure 4.6,** were available as well so that the test layout could be modified easily. Both the orifice plate and the conditioner, and finally the "damper", were properly designed in accordance with **(BS. 1042)** as shown in **Figures 4.7-4.9b** respectively, to fit in all the flanges. The orifice plate had a *beta ratio 0.68* and the throat was 45^0 sharp edged at the downstream face. Four D and D/2 tappings were positioned at about 45^0 to the vertical at the lower and upper half of the flow meter when it was installed 20D or 40D downstream the bend. Almost all the measurements were made using the pressure tappings at the lower half of the flow meter. This was done in order to avoid entrapment of bubbles in the impulse lines which caused a problem at the beginning of the experiments. Moreover, in order to avoid problems of blockage by rust or other heavy extraneous matter the angle of the tappings was not less than 45^0 in accordance with **Battye, 1988**. The pressure tapping holes had a diameter of 2mm. The upstream and the downstream pressure transducers were always positioned at a 0^0 angle (on the same line). Four additional pressure tappings with the same orientation and dimensions were positioned 1D upstream and 1D downstream the flow conditioner.

4.2.3 Secondary Instrumentation (Pressure transducers - Data Acquisition board).

All the measurements were carried out using three unbonded strain gauge pressure transducers. Manufactured by Keller L.T.D to measure absolute pressures, they featured a four active arm Wheatstone Bridge strain gauge diffused directly into a silicon

diaphragm as shown in **Figure 4.10**. A constant voltage of *15 Volts* was supplied to the transducers. The output ranges were *0 to 10V*, thus, avoiding range switching at the data acquisition board. Three wire cables were used to connect the pressure transducers to the power supply and to the data acquisition board. In order to avoid earth loops all wires were earthed to the data acquisition board via the RS 232 interface. The lengths of the wires used to connect the pressure transducers with the data logger, when they were installed at the tappings, were 3m for each transducer.

The pressure ranges of the transducers were *0 - 10 Bar* or *0 - 150 psi* and their line pressure sensitivity was smaller than 0.003 mV/psi. The effective frequency response of the transducers was up to 3KHz. Calibration checks on the transducers were made frequently throughout the test program. Calibration curves were plotted for each transducer and can be seen in **Appendix A** in **Tables A1** and **A2**.

A 16 channel, 12bit Data Acquisition Board with counter/timers installed on an AT/286 computer was used to collect the output signals of the pressure transducers. Having the fixed *resolution* of the 12Bit A/D converter, that is 0.024% of full scale (1 divided by 4.096) and setting the input range of the acquisition board at 0 to 10V, unipolar (the same range as the output range of the transducers) a 2.44mV change could be detected. During the A/D conversion the sampling operation was performed by a *Sample and Hold* amplifier inserted prior to the ADC with a typical track time 2μSecs. This is used to ensure that the level of the analogue voltage does not alter during the conversion time by freezing the input voltage at the precise instant at which the sampling process takes place. It is important to point out here that in the signal conditioning circuit there was no low pass filter installed as would normally be, in order to obtain the widest frequency response from the unit. A diagram of the data acquisition system is shown in **figure 4.11** while all the electronics are shown in the photo of **Figure 4.2.**

The calibration of the acquisition board showed that a *sample rate* up to 8kHz could be used to acquire the data via interrupt control. This speed was sufficient and in accordance with the Niquist Theorem in order to avoid aliasing effects. All the measurements were carried out with the above sample rate.

4.2.4 Computer software used for the Data Acquisition, Analysis and Presentation.

The data acquisition software that supported the board (written in Microsoft C) was a *menu-based* software where via commands it was possible to specify things like which channels on the hardware to use, how many data points to collect, which voltage range to use, what rate samples were to be taken at, etc. The output data had been arranged by this software to be in Volts in the range 0 to 10V and were written into files. These files were analysed using digital signal analysis techniques.

The *analysis* and *presentation* software was a signal processing package called **MSPECT** available on the PCs and Vax computers in ESD Dpt.(Electronic Systems Design) in the College of Aeronautics. This software package provided most of the analytical tools necessary for signal analysis. Operations such as time domain manipulation and editing of real or complex data, Fast Fourier transforms, convolution, filtering, etc. were available. The software operated on an internal pair of buffers. The first was the active buffer upon which most of the commands operated. The second was a backup buffer used for temporary data storage. The display screen was divided into two areas one on the upper half and one on the lower half. Generally the unprocessed data were displayed on the upper half and the processed on the lower half. It was proved to be a powerful and very useful tool throughout this project.

In order to obtain some statistical analysis of the data, another software package called **SIMAN,** coming from the *Department of Computer Engineering, University of Patras,* was used. It was possible to draw the *cdf* (Cumulative density function) and *pdf* (probability density function) of the sampled data in order to examine for possible information from the amplitude's distribution within the signals.

From the *pdf* plot, the mean value of the signal that corresponds to the maximum value of pdf could be determined as well. The above statistical technique was not extensively used and other techniques were preferred as will be explained in later sections; however, typical results from **SIMAN** are shown in **Appendix A,** in **Table A3.** All other calculations, such as linear regressions, correlation, etc., as well as most of the plots were carried out in **EXCEL 5.0** that was proved to be a very powerful tool as well.

4.2.5 Procedure of pressure measurements - (Codification).

As mentioned previously in **section 4.1** the measurements were carried out in eight different pipe layouts. Thus, the first codification, was based on the eight different tests, i.e. in every plot there is a T1,T2,....T8 meaning Test1, Test2 e.t.c. Moreover, measurements were taken for 19 different flow rates for the first four tests and for 11 different flow rates during the last four tests. For every flow rate 9 time records per transducer were collected. Each flow rate was encoded with a letter from **A** to **S** and each transducer was encoded with a number that characterised its position as well. Thus, transducer number **2** was upstream of the conditioner, **1** was upstream of the orifice plate and **0** was downstream of the orifice plate. For example, the amplitude spectrum plot T2/P13 means Test 2 (orifice meter 40D downstream the bend -No conditioner installed), flow rate 138.7 m^3/hr (P), pressure transducer No 1 (upstream the orifice), measurement No 3. The whole codification is summarised in **Appendix A** in **Table A4.**

A sample rate of 8kHz was used in all measurements made. 9 records per transducer were taken for each experiment, five of which were of 4,096 samples giving a time record of 0.512 sec, three were of 8,192 samples giving a time record of 1.024 sec and one was of 65,536 samples in a time interval of 8.192 sec. The last time record was used in order to check for large scale changes that could possibly occur and was obtained via DMA (Direct Memory Access).

However, for the first two objectives of my research, as mentioned previously in **section 4.1,** it was necessary to obtain only the mean value of those time records. Thus any random effects were removed out of the signal by averaging across the same time interval (0.512sec) a collection of 9 transducer time records, called an *ensemble*, of the same measurement. The large time records were divided in time records of 0.512sec. In this way the resulting signal was a true record of the phenomenon being measured over that time of period. Then the mean value of the signal, xi was:

$$\bar{x} = \frac{1}{N}\sum_{i=0}^{N-1} x_i$$

It must be pointed out here that there were not significant changes of the mean value between all these time records, implying that the flow could be characterised almost as a *mean steady flow* although fluctuations always existed. **Table 1** shows the experimental results of all the pressure measurements carried out and **Table 2** all the calculations made to obtain the theoretical values of the discharge Coefficient for the flow range that the experiments were carried out. From the values of **Table 2** a theoretical curve was drawn and is shown in **Figure 4.12a.** The theoretical value of Cd was found to be around 0.621.

5. RESULTS

5.1 RESULTS OF THE DIFFERENTIAL PRESSURE MEASUREMENTS K FACTOR.

Although in the theoretical estimations of the K factor that have been described in **section 3.2.5** we have assumed an equation of the form: $Q = K * \Delta p^n$ where n=0.5, in real cases this power is not 0.5 but slightly different. Thus, in all correlation methods that were carried out the objective was to establish both the values of **K** factor and **n.** Using the functions of the **section 3.2.5** the theoretical values of K(2,1) and K(2,0) were calculated for the first six tests layouts (where the conditioner has been used) and are shown in the next table followed by the respective experimental values that have been obtained for all tests, including the last two with the "damper". For the theoretical calculations the loss coefficient of the orifice was taken Kor=5.5, the loss coefficient of the Mitsubishi conditioner Kco=1.35 and the relative roughness of the pipe k=0.0025mm since we used a new ABS smooth pipe. The theoretical value of exponent **n** was assumed to be equal to 0.5 for all the cases.

FACTOR	WITH CONDITIONER				WITHOUT CONDITIONER			
K (Orifice Distance)	TEST 1 (40D)		TEST 4 (20D)		TEST 2 (40D)		TEST 3 (20D)	
	K(2,0)	n	K(2,0)	n	K(2,0)	n	K(2,0)	n
Theoretical	0.4814	0.5	0.4911	0.5	0.5327	0.5	0.5459	0.5
Experimental	0.5101	0.476	0.3969	0.4977	0.309	0.5223	0.3718	0.5067
	K(2,1)		K(2,1)		K(2,1)		K(2,1)	
Theoretical	0.9635	0.5	1.049	0.5	1.871	0.5	2.916	0.5
Experimental	3.9772	0.3618	2.6812	0.4104	very scattered data		very scattered data	
K (Orifice Distance)	TEST 6 (11D)		TEST 7 (18D)		TEST 8 (11D - Damper)		TEST 9 (13D -Damper)	
	K(2,0)	n	K(2,0)	n	K(2,0)	n	K(2,0)	n
Theoretical	0.4956	0.5	0.4920	0.5		0.5		0.5
Experimental	0.3815	0.5074	0.3501	0.5045	11.005	0.2687	10.112	0.2817
	K(2,1)		K(2,1)		K(2,1)		K(2,1)	
Theoretical	1.095	0.5	1.059	0.5		0.5		0.5
Experimental	3.7256	0.4736	3.9466	0.4653	0.3816	**0.5**	0.4114	0.5039

Table 5.1a Theoretical and experimental values of the factors K(2,1), K(2,0) and n

The regression lines and their respective equations obtained for the **K** factor and the exponent **n** for the eight different test layouts are shown in **figures 5.1** to **5.7**. For all the plots the flow rate Q=Q(2,1)=Q(2,0). It could be said that only in few cases, there is good approximation between the experimental values of K factor and those estimated by the theoretical functions. However, it must be kept in mind that the pressure transducer No 2 was positioned almost 5D downstream the bend inside an acceleration region due to the bend.

For the best comprehension of the results it must be mentioned that those tests where the Mitsubishi conditioner was installed permanently 6D downstream the bend have been positioned in the first half of the table above. Studying the first half of **Table 5.1a** it can be seen that the distance of the orifice from the bend is reduced clockwise from Test 1 to Test 6 (Test 1 - 4 - 7 - 6). From the theoretical estimations it is clear that the values of K(2,0) and K(2,1) increase while the distance orifice - bend or orifice - conditioner decreases since the total and the partial resistances of the orifice conditioner package decrease. Although we could not say the same for the experimental values of K(2,1) and K(2,0), on the other hand **the exponent n is increased** with the decrease of the distance. We could assert that this indicates **stronger** the decrease of the relative resistances or in a similar manner the decrease of losses, and emphasises the fact that the exponent n is as important as the K factor. It is vital to keep this fact in mind since it is one of the few things that we could rely on in order to be able to distinguish the different scenarios in our Tests.

The same thing as above happened in Tests 2 and 3 when removing the conditioner and decreasing this way the losses; the exponent n was increased compared with the respective Tests 1 and 4. Tests 8 and 9 have to be distinguished from the other

Tests not only for the presence of the "Damper" but also for the unusual and interesting results that were obtained from the regression lines of K(2,0).

The previous observations gave rise to an effort to find out the exact causes of different tendencies of the factors and the possible effects in the general performance of the orifice through the changes of the discharge coefficient. Many assumptions have been made and many possible explanations have been given where some of them led to very interesting conclusions and will be described in later sections in conjunction with the amplitude spectrum plots obtained. It was apparent from the variability of the results conserning the K(2,1) and K(2,0) that possibly we had to confront eight different cases with not so many common factors, revealing the difficulty to comprehend the possible operation mechanisms. Because of this, the only statement that could be made at this point is that the variability of the results obtained for the different cases is due possibly to the different mechanisms of turbulence redistibution through the test section since it is the only term that we could use with some confidence in order to describe all the possible scenarios.

The possible benefits of using the above technique could be multiple and some of them will be described. Having virtually three simultaneous measurements of the flow are certainly better than one. However there are no same standards for the measurement of flow through a flow conditioner as for the orifice and surely it would be very difficult to have because of the wide variety of the flow conditioners with different characteristics. For all that, the relationship could be obtained when the system is first commissioned or after an in situ-calibration of the orifice meter. Although the above constraints exist, by knowing the loss coefficient of the conditioner which is always known, it is possible to have a good check of the flow rate measured by the orifice.

The combined observation of the **K** factors (K(2,1), K(2,0)) and the exponent **n** with the coefficient of discharge or the factor K(1,0) could give us to some extent, the cause of changes in the performance of the orifice meter. For example, a change in the Cd resulting by a change in the differential pressure across the orifice could be detected more precisely as well as the cause (e.g. asymmetry,swirl etc) of this change by a respective change in one or both the K factors. We could simply expess the factor K(1,0) as a function of Cd :

$$K(1,0) = Cd * \frac{1}{\sqrt{1-m^2}} * \frac{\pi d^2}{4} * \left(\frac{2}{\rho}\right)^n$$

The respective values of K(1,0) have been estimated for all tests and are shown in the next Table:

With Conditioner				Without Conditioner			
TEST 1		TEST 4		TEST 2		TEST 3	
K(1,0)	n	K(1,0)	n	K(1,0)	n	K(1,0)	n
0.4392	0.495	0.3701	0.5089	0.3622	0.5115	0.4406	0.4938
TEST 6		TEST 7		TEST 8		TEST 9	
K(1,0)	n	K(1,0)	n	K(1,0)	n	K(1,0)	n
0.2853	0.5415	0.264	0.5361	0.2967	0.5254	0.2704	0.5455

Table 5.1b Experimental values of factors K(1,0) and n

In addition the respective theoretical values of K(1,0) and n have been estimated from the curve of **figure 4.12b** that has been drawn using the data from **Table 2**. Two main things have to be emphasised:

1. The theoretically estimated exponent n was not equal to 0.5 since it was found to be **n=0.4918,** indicating the separation losses introduced by the orifice.

2. There is an obvious proximity of the theoretical values of K and n with the values obtained in Test 3. In Tests 3 and 4, as it will be described in the next section, the values of the discharge coefficient (Cd) approached the respective theoretical values and the orifice meter could be said that had performed better.

Another important fact that was revealed, comparable with some previous thoughts, is that in Tests 6 and 9 the exponent n is quite increased indicating a low resistance to the flow from the orifice and subsequently a low pressure drop. This fact could be distinguished as well by looking at **Tables 3** to **10** where it is clear that the differential pressure across the orifice is the smaller in those two Tests.

The possible benefits of the above analysis would become obvious after a possible failure of one of the three pressure transducers. The flow measurement would not be lost since it could be obtained by the other two transducers. The use of differential pressure transducers in flow measurement by orifice meters in conjunction with the filtering of the high frequencies in measurement signals, confine the information that could be obtained using pressure transducers. In addition recent advances in electronics could give us the opportunity for a continual and precise measurement and acquisition not only of the measured variable and its changes but the precise cause and effect as well.

5.2 RESULTS ON THE PERFORMANCE OF THE ORIFICE PLATE USING A MITSUBISHI FLOW CONDITIONER AND A "DAMPER" BY EXAMINING THE DISCHARGE COEFFICIENT.

Many comparative measurements and further estimations have been carried out in order to identify first of all the characteristic performance of the Mitsubishi conditioner upstream of the orifice plate and then to compare it with a simple-design pipe configuration that was described as a "damper" for the purposes of this project. All the results are summarised in **Tables 3** to **10**. At this stage the performance of the orifice, the conditioner and the damper will be presented having as measure the discharge coefficient and its changes. In Test 1 the orifice was installed 40D downstream of the bend having the conditioner positioned 6D downstream of the bend as well. The previous layout or the layout in Test 2 (without the conditioner installed) could be regarded as the most proper in order to obtain a calibration curve for the orifice, following the standards. This could be the reference curve for all comparisons made. However, it was decided all comparisons were to be made against the theoretical values of Cd. The curve of those values is shown in **figure 4.12a**.

The above decision seemed to be correct, since as it was shown later, the performance of the orifice was not the best one at these layouts. **Figures 5.8 - 5.15** show the Cd curves of eight different layouts as well as the percentage difference of all the estimated values from the respective theoretical values. In most cases the estimated Cd was higher from the theoretical values except for a few cases where for the lower Reynolds number the Cd was lower.

Generally, we could say that in the first four tests in which the orifice was installed 20D or more downstream of the bend, the Cd differed from the theoretical values from -1% to +3% and it was mainly positive. It is obvious that the orifice

presented its "best" performance, (the Cd values were closer to the theoretical values), in test 3 where it was installed 20D downstream of the bend and the Mitsubishi conditioner was not installed; and then in Test 4 when the Mitsubishi conditioner was installed 6D downstream of the bend with the orifice positioned at the same distance. In Test 3 the Cd had a difference of 0% to 1.5% from the theoretical values for the whole range of Reynolds numbers while in Test 4 the difference was between -1% and 1%. However, in Test 3 the Cd had not any particular slope, its values were very changeable compared with the respective theoretical values and from this point of view this could not be characterised as fully satisfactory. On the other hand, in Test 4, although the slope of Cd is opposite to the theoretical, its values followed a more steady "attitude".

When the orifice was positioned closer to the bend (11D downstream) in Test 6 and the conditioner was installed 6D downstream of the bend as well the Cd had a large positive percentage difference from the theoretical (10%). The fact that in Test 7, and for the most of the flow range, the percentage differences of Cd values from the theoretical could be characterised as satisfactory as they were quite steady and had a difference of 1% to -2%. Similar results to the Tests 6 and 7 were obtained in Tests 9 and 8 respectively when the "Damper" had replaced the Mitsubishi conditioner. Thus, in Test 8 the Cd values had a negative difference at around -2% from the theoretical values while in Test 9 a high positive difference at around 10% for the higher flow rates. The slope of the Cd curves in all tests was opposite to the theoretical since Cd increased with the increase of the flow rate.

These high positive differences of Cd values in Tests 6 and 9 created a lot of questions and it was decided later to have a second check of those results. For this purpose the rig that had already been modified for other experiments was rebuilt and these two measurements were repeated. The fact that it was almost impossible to obtain exactly the same pipe configuration since the pump had already been shifted for some

other series of experiments, the suction part was longer than before and some pipe components that had been used in the first measurements were no longer available, resulted in obtaining some different results that are presented in **Appendix B**. However, these two additional measurements revealed some additional information that led us to some further considerations regarding the various results which had already been obtained.

As it was mentioned earlier and could be easily observed in test 3, where the orifice was installed 20D downstream the bend without the flow conditioner, that the values of Cd had a good approximation with the theoretical, especially for the medium range of Reynolds numbers. This fact could be related as well with the very good approximation of the experimental values of K(1,0) and exponent n with the respective theoretical values as this has been described in the previous section.

Some comparative plots of the orifice plate performance 40D and 20D downstream of the bend are presented in **figure 5.16.** Generally, for the layouts used in these experiments it was proved that it was better to install the orifice closer (20D or even 11D with the damper) than further (40D) downstream of the bend either with or without the conditioner. Thus, some useful considerations could be observed in terms of the comparative performance of the orifice downstream a single 90^0 bend:

- When the orifice was installed 40D downstream of the bend, which is a sufficient length of straight pipe after a single bend (for the present test conditions defined a 0.68% uncertainty apart from errors due to other parameters of improper construction e.t.c) for a good performance of the orifice according to the standards, it proved not to be enough. Moreover, the presence of the flow conditioner in good flow conditions led to a positive shift in the discharge coefficient.

- It could be easily observed that in all the cases the Cd had the tendency to increase with the increase of Reynolds number whic was in contrast with the theoretical values where the slope was exactly the opposite. This could be explained by the fact that those disturbances created by the presence of the bend (asymmetrical flow and probably some swirl) were becoming amplified as the flow rate was increasing and were travelling at a longer distance across the pipe. Thus, almost in all cases the D pressure tapping of the orifice was reading a lower pressure value than we could say its theoretically predicted value, due to the acceleration near the wall and the result was a positive Cd. However, this consideration is not enough since if we look at the summary **Table 1** we can see that the pressure increased in all three pressure measurement positions as the orifice shifted closer to the bend.

- The fact that the orifice presented its better performance near the bend without the conditioner probably suggests that the crucial distance is that of the orifice from the bend and then the distance orifice - conditioner. We could say that in only few cases the conditioner improved the performance of the orifice and this happened in only a limited envelope of the flow range. For example in Tests 3 & 4 and in the range between 3.46E+05 up to 3.94E+05 it would be preferable for the conditioner not to have been installed and to use the orifice alone just 20D downstream of the bend although in actual installations and having in mind the possible flow variations, this would not be wise.

In order to have a complete view of how this distance affected the performance of the orifice, combined with the presence or not of the flow conditioner, it would be better to present the amplitude spectrum of the pressure signals combined with the mean values of the pressure in the three measurement positions as will be described in the next section.

5.3 AMPLITUDE SPECTRUM ESTIMATION OF PRESSURE TRANSDUCER SIGNALS AND ITS MONITORING CAPACITY. FAST FOURIER TRANSFORM.

5.3.1 Basic result analysis.

It is well known fact that there is a lack of understanding of the physical meaning of spectrum from pressure transducers and for this purpose it was thought necessary to present at this moment a short analysis on this matter in conjunction with the presentation of the data obtained during this project. This will be very helpful to better understand the results and their significance.

Non-periodic or random discrete signals could be analysed in the frequency domain by the use of the Discrete Fourier Transform (DFT) and for its fast computation by the Fast Fourier transform (FFT). The signals collected from the pressure transducers in this project will be described in voltage versus time and amplitude versus frequency representations. Virtually our interest has been concentrated on the frequency domain and mainly on the pattern of the amplitude spectrum, its physical meaning and the possible information that could be extracted by particular changes in its frequency components. We could generally say that the continuous Fourier Transform of a non - periodic signal f(t) is defined by:

$$F(j\omega) = \int_{-\infty}^{\infty} f(t) * e^{-j\omega t} dt \qquad \textbf{(5.1)}$$

where $F(j\omega)$ is complex and is known as the Fourier integral or, more commonly, the Fourier transform and ω represents in this case a continuous frequency variable. If we put

$$F(j\omega) = \mathrm{Re}(F(j\omega)) + j * \mathrm{Im}(F(j\omega)) = |F(j\omega)| * e^{j\varphi(\omega)}$$

then we have

$$|F(j\omega)| = \left[\mathrm{Re}^2(F(j\omega)) + \mathrm{Im}^2(F(j\omega))\right]^{1/2}$$

which is in units of **volts per hertz** rather than **volts,** something quite important in our case. Thus, we could simply say that $|F(j\omega)|$ is an amplitude density called *amplitude spectral density.* Subsequently, $\varphi(\omega)$ is the associated phase angle given by :

$$\varphi(\omega) = \tan^{-1}\left[\mathrm{Im}(F(j\omega))/\mathrm{Re}(F(j\omega))\right]$$

The data obtained in these experiments were discrete and so it is not possible to apply the Fourier transform since it is for continuous data. However, the analogous Fast Fourier Transform was applied. It was mentioned earlier in section **4.2.3** that all the data sequences had been sampled at 8 KHz, which means that the signals were sampled at regular time intervals, $T = 1/8{,}000 = 125\mu$ sec. Therefore the produced sample sequences are of the form:

$$\{x(nT)\} = x(0), x(T), ..., x[(N-1)T]$$

where N is the number of samples. In some of the signals presented in this project the number of samples N=4,096 while in others N=8,192. Furthermore, n is the sample number from n=0 to n=N-1. The FFT of x(nT) is then defined as the sequence of complex values $\{X(k\Omega)\} = X(0), X(\Omega), ..., X[(N-1)\Omega]$ in the frequency domain, where Ω is the first harmonic frequency given by $\Omega = 2\pi/NT = 2\pi f$. Amplitude nulls occur at f=1/T, 2/T, 3/T..... Therefore, in our measurements we could say that the first and second harmonic frequencies f, when N=4,096, were f_1=1.95 Hz and f_2=3.9 Hz respectively and when N=8,192 they were f_1=0.98 Hz and f_2=1.95 Hz. It is obvious that an increased number of samples produces better frequency resolution. Noting that N real data values (in the time domain) are transformed to N complex FFT values (in the frequency domain) then we could say that the FFT values, X(k), are given by:

$$X(\kappa) = FFT[x(nT)] = \sum_{n=0}^{N-1} x(nT) * e^{-jk\Omega nt} \qquad \textbf{(5.2)}$$

where k=0,1,.....N-1 and represents the harmonic number of the transform component while FFT denotes the fast Fourier transformation. It can be seen that equation 5.2 is analogous to the Fourier transform of equation 5.1 when f(t)=0 for t<0 and t>(N-1)T by putting x(nT)=f(t), nT=t and $k\Omega = \omega$ and so it is expected that the two transforms must have similar properties. However, they are not equal but by making the previous substitutions in equation 5.1 and replacing the integral by summation we obtain:

$$\sum_{n=0}^{N-1} x(nT) * e^{-jk\Omega nT} * T = F(j\omega) = T * X(k)$$

for $0 \le t \le (N-1)T$. This reveals that the Fourier transform components are related to the FFT components by the sampling interval and may be obtained by multiplying the FFT components by the sampling interval. Therefore in our plots of X(k) versus f we may say that X(k) is in V/Hz or subsequently Pressure units/Hz (e.g. Bars/Hz). To the authors point of view this is such an **important yet simple** fact and its importance will become clear in the next example.

In **figure 5.17** we could see a voltage versus time and an amplitude versus frequency plot as collected and analysed with the MSPECT. We could easily observe two sharp peaks at 667 Hz and at 652 Hz. Since it is well known that the area under the $|F(j\omega)|$ versus f plot gives the mean voltage and similarly for X(k) versus f after multiplying by T=0.000125sec, it could be easily verified **that the biggest portion of the mean voltage value (and subsequently of the pressure) is mainly coming from the area under those two high frequency - high amplitude peaks**. Inevitably, this fact formed the basis for further estimations. Subsequently many efforts focused into explaining the difference and the possible physical meaning of an energy (or pressure) where its mean value is mostly coming from high frequencies and that where its value is coming from low frequencies and the particular effects of this on the performance of the orifice meter.

5.3.2 Results on the performance of the orifice - conditioner (and Damper) package using the amplitude spectral density.

Among the Tests that were carried out during this project the values of Cd approached the standard empirical values or they performed steadily when two factors related with the pressure gradient existed together. The improvement on the pressure gradient was identified and explained by the next two factors as they were observed after a very detailed estimation of the pressure signals in the time and frequency domain.

1. The removal of the large amplitude - high frequency pressure fluctuations in the three measurement positions and mainly upstream of the orifice plate seemed to be of major importance. The main factor for the elimination of those high frequencies seemed to be the distance of the orifice from the bend and as a second reason the presence of the flow conditioner, but this was not valid in all cases. In some cases it was observed that the flow conditioner had introduced or supported the evolution of those high frequency pressure fluctuations and worsened the conditions.

2. The above factor, as it has been highlighted and will be extensively explained in this section, was not enough to give better results in terms of the performance of the orifice. For example, in some cases although those significant amplitude high frequencies had been eliminated, the performance of the orifice did not been improve. Thus, the second factor that was identified, which in addition was valid in all cases where the performance of the orifice was improved, appeared to be the simultaneous reduction of the mean squared value of the relative signals with the increase of the flow rate and mainly upstream the orifice (D tapping). This is a measure of the signal amplitude, it is directly related to the signal's power and is given by the next equation:

$$\overline{x^2} = \frac{1}{N}\sum_{i=0}^{N-1} x_i^{\,2}$$

Particularly, as we moved downstream from the bend the pressure gradient seemed to improve when a "transfer" of energy from the higher frequencies to the lower followed by a simoutlaneous decrease of their respective amplitude was taking place. It is clear from the above considerations the two factors mentioned above are the two apparent effects of "Damping". The conclusion mentioned before seemed to be very important and combined with the ideas mentioned in section 3.2.5 could be extensively used for a better and continual on-line check of the performance of the orifice; and not only this. It could provide some useful information in terms of the design of the flow conditioners and their ability to remove (or to support properly in some cases) those high frequency pressure fluctuations as well as at the same time to shape downstream a desirable pressure gradient. Naturally, a desirable pressure gradient is that of a straigh smooth pipe.

The case of those high frequency pressure fluctuations, what they may represent and what their significance may be was examined extensively and some ideas were described in the previous section. However, it should be mentioned here that such fluctuations could possibly be characterised as strong turbulence supported by the asymmetrical flow due to the bend and were manifest in the pressure transducer's signals just downstream the bend for the entire range of flow rates. The term *strong turbulence* was used although we are in the region of the wall (no slip conditions) in order to perform possibly a turbulent boundary layer.

Although these factors seemed to be of major importance in understanding the improvement of the orifice performance they did not fully explain its performance in cases such as in Tests 7 and 8 which could be characterised as satisfactory despite the deviation of Cd. Thus, an effort was placed in finding out a third possible common factor existing in all cases that could complete the picture.

It is necessery to mention briefly at this stage that as the pump was rated at 2.900rpm, its rotation frequency was at around 48.3Hz. Since the impeller of the pump was made of 6 blades we estimated that the pump was introducing into the pipe system roughly 6*48.3=290 volumes of fluid per second. At the beginning of this research there was a thought that probably a frequency of around 290Hz could be present in the signals but was not fully understood when and where it could be present then.

It must be reminded at this stage that the flow rate was being controlled with a gate valve that was installed **at the far end of the pipe**. Examining **figures 5.18-5.19** we could easily distinguish those high frequency peaks of significant amplitude in Test 1, just 5D downstream of the bend and 1D upstream of the conditioner. Only in Test 4 these have been totally eliminated by the three positions of pressure measurements and this is one of the cases in which the orifice performance approached the theoretical considerations. It is clear that the evolution of these peaks followed a very distinct manner since they were moving steadily to higher frequncies with the decrease of the flow rate and they were always present until the lower tested flow rate. In **Figure 5.18a** the control gate valve was almost **fully open** and we could see a very distinct peak at 313Hz (very close to 290HZ). When the gate valve closed further the pressure increased and the distinct peak shifted to a higher frequency (**figure 5.18b**). Inevitably, some preliminary thoughts follow:

1. A permanent change of the conditions at the far end of the flow loop (partial closure of a valve) affects permantly and discernably the conditions at a long distance **upstream.** It is necessary at this stage to emphasise the fact that these unsteady conditions were not the result of a rapid valve operation. It could be regarded as a passage from one equilibrium condition to another. This was strongly supported by the excellent repeatability of the pressure measurements at the same point and under the

same conditions and particularly by the permanent shape of the amplitude spectrum in a whole set of measurements carried out at irregular time intervals.

2. Since a partial closure of a valve introduced an additive flow resistance to the system, this resistance was depicted at the amplitude spectrum of the pressure signals with the shift of distinct components to higher frequencies. This second thought could possibly give an explanation for the presence of those components at frequencies slightly higher than 290Hz when the gate valve was fully open considering the primitive resistance of the system.

The main result of the previous estimations is that the pressure at some point of a flow system depends on the prevalent conditions, not only upstream to that point but further downstream as well. Furthermore, every item of equipment installed in a pipe layout affects more or less the pressure at **every point** of the pipe system either downstream or upstream. The importance of this is easily understood for monitoring purposes. So, in the authors opinion, **a permanent adverse propagation of pressure waves must exist within the pipe layout, caused by every single pipe component.** These waves are something different from the well known pressure transients that are characterised by a short duration. This idea has several common points with the *rigid column theory* which is a limiting case of wave theory **(Douglas J.F, et al, 1995)** and whose principles seem to have an increasing potential for extensive use.

The particular conditions present in Test 1 resulted in the shifting of these peaks to higher frequencies with the closure of the valve (decrease of the flow rate) 1D upstream the orifice (D tapping) while they "disappeared" at a flow rate of 135 m^3/Hr as it can be seen in **Figures 5.20-5.22.** They were absent at the lower flow rates. In **figure 5.21c** it is easily seen that this band of frequencies "disappeared" **when it approached the sixth harmonic** of the pump frequency (6*290Hz=1740Hz).

The same band of high-ampitude frequencies was present in the spectra downstream the orifice in Test 1, at around 290Hz, when the control valve was almost fully open and they evoluted with the same way as before, as shown in **Figures 5.23-5.25**. They "disappeared" at a lower flow rate, 102 m^3/Hr, (**figure 5.25a**) while the spectrum was "flat" at the lower flow rates. The interesting point is that this band was totally eliminated when it almost approached the sixth harmonic of the pump frequency (1740Hz) as well. The presence of the orifice shifted this band at lower frequencies (**figure 5.23a**) downstream, at the D/2 tapping, than upstream (**figure 5.20a**) so they approached the sixth harmonic at a lower flow rate. Furthermore, the D/2 tapping was closer to the control valve and so was more sensistive to every change in the status of the valve. It was apparent by the results that the frequency response of the pressure transducers was proved inadequate since it seemed that frequencies higher than 3.5KHz of distinct amplitude were possibly present in some cases into the pipe flow (see **figure 5.29c**).

Figures 5.26-5.29 show the amplitude spectra obtained in the three measurement positions when the control valve was fully open (full flow) in Tests 6 to 9. Although the peaks close to the pump frequency are very clear in all tests we could distinguish four totally different scripts. For example, in Test 6 and upstream the conditioner (**figure 5.26a**) we could see the two peaks at 270Hz and 313Hz at the left and right of the frequency of 290Hz. Although the amplitude scale in all these plots is in arbitrary units the indicated values represent the true relative magnitude of the harmonics. So we could say that the energy (or pressure) at this point is mainly coming from this band of frequencies.

The presence of the conditioner resulted in a slight shift of the above band of frequencies to lower values just 1D upstream the orifice with a slight reduction in their

magnitudes and it also transfered an amount of the energy to a band of very high frequencies (**figure 5.26b**). The main component of the lower band appeared at a **superimposed** frequency of the flow (coming from the pump) frequency (290-1/6*290) and this happened in more than one case. However, only in this case two distinct and different bands of frequencies appeared in the same spectrum and so the fact that the distance orifice - conditioner in this Test was just 5D led to the thought that this band of very high frequencies indicated the presence of the conditioner. On the other hand, downstream the orifice (**figure 5.26c**), most of the energy was transfered to lower frequencies and mainly to the fifth harmonic of the spectrum or more precisely to the sixtieth sub-harmonic of the flow frequency (4.8 Hz). This peak was present in all signals and seemed to exert a "balance" in every change regarding the amplitude and the frequency of the higher harmonics.

In Test 7, **Figure 5.27**, we see a very different situation than in Test 6. Before we explain the difference it is worth mentioning that in all cases the decrease or increase of the pressure at a certain point was usually indicated by the shift of the distinct amplitude frequency components to lower and higher frequencies respectively. The presence of the conditioner in Test 7 shifted the energy upstream the orifice at a higher and narrower band of frequencies, with the decrease of the flow rate. In addition these frequencies appeared with a powered amplitude in contrast to the previous statement and to the respective case in Test 6. Furthermore, downstream the orifice the energy was distributed to a wide band of higher frequencies with decreased amplitude and with a sharp peak at 453Hz. The totally different behaviour could be possibly explained by looking at relative distances bend - conditioner - orifice and to the distance orifice - control valve after a partial closure. In Test 6, since the distance orifice - conditioner was just 5D, the created jets due to the conditioner possibly had not the time to expand downstream, leading to an accelarated flow upstream the orifice. This had the effect that the D tapping recorded a low pressure value resulting in an increased discharge

coefficient (see Table 7). In contrast, the created jets of the conditioner in Test 7 expanded leading to increased ampitude high frequency fluctuations upstream the orifice as well as to a higher pressure than in Test 6. From another point of view, the orifice installation at a further distance from the conditioner in Test 7 seemed to cause a relatively increased resistance to the flow. This fact could be supported as well from the results of K(1,0) and exponent n as they have been shown in the **Table 5.1b** of page 47.

Among all the Tests that were carried out there are particular reasons that drove us to distinguish the case of Test 8 and Test 4. In these cases, as it has been described in previous sections, the orifice showed a relatively satisfactory performance although this was judged from a different point of view. **Figure 5.28** shows the very interesting case of Test 8. Upstream the "Damper" (**figure 5.28a**) the energy is mainly shared by two band of frequencies with the distinct components at 107 Hz and 328Hz. We must also note the quite distinct component at 4.8Hz. Downstream the damper and upstream the orifice in **figure 5.28b,** (the distance damper orifice was just 2D) something similar with the case of Test 7 happened but the differences are worth mentioning. The energy was concentrated on a band of frequencies with main peak at 435Hz which seemed clearly to come from the **addition** of the previous peaks (107Hz+328Hz=435Hz). Morever the frequency of 435Hz is a superimposed frequency of 290Hz (290+290/2) and subsequently, after a few simple estimations, the frequencies at 107Hz and 328Hz are also linearly superimposed with the flow frequency. Noting also the component at 4.8Hz we saw only a slight (compared to other cases) decrease in its amplitude since the frequency of 435Hz appeared to have significant amplitude. Finally, downstream the orifice most of the energy had shifted at frequencies close to 145Hz which is a sub-harmonic of the flow frequency (290/2). Although there is a slight decrease in the amplitude of higher frequency peaks at the same time there is a slight increase of the amplitude at 4.8Hz. Another fact that must be emphasised, since it differentiates Test 8 and Test 4 from the other cases, is the relatively small variation of the amplitude of those

harmonic components where most of the energy was concentrated. Some typical results of Test 4 are shown in **Figures 5.32-5.34**. The total elimination of large amplitude variations in high frequencies is evident since all the energy is canalised in relatively low frequencies. Morever, upstream and downstream the orifice there is no signifigant variation of the amplitude especially of the lower distinct component at 4.8Hz. For the a complete view, it must also be reminded that in Test 8 the exponent n was found (estimating the K(2,1)) to be exactly 0.5

A very interesting situation was observed in Test 6 when the flow rate was 111.7 m^3/Hr (NRe= 3.41E+05) and as shown in **figure 5.12** and in the **Table 7** the value of Cd presented a sharp decrease. By looking at **figure 5.30a,** which shows the recorded signal at the D tapping, we could clearly distinguish an unsteady situation with the particular characteristic that the dc (or mean) value performed a very steep and **parallel** change, sweeping along as well the higher frequencies. This lasted only a few microseconds,. In other words we observed a sharp passage from one "steady" or better equilibrium condition, to another. In **Figure 5.31,** the two different states have been analysed separately and the effect of this "transition" on the amplitude spectrum could be seen in more detail. The increase of the energy level was achieved by a concentration of a band of high frequencies to a lower and narrower band (mainly to one distinct peak at 480Hz that is also a superimposed frequency of the pump frequency) and an increase of the amplitude of all harmonic components. It must be noticed and emphasised as well that the high frequencies in figure 5.30a examined in the time domain, very clearly seem to follow the lower frequencies. In other words they seem to be "locked in" with the lower frequencies, something quite important suggesting for further considerations and research.

The above cases produced the evidence based on which we may express some preliminary thoughts about a possible third and more important factor for the

improvement of the orifice meter performance. However, its complex nature and the strong association with the general subject, called "flow conditioning", require further research efforts for its accurate determination. Therefore, some preliminary efforts towards its description have been placed in the general discussion in the next Chapter.

6. DISCUSSION

In this chapter some general discussion will follow regarding the valuable pieces of information obtained during this project, since a lot of ideas have already been described in the presentation of the results. In today's metering conditions where accuracy and repeatability are critical, flow conditioning is essential. An acceptable flow conditioner is judged by its ability to fulfil the following requirements:

1. To ensure that the flow approaching a meter is equivalent to "ideal", that is swirl, asymmetry and pulsation free fully developed flow.
2. To achieve condition 1 in a relatively short distance from the source of the particular disturbance,
3. To succeed in all these with the lowest pressure loss and
4. To ensure a meter accuracy and repeatability for the wider possible flow range.

The selection of the proper flow conditioner from the extensive variety of them is not an easy task. On the other hand, until now, none of the existing conditioners could be characterised as a "panacea" for all flow conditions. In terms of differential pressure meters, although their accuracy is well known and accepted, their high sensitivity under distorted flow also exists.

Examining in detail the particular conditions present in this project we could say that we had to confront an asymmetric flow upstream the orifice due to the presence of the single bend, possibly followed by swirl, and pulsatile as well due to the operation of the pump. All the unwanted flow conditions were present more or less. However, it could be said that all these conditions have had a specific common factor or better yet they were the different views of the same question, that is the distribution of momentum. To the author's point of view the subject of flow conditioning has to be included in the

general and very big issue of **turbulence control**. This statement will be explained after we make some other considerations.

First of all the results obtained in this project are in accordance with the suggetions of **Irving, (1977)** and **Avery & Moore (1983)** regarding the values of discharge coefficient for bends given in **ISO 5167** that seem to *overestimate* the mass flow rate. In addition, the author would like to point out the fact that the proposed lengths of staight pipe downstream of the orifice meter have to be reconsidered with increased care as well since they seem to play a signifigant role in the performance of the orifice meter.

It should also be noted that we were in agreement with the results of **Blake K.A. et al (1976)** as those were presented by **Reader-Harris, M.J., Hutton, S.P., and Laws, E.M. (1989)** and are shown in **Table 11.** These show that the change in the orifice plate discharge coefficient was found to depend on the separation between the perforated plate and the orifice but we are unable for the time being to make any statement with certainty about the effect of distance between the bend and perforated plate.

In addition, as **Humprheys, J.S and Hobbs, J.M, (1986)** have shown and our results in Test 1 have revealed, inclusion of a Mitsubishi conditioner in relatively good flow conditions leads to a positive shift in the discharge coefficient. We should add here that this positive shift of Cd could be the result of the following:

1. The first cause could be the angular momentum associated with the presence of swirl that is conserved downstream the orifice throat leading to a smaller contraction of the flow at the vena contracta. The result is a positive Cd error mostly in small area ratio orifice plates. This is the second mechanism of swirl effects as described by **Avery and Moore, (1983)** and is presented in section 3.3.1.

2. The second cause could be simply a sharper (high core type) flow profile as it has been described by **Ghazi, (1962).**

Examining the cases of Tests 6 and 9 in conjuction with the **table 1** the high positive Cd values that were obtained in Test 9 were mainly the result of the first cause since the pressures upstream and downstream the orifice were both relatively increased. On the other hand the resulted high Cd values of Test 6 were possibly the product of both previous mechanisms.

It is necessary at this stage to present some additional information that was obtained at the latest stages of this project and is included in the Appendices. **Appendix B** shows the results of the repeated mesurements of Tests 6 and 9 under somewhat different conditions as it has already been described. The discontinuity in the curve of Cd for a specific flow rate as shown in **figure B1** is very clear. A more interesting case is presented in **figures C1** and **C2** of **Appendix C**. These plots reveal something that was not so clear by first observation of the plots of Cd with Reynolds number.

After a carefull observation of the Cd plots with Reynolds number we could distinguish a change at around 3.4E+05 Reynolds at almost all plots. This became clearer in the last four Tests and mainly in Test 6, where the Cd presents a sharp decrease close to this Reynolds number. The same case clearly appeared at a lower Reynolds number in Test 6B without excluding a possible discontinuity as well at 3.4E+05 Reynolds or the fact that a kind of multiple transitions at different states could have taken place. The interesting case of figure 5.30 observed at the same Reynolds number is also worth mentioning. This subject also suggests further research.

Pulsations of any magnitude seem to play a significant role in the performance of the orifice plate. Their evolution and particular characteristics could define the mean

value of the wall static pressure. As it is well known the threshold between steady and pulsating flow can be defined in terms of the pulsation amplitude as: $\Delta prms / \Delta \overline{p}_p \leq 0.10$. For the measurements recorded in this project the previous quotient was varied for different positions, different flow rates and different layouts with minimum and maximum values of 0.08 and 0.65 respectively. Pulsations can affect the performance of the flow meter in two ways: Firstly, they can change the relationship between flow rate and the differential pressure generated. Secondly, they can cause the secondary element (pressure transducer) to indicate a false differential pressure, **Mottram and Sproston, 1989**. However for the calculations that were carried out in this project these effects were neglected:

1. By using fast response pressure transducers with a frequency limit up to 3KHz although a higher frequency response would have been more desirable.

2. By obtaining several long time records of the pressures measured upstream and downstream the orifice and using the averaging technique presented in section 4.2.5.

In **Foxboro's** recommendations (see chapter one), it is emphasised that *whereas the pressure component of the pulsation may be reduced, the velocity component might be increased* and it is the velocity component that affects metering performance. However, in a differential pressure flowmeter the author would emphasise more the effects of the pressure components since it is they that carry and decode the velocity information. These two different aspects suggest a new approach in terms of flow conditioning in differential pressure flow meters.

The idea is quite simple. The use of a flow conditioner upstream of a differential pressure meter, as it is well known, aims to improve a distorted flow or particularly to bring the flow in a form as close as possible to that of a fully developed flow, so that the

created differential pressure across the meter approaches a theoretical differential pressure specified by Bernoulis' equation. So the question was, whether by knowing the specific flow conditions indroduced by a single bend and the operation of the pump, we could improve the performance of the orifice plate by controling the wall static pressure, especially using the information obtained from the amplitude spectrum. To the authors point of view this could be possible and should be less expensive as far as the cost is concerned. This idea originated after some strong evidence, incuding the ideas described in section 3.3.2, that there must be a certain relationship between the mean values of wall static pressure and axial velocity. Thus, by controling the static pressure we could possibly affect the flow development as well. This idea applies to the general subject of turbulence control which led to the tested preliminary design of the "damper".

The experience gained during this project revealed the fact that there are at least two different mechanisms in order to succeed in the better performance of the orifice plate under the reference conditions:

1. Prevent the growth and the evolution of those distinct high frequency fluctuations, which are possibly marks of a kind of transition as it will be shown later, with a mechanism that reduces the asymetrically accelerated flow due to the bend and eliminates the powered fluctuations at their birth, possibly at the bend itself. This approach could explain the case of Test 4 and to the author's point of view the elimination of the peaks was mainly a result of the spesific distance of the orifice from the bend.

2. Remove these fluctuations with a "damper" positioned downstream of the bend and simultaneously support the accelerated flow due to the bend but with a more symmetrical distribution of momentum. This symmetrical distribution could be possibly indicated either by the total elimination of those peaks or by the appearance and

evolution of *significant* and *particular* harmonic components as shown in Test 8. The performance of the orifice in Test 8, considering the fact that the distance orifice - bend was the smallest, could be characterised as satisfactory since the Cd for the medium and higher Reynolds numbers was around -2% from its theoretical values.

Finally, **Foxboro** recommended that if the addition of extra capacitance is not possible, then the remaining solution is the use of Sprenkle or Zanker flow conditioners together with installation of a throttling valve downstream of the flowmeter at a distance according to the standards. However, these kind of conditioners produce a significant non-recoverable pressure loss and this probably could be their weak point. Particularly, the fact that a flow conditioner is a component installed inside the flow, as the rest, it could be possibly a source of distortion although it is used for its ability to improve a distorted velocity profile.

It is regarded more than necessary to consider carefully the new proposals in terms of flow conditioning coming from **Fluid Components, Inc**. and **Vortab Co**. (see chapter one). Their claim that these inserted sleeves could eliminate undesired flow conditions such as swirl and flow asymmetry sounds quite strange. However, to the author's point of view their effort is in the right direction since, as it was said before the subject of flow conditioning is included in the general subject of turbulence control together with other aspects such as mixing and separation control. Thus, all efforts to explain and find out possible solutions to all these problems have to be focused on the birth of turbulence itself, that is the wall. The idea of the use of the damper, virtually was aimed at changing the characteristics of a previously used pipe wall upstream the orifice with a "smoother" pipe component that could damp some unwanted fluctuations as well.

The discussion will be completed with some very interesting theoretical aspects of secondary instability as described by **Sherman S.F., (1990)** and could have a strong

relation to the results obtained in this project. First of all, Sherman mentioned that in a statistically stationary turbulent flow, only the amplitude spectrum converges to something usefull as we repeat the sampling process. Morever, individual records that look entirely different may have the same amplitude spectrum and so the phase data are needed to distinguish between them. Sherman's conclusions were more than obvious in our measurements and were strongly supported by the fascinating repeatability of every set of spectrum obtained under the same conditions at a specific point.

Furthermore, he mentioned that a typical energy spectrum from a turbulent pipeflow or boundary layer exhibits a **gradual variation without sharp peaks**. This could be easily seen in the case of Test 4, **Figure 5.33**. He added as well, that if peaks are present they can usually be traced to some measurable periodicity in the nominal constraints, **such as pump discharge pulsations at a blade passing frequency**. This was another fact that was apparent in most of the spectra obtained in our measurements when the control valve was fully open.

Sherman also mentioned that when turbulence evolves from a steady laminar flow, meaning at the boundary layer, the shape of the spectrum of **velocity** fluctuations changes in a distinctive way as the point of observation is taken further downstream or a similar evolution is observed at a fixed point if the flow rate is very slowly increased with time. In other words the appearance and evolution of those fluctuations is strongly connected with the aspect of transition. For comparison purposes it was regarded nessecary to present in **Figure 5.35** the evolution of this velocity fluctuations as they were shown by Sherman. We could easily note the similarities with **Figures 5.21 and 5.24**. We could also mention several other events, such as **turbulent spots,** and their possible connection with high-frequency motions near the wall, as well as many other interesting aspects of the theory of secondary instability.

The author would like to place additional emphasis on one extra point in order to complete this discussion. As it has been mentioned by Sherman and many other researchers as well, the first observable fluctuations connected with the primary disturbances of the instability theory (in our case the primary disturbances are around the pump flow frequency, at 290Hz) usually occupy a relatively narrow band of frequencies. Harmonics of this narrow band may next appear as the primary disturbances amplify and lose their sinusoidal waveforms. The perturbed flow may next become unstable to a different class of disturbances, possibly leading to subharmonics of the original frequency or to frequencies that are neither integral multiples nor fractions of the original.

Indications that the growing secondary disturbances are **phased-locked** with the primary disturbance and the two disturbances move downstream with the same phase speed have also been analysed by Sherman as well. Because of the coupling of the ordinary differential equations, all the Fourier components of the secondary disturbances move with the same speed and have the same rate of amplification or decay. The close relation of the above considerations by Sherman to the results obtained in this project and the fascinating similarity of near wall pressure and axial velocity fluctuations indicated by other researchers as well may be easily appreciated. However, the subject is quite extensive and further research is nessecary.

Although the theory of secondary instabilities has succeed in explaining to some extent many aspects of fluids flow, the author would like to add that evidences such as

the frequent appearance of linearly superimposed solutions imply possibly a full linear theory rather for the non-linear interactions of the secondary instabilities.

7. CONCLUSIONS - PROPOSALS FOR FUTURE WORK

The work presented in this thesis has shown the muptiple and valuable information that can be obtained from an orifice - conditioner package using three resonant type pressure transducers. In summary we have the following:

1. Obtaining the relationship of the differential pressure across the flow conditioner and the orifice with the flow rate we can secure the flow rate information in case of failure of one of the three pressure transducers. On the other hand we have a continious check of the flow rate measured by the orifice meter.

2. Using the K factor and the exponent n as indicators of the total and spatial resistances of the orifice - conditioner package it is possible to obtain additional information for their proper performance. Additional details concerning the nature and the magnitude of separation losses which play such an important role in this region, could be revealed. The author would like to emphasize the importance of a more detailed research regarding the nature of the K factor whose units as a combination of mass, space and time should not be underestimated.

3. The discharge coefficient was clearly affected by the distance between orifice - conditioner and orifice-bend. Nevertheless, nothing certain could be said about the distance between conditioner-bend.

4. Inclusion of a Mitsubishi conditioner in good flow conditions led to a positive shift in the discharge Coefficient.

5. The main factor that affects the performance of the orifice meter downstream of a single 90^0 bend and possibly downstream of any other type of disturbance, is its distance from the disturbance, a known fact. The important thing is to comprehend the specific mechanisms that change the meter's performance. In our case, we could say that since the orifice plate introduced the higher resistance (or pressure loss) inside the flow measurement system, every shift in its position affected the flow pattern at the exit from the bend and subsequently its further evolution, resulting in affecting the performance of the orifice itself. If we examine the same thing as a package orifice - conditioner the things are different since the closer those two are the more the resistance of the package is reduced.

6. The use of two static pressure transducers upstream and downstream the orifice, instead of one differential pressure type, should offer many more details regarding its performance and simultaneously could be used to monitor the condition of the associated process plant. The amplitude spectrum estimation method seem to offer invaluable capabilities in terms of an effective monitoring, combined always with enhanced sensors of resonant type, since the sensitivity of Fourier components to any change in the status of the process plant is instantaneous. Still remains the problem of distinguishing the particular cause and the position of this change inside a flow system.

However, in the simple scheme that has been used in this project we could say that although any change in the process plant affects the static pressures upstream and downstream the orifice plate almost simultaneously there will be a clear quantitative difference in the amplitude spectra downstream and upstream of the orifice that could suggest for the direction and possibly the exact point of this change. It was evident in our results that the amplitude spectra coming from the downstream obtained signals were more sensitive to downstream changes. This subject suggests for further research. Additionally, we could easily distinguish the case of failure due to one of the two

pressure transducers (compared with the use of a differential type pressure transducer where the origin of abnormal records may not be so clear) in conjuction with the use of the third transducer upstream the conditioner thus making the failure to be more clear.

Finally, the author would like to point out that the wall static pressure in a pipe is a variable that could offer, using enhanced methods such the amplitude spectrum estimation, much more information than we probably know today. We must always bear in mind the fact that the wall in a pipe is the crucial region of turbulence production and subsequently of further flow development. Thus, when we concern ourselfs with aspects such as flow conditioning or improvement of the velocity profile the best solutions to these problems could possibly start by a thorough and extensive research in the near-wall region. The proposals of *Fluid Components, Inc* and *Vortab Co.* and their designed flow conditioner with the inserted sleeves in the wall sounds very promising.

The last conclusions suggest for a possible relationship between the instantaneous values of wall static pressure and axial velocity in a pipe. Although this relationship is not yet known, it may be revealed by further research taking into account the initial and final (boundary) conditions of the flow system.

REFERENCES

1.- **Amadi-Echendu J.E.,(5-9 Sep. 1988)** - *Condition monitoring of process plant and associated equipment - analytical approach* - 2nd International Symposium on fluid control measurement mechanics and flow visualisation (FLUCOME), Sheffield.

2.- **Amadi-Echendu J.E, Hurren P.J.,(1990)** - *Identification of process plant signatures using flow measurement signals* - IEEE Transactions on Instrumentation and Control, Vol 39, No2.

3.- **ASME.,(1971)** - Fluid Meters-Their theory and Application.- Sixth edition, Part II, Chapter II-II.- *General requirements for fluid metering :Installation./* Edited by Howard S., New York.

4.- **Avery P., Moore A.E.,(Dec. 1983)** - *Orifice plate errors due to upstream disturbances from bend arrangements* - BHRA.

5.- **Baker R.C.,(1989)** - *An introductory guide to flow measurement/* London: Mechanical Engineering - 148p.

6.- **Blake K.A.,(April 1973)** - *Development of velocity profiles downstream of swept and simple mitre bends* - NEL Flow Measurement Memo 107.

7.- **Blake K.A., Kennedy A., Kinghorn, F.C., (1976)** - *The use of orifice plates and Venturi nozzles in swirling or asymmetric flow.* - Proc. 7th IMEKO Congress pp 279-292, Institute of Measurement and Control, London.

8.- **Battye J.S.,(1985)** - *Shell flowmeter engineering handbook* - Edited by G.W.A. Danen (Royal Dutch/ Shell Group)-2nd edition.

9.- **De Gray B.G.,(1992)** - *Low speed Wind Tunnel Tests on Perforated Square flat plates normal to the airstream: Drag and Velocity fluctuation measurements* - ARC - SR/5635.

10.- **Fell R., Ajayi A.A., Tsiknakis E.,(Feb. 1987)** - *Signal processing for flow measurement* - Trends in instrumentation -Proccedings of a meeting of the Instrument Science and Technology Group - IOP Short meetings, No5.

11.- **Gebhart Pardue S.J., Munukutla S.S.,(6-9, Jan.1992)** - *Experimental studies on turbulence behind screens and perforated plates* - 30th Aerospace Sciences Meeting & Exhibit, AIAA 92-0556.

12.- **Ghazi H.,(1962)** - *Effects of upstream flow non - uniformities on orifice meter* - PhD Thesis - Ohio State University, Ann Arbor Michigan: University microfilms, 1974.

13.- **Haritonidis J.H., Gresko L.S., Breuer K.S., (1988)** - *Wall Pressure peaks and waves* - Dept. of Aeronautics and Astronautics, M.I.T - 1988 Zoran Zaric Memorial Conference, pp. 397 - 417.

14.- **Higham E.H., Fell R., Ajaya A.,(June 1986)** - *Signal analysis and inteligent flow meters* - Measurement and control special issue,pp 47-50.

15.- **Humprheys, J.S., Hobbs, J.M., (1986)** - *An investigation of the effectiveness of flow conditioners* - Proceedings of the International symposium on Fluid Flow Measurement, Paper 16.2, American Gas Association, Washington, D.C.

16.- **Hurren P.J., Amadi-Echendu J.E., Higham E.H.,(11-13 May 1988)** - *Condition monitoring using a resonant wire differential pressure sensor* - 2nd International Conf. on flow measurement, London, Publ. BHRA, pp 199-206.

17.- **Irving S.J.,(June 1976)** - *Effect of system layout on the discharge coefficient of orifice plates* - Part 1, Literature review - BHRA.

18.- **Irving S.J.,(Aug. 1977)** - *Effect of system layout on the discharge coefficients of orifice plates.*-Part II, Experimental investigation into the effect of isolated fittings - BHRA.

19.- **ISO 5167-1:1991/BS 1042: Section 1.1: (1992)** - *Measurement of fluid flow in closed conduits.-Specification for square-edged orifice plates, nozzles and Venturi tubes inserted in circular cross-section conduits running full.*

20.- **Laws E.M.,(16-18 July 1990)** - *Optimal flow conditioner design* - 26th Joint Propulsion Conference, AIAA 90-2385.

21.- **Miller R.W.,(1983)** - *Flow measurement Engineering Handbook* - McGraw Hill.

22.- **Mottram R.C., Sproston J.L., (Sept. 1989)** - *The effect of pulsation on the performance of flowmeters.* - FLOMIC Report No. 8.

23.- **Reader - Harris M.J., Hutton S.P., Laws E.M.,(Sept. 1989)** - *Flow straighteners and flow conditioning devices* - FLOMIC Report No. 7.

24.- **Sanderson M.L., Laws E.M., Sweetland D.,(July 1991)** - *A preliminary evaluation of the comparative performance of flow conditioners* - FLOMIC Report No1, Cat. 2A.

25.- **Shaw, R.(1960)** - *The influence of hole dimensions on static pressure measurements* - Journal of Fluid Mechanics, Vol. No 7.

26.- **Sherman F.S., (1990)** - *Viscous flow* - University of California at Berkeley, McGraw-Hill.

27.- **Spitzer D.W.,(1991)** - *Flow measurement - Practical guides for measurement and control* - ISA.

28.- **Stokes G.M., Davis D.D., Sellers T.B.,(1993)** - *An experimental study of porosity characteristics of perforated materials in normal and parallel flow* - NACA - Technical Note 3085.

29.- **Tinham B.S.,(Feb. 1988)** - *Is Flow technology still in its infancy?*- Control and Instrumentation Journal, pages 22-45.

30.- **Turner J.T., Wynne R.J., Tong F.,(Apr. 1993)** - *Experimental study of intelligent flow meters* - FLOMIC Report Cat.2A, No5.

31.- **Walpole R.E., Myers R.H. (1993)** - *Probability and statistics for Engineers and Scientists*, Fifth Edition, MacMillan.

32.- **Zhu H., Higham E.H., Amadi-Echendu J.E.,(1992)** - *The application of signal analysis methods in orifice plate differential pressure flow measurements.*

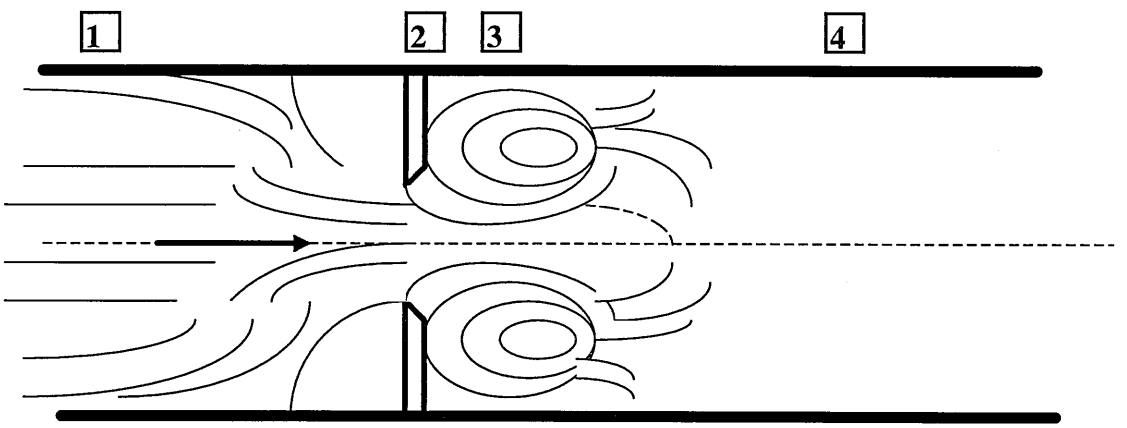

1 Upstream conditions

2 Plane of orifice

3 Vena contracta

4 Recovery plane

Figure 3.1 Turbulent flow through an Orifice plate.

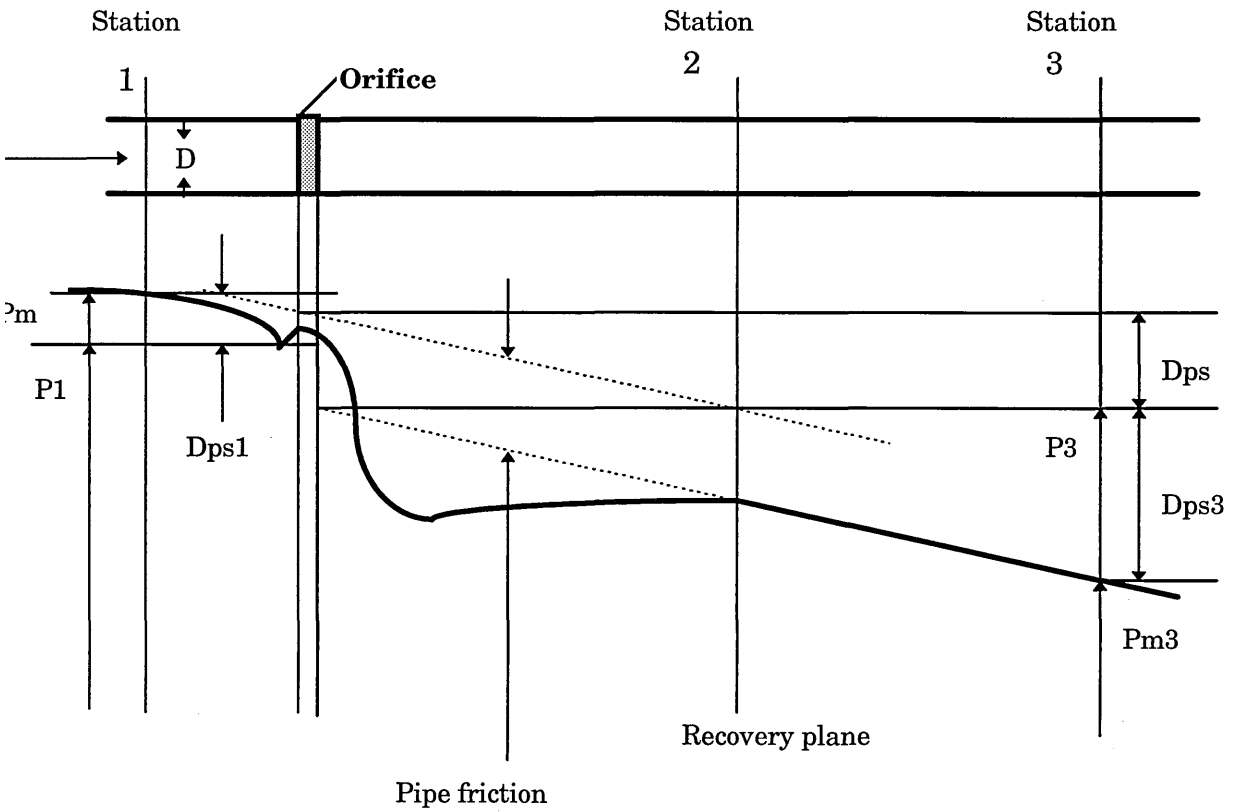

Pm1, pm2: Static pressures at stations 1,2
P1, P3: Static pressures corrected for pipe friction losses
Dps1, Dps2: Friction losses in the straight pipe upstream and downstream of the orifice.

Figure 3.2 Pressure distribution in an orifice plate

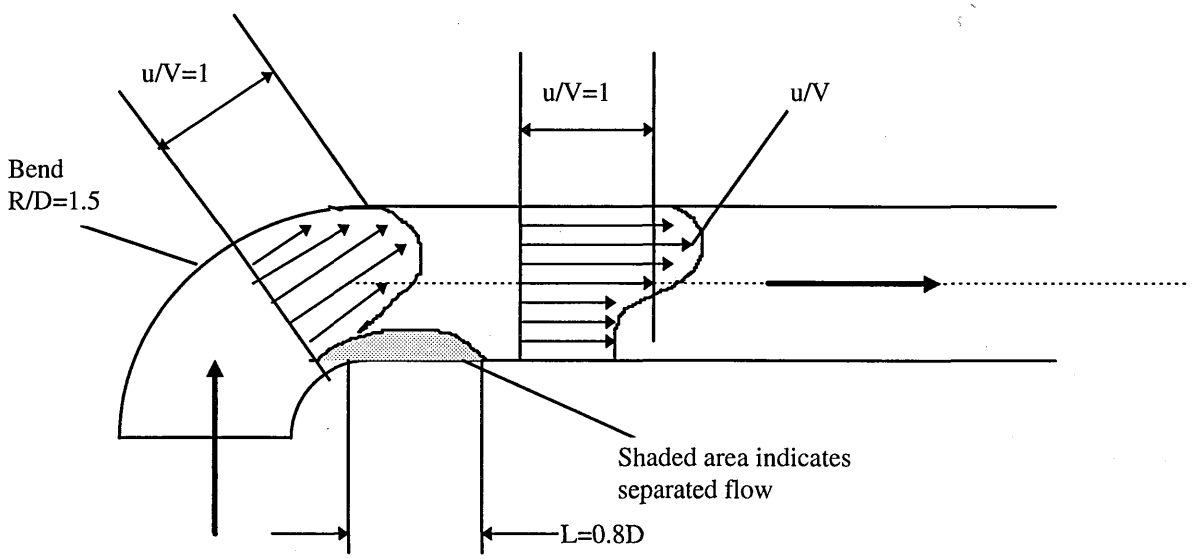

Recovery of the normal axisymmetric velocity profile requires about 50D of straight pipe length.

Figure 3.3 Flow through a 90^0 bend.

FRONT VIEW OF THE RIG

(All the valves are gate)

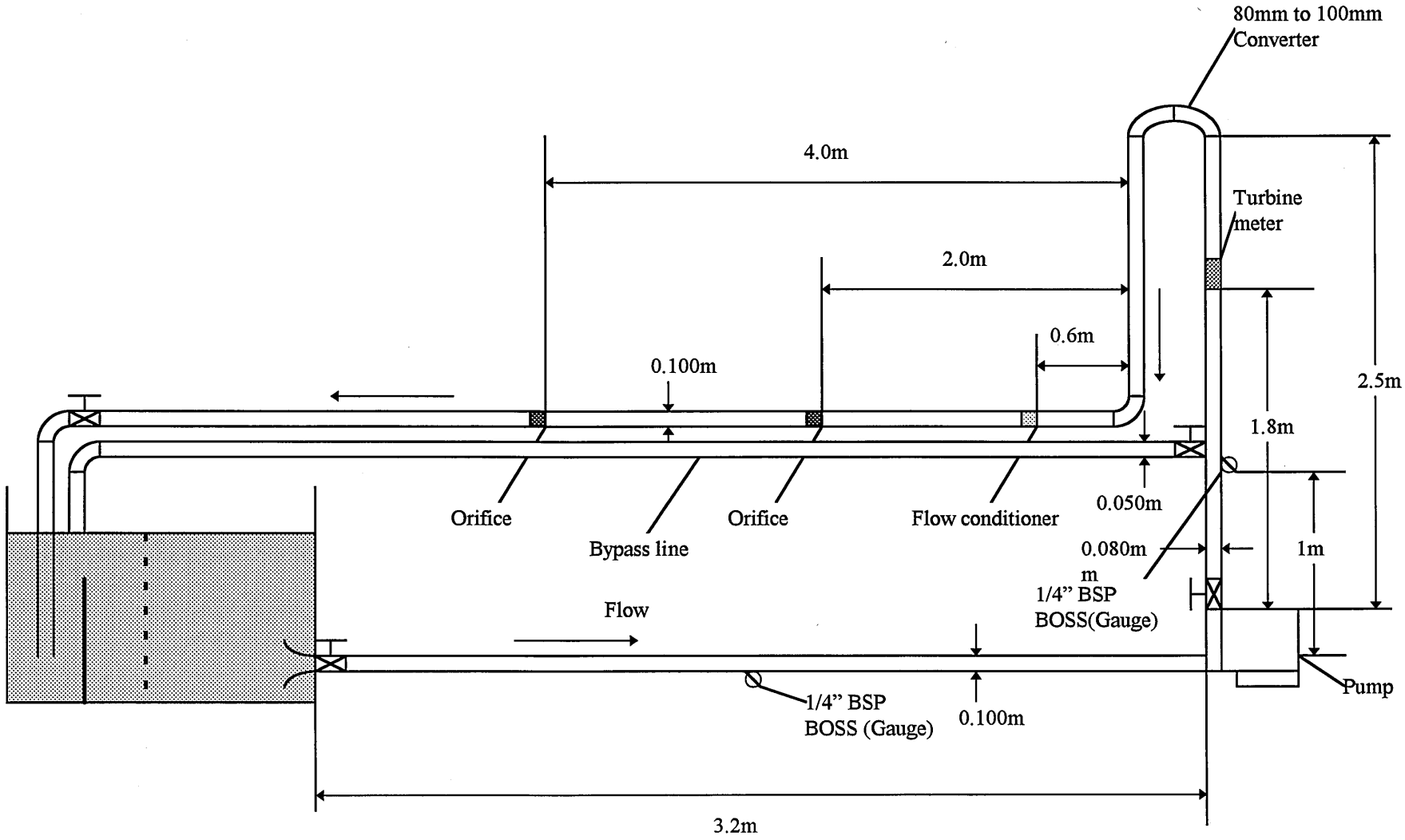

Figure 4.1 The experimantal flow loop.

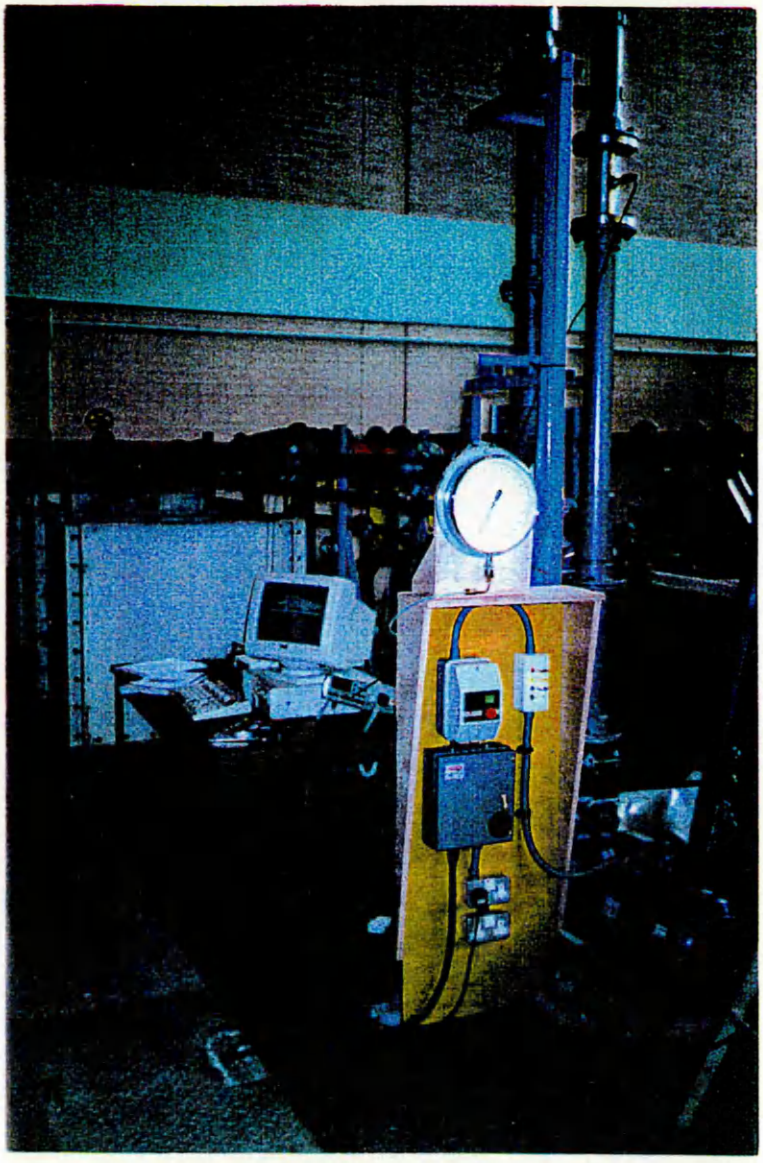

Figure 4.2 Overall view of the flow loop and the electronics.

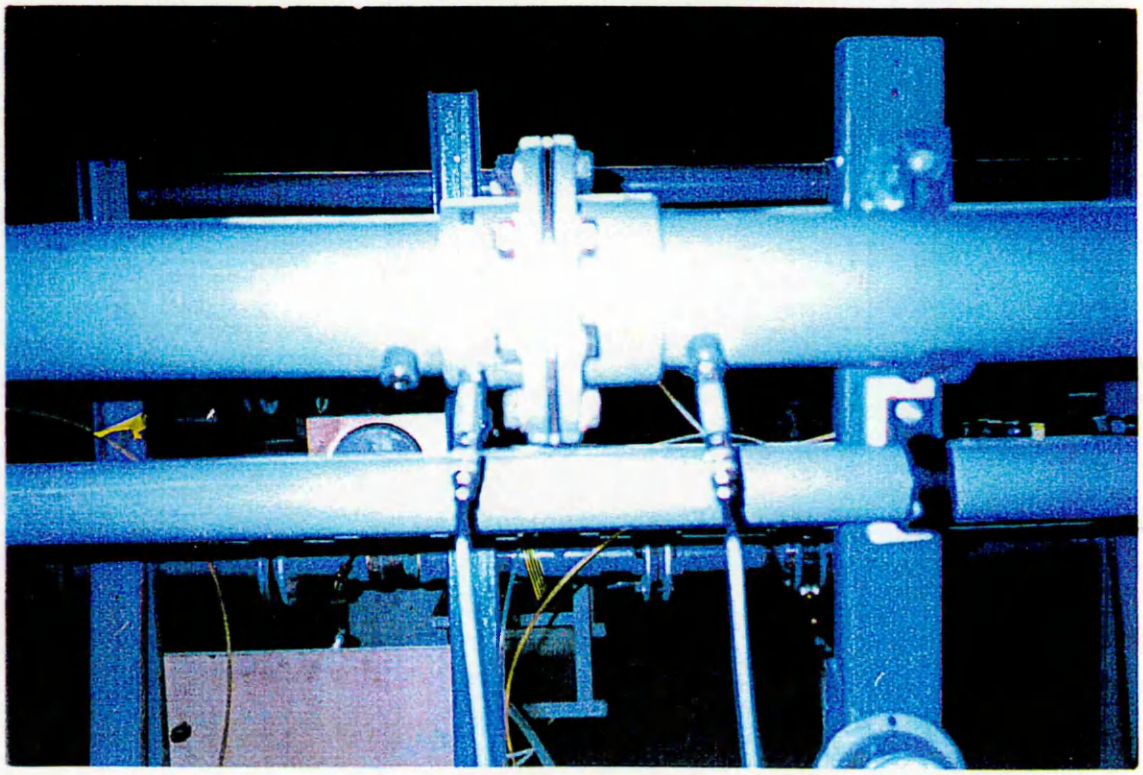

Figure 4.3 The orifice plate.

Weight (lbs)	Counts	Time (sec)	Flow rate (m^3/Hr)	Frequency (Hz)	Factor (pulse/m^3)
1092	3194	158.31	11.29	20.17	6432.93
1092	3237	108.5	16.473	29.83	6519.53
1092	3219	105.76	16.9	30.43	6483.28
1092	3193	78.41	22.795	40.72	6430.91
1092	3185	64.08	27.893	49.7	6414.8
1092	3177	44.38	40.275	71.58	6398.69
2184.1	6357	70.45	50.743	90.23	6401.71
2184.1	6346	52.91	67.564	119.93	6390.63
2184.1	6335	42.49	84.134	149.09	6379.55
2184.1	6335	37.55	95.202	168.7	6379.55
2184.1	6338	33.71	106.047	188.01	6382.57
2184.1	6331	29.03	123.143	218.08	6375.53
2184.1	6350	25.67	130.262	247.37	6394.66
2184.1	6327	23.71	150.774	266.84	6371.5
2184.1	6336	21.26	168.149	298.02	6380.56
2184.1	6332	19.97	179.011	317.07	6376.53

Calibration conditions:

Fluid:Water Pressure:60 psig Temperature:16.3 C^0
S.G:0.9982 Viscosity:1 cst Pickup time:Magnetic

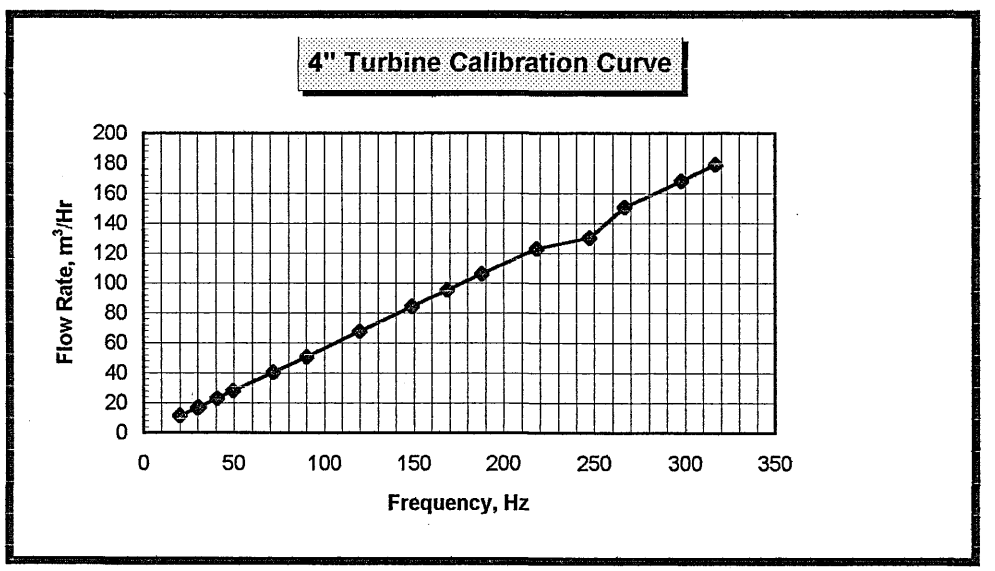

Figure 4.4 Calibration data and curve of the 4" Turbine meter.

4" Turbine (Hz)	3" Turbine (Hz)
57	166
73	212
100	291
116	337
130	378
156	453
180	523
212	616
237	689
250	726
262	761
280	814

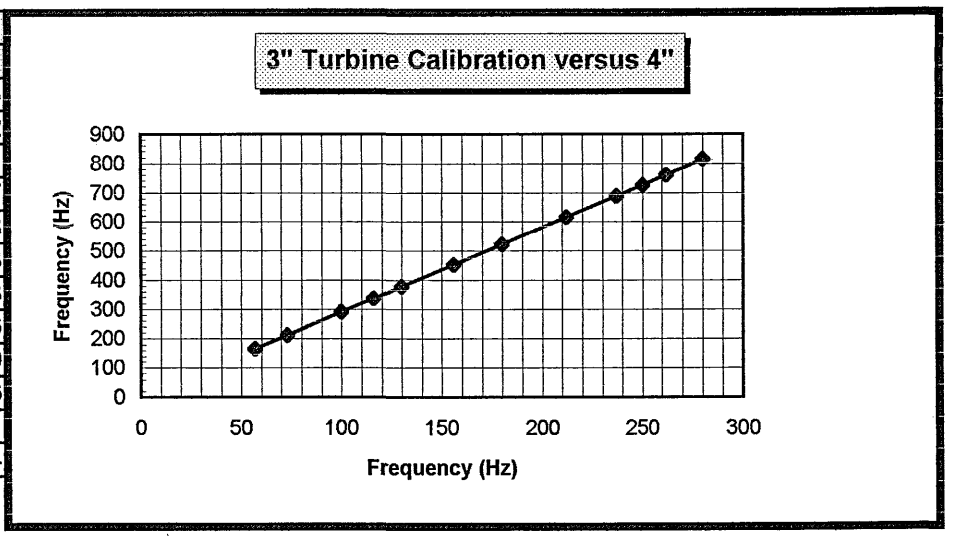

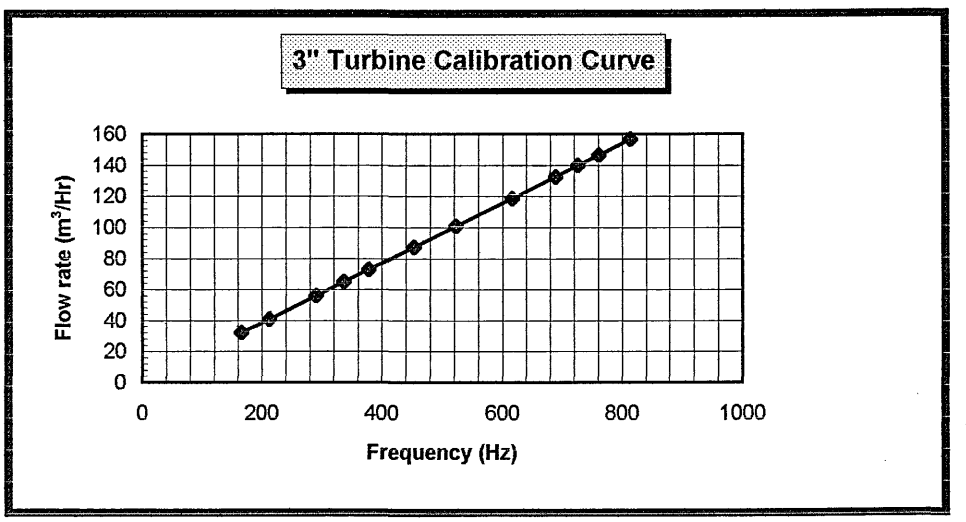

Figure 4.5 Calibration data and curves of the 3" Turbine meter.

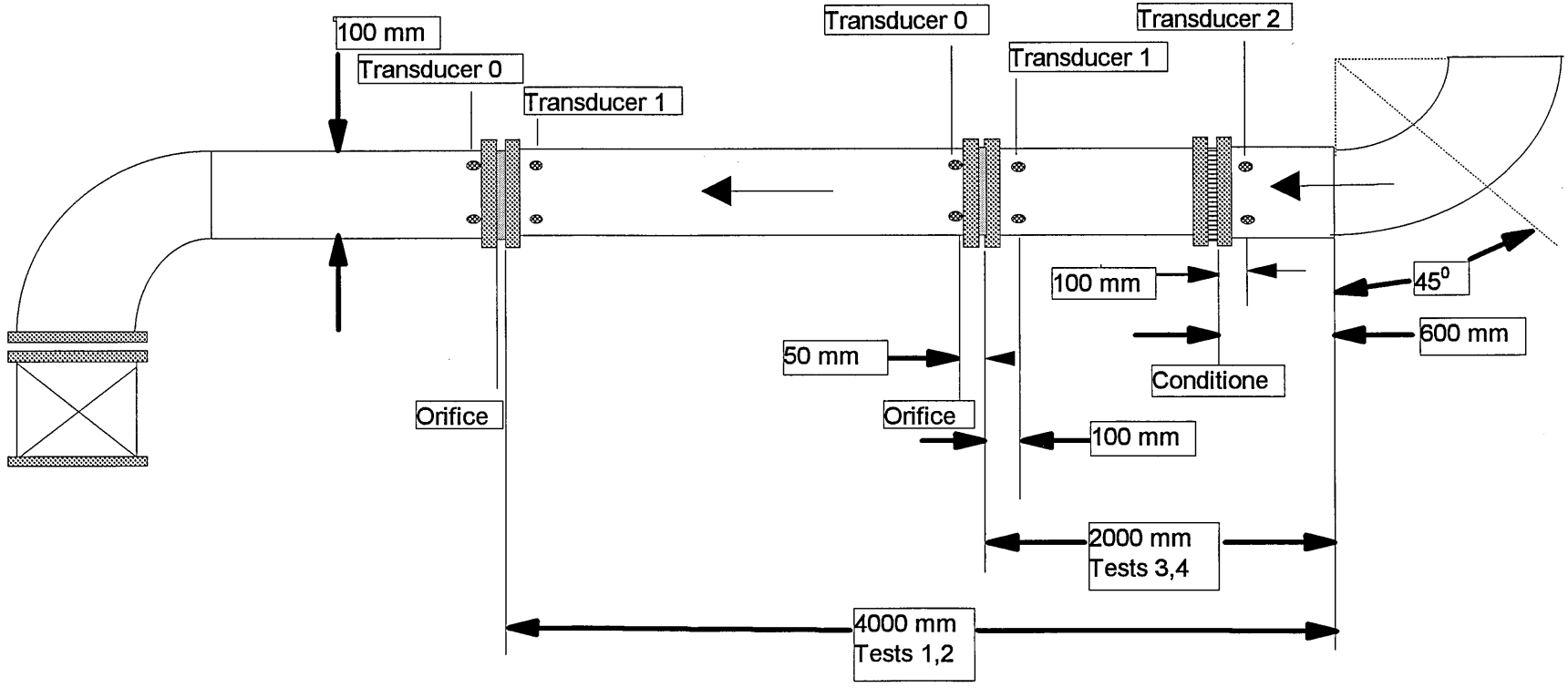

Figure 4.6 The Test Section

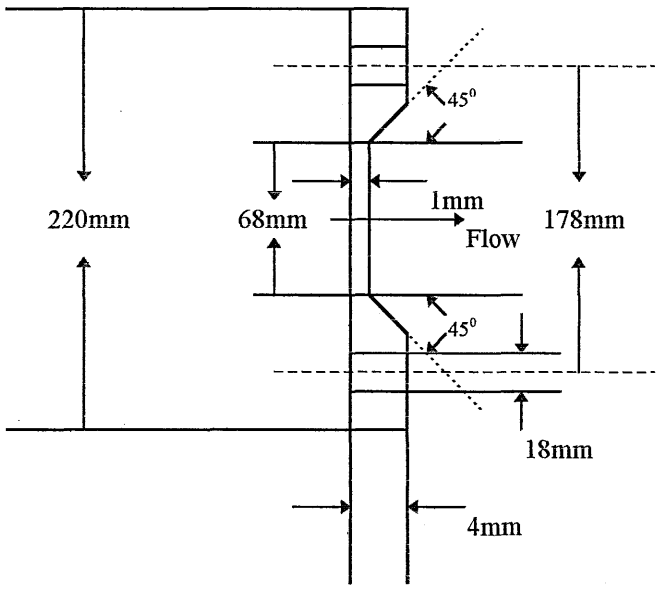

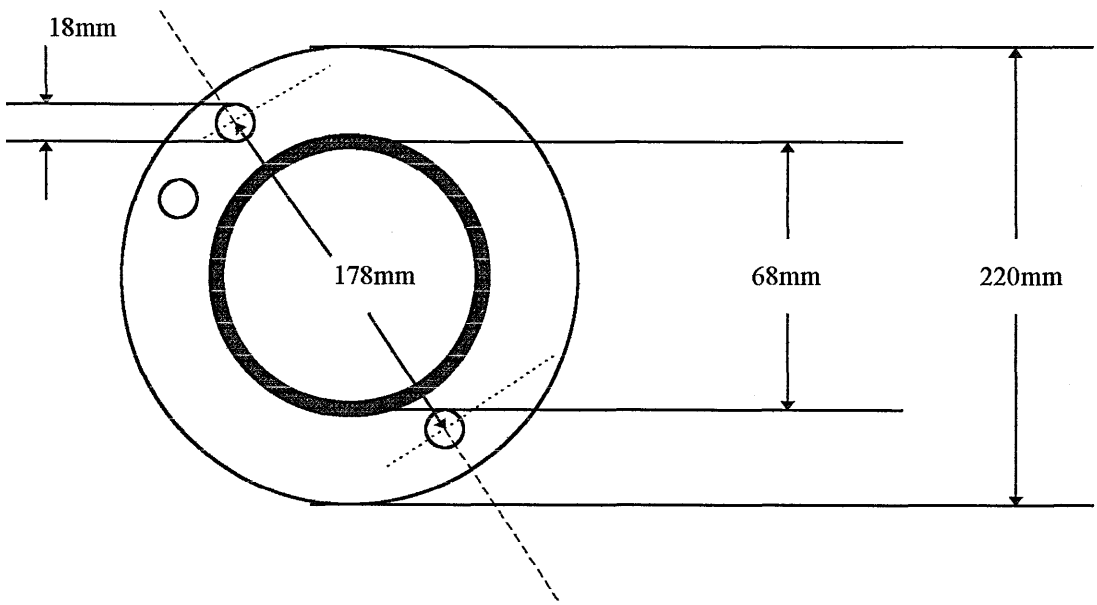

Figure 4.7 The orifice plate.

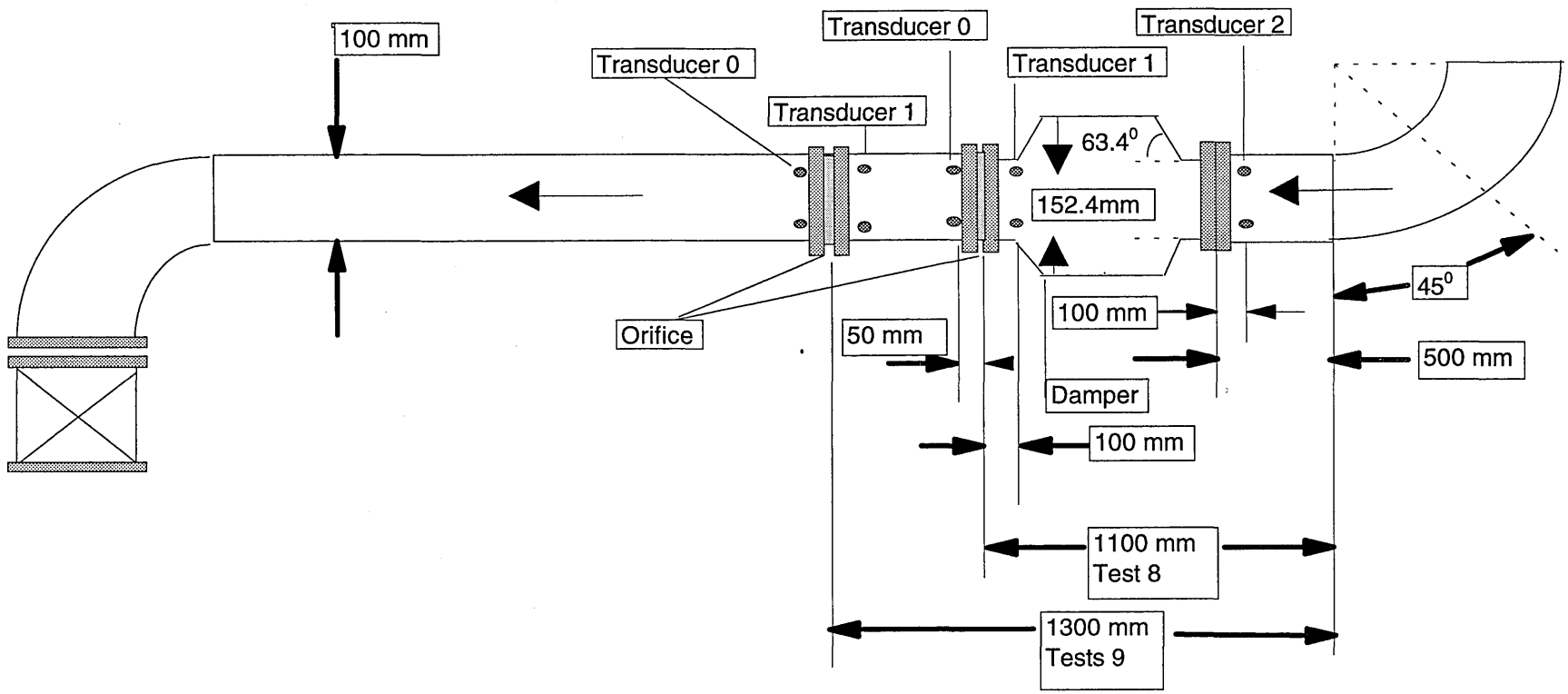

Figure 4.8 The Test Section with the "Damper"

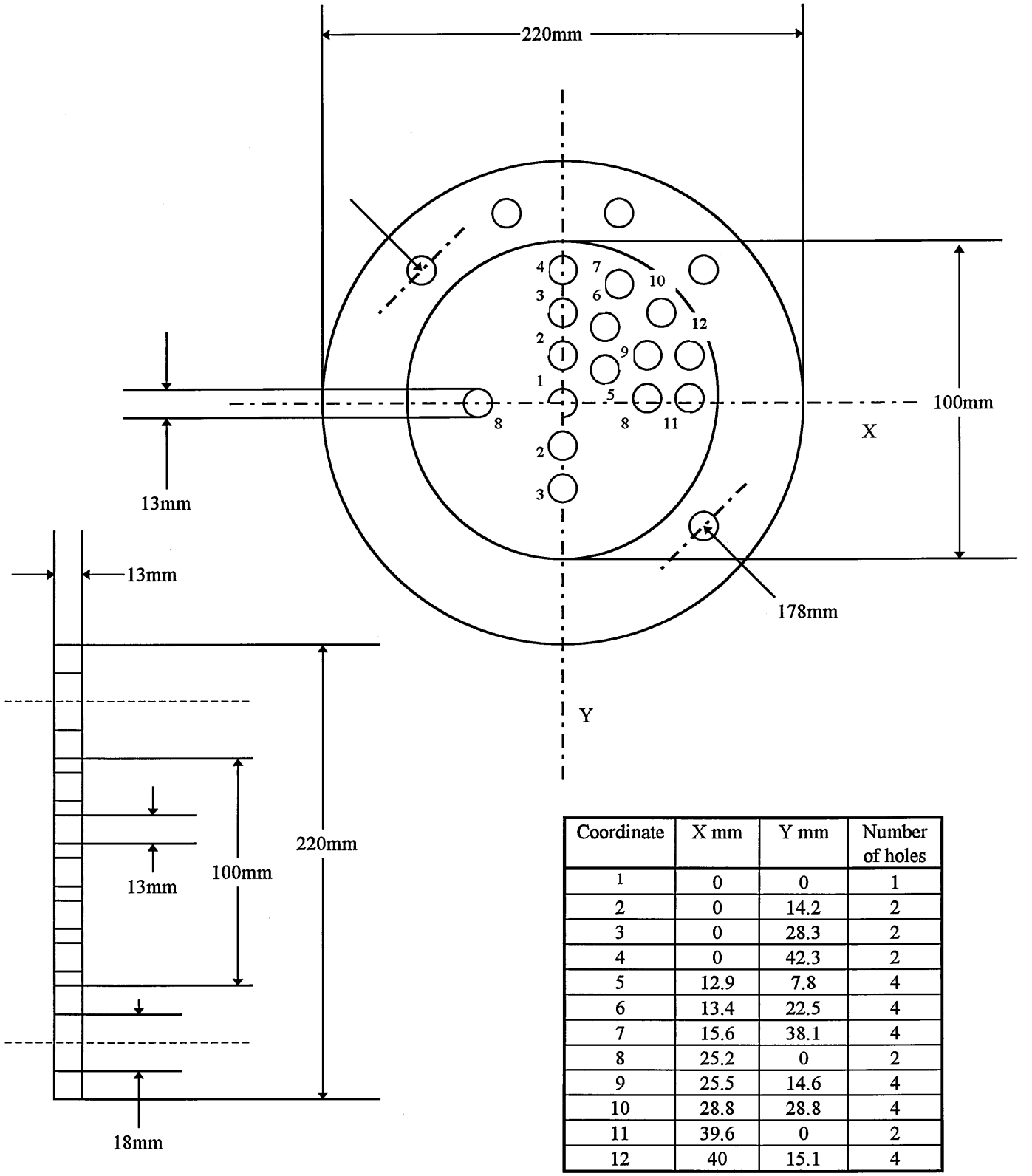

Coordinate	X mm	Y mm	Number of holes
1	0	0	1
2	0	14.2	2
3	0	28.3	2
4	0	42.3	2
5	12.9	7.8	4
6	13.4	22.5	4
7	15.6	38.1	4
8	25.2	0	2
9	25.5	14.6	4
10	28.8	28.8	4
11	39.6	0	2
12	40	15.1	4

Figutre 4.9 The Mitsubishi flow conditioner.

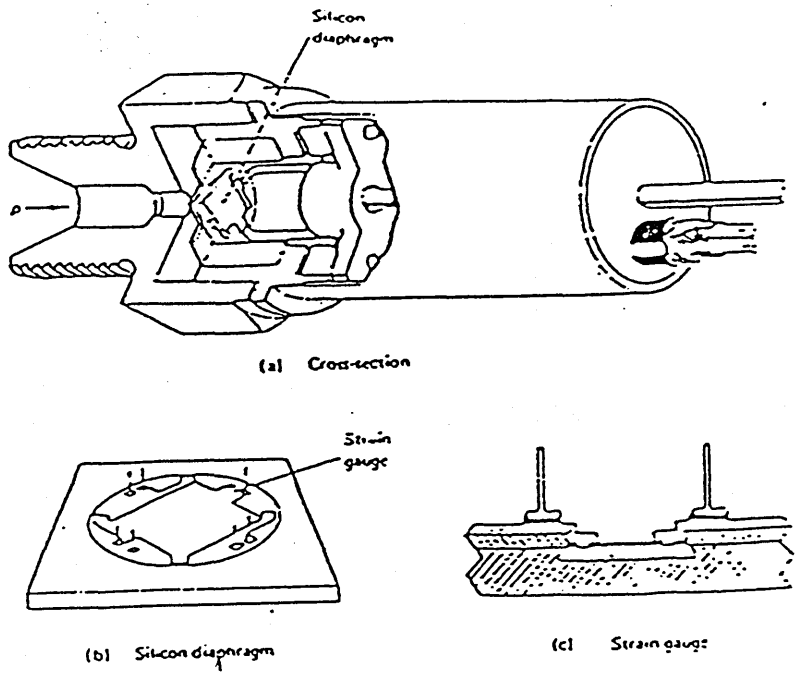

Figure 4.10 Silicon strain gauge pressure transducer

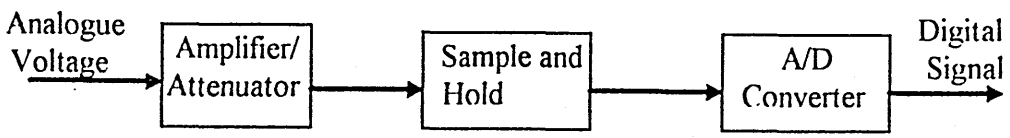

Figure 4.11 The Data Acquisition System

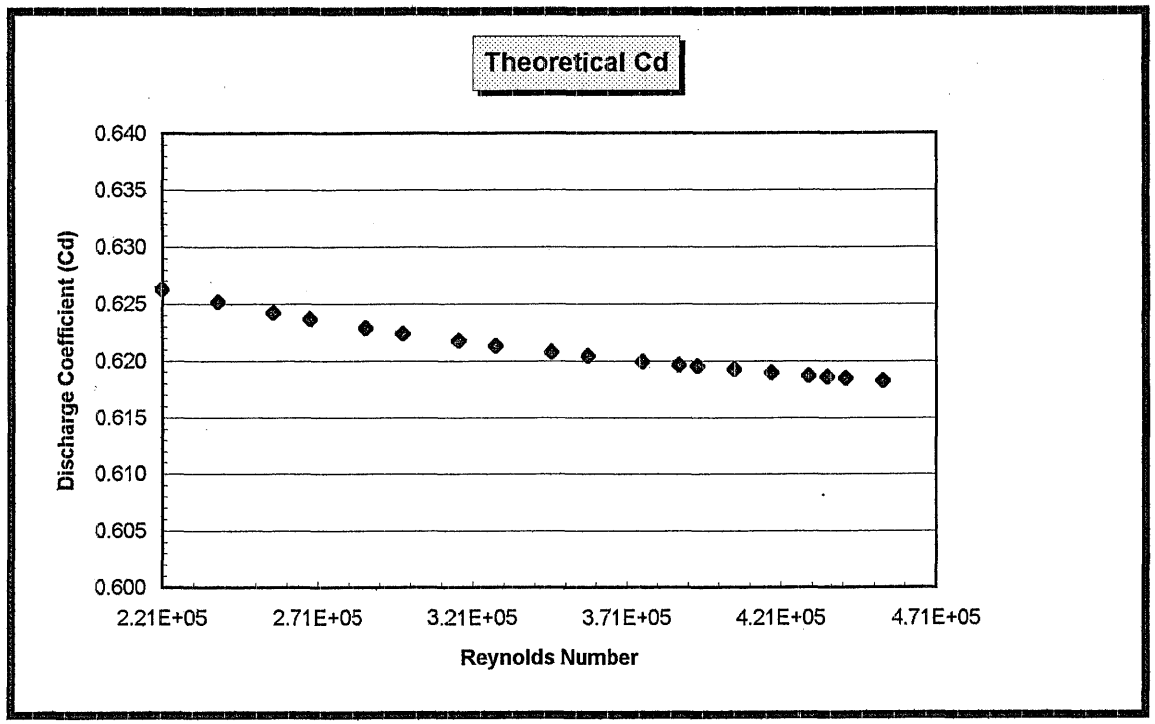

Figure 4.12a. Theoretical values of Discharge Coefficient (Cd).

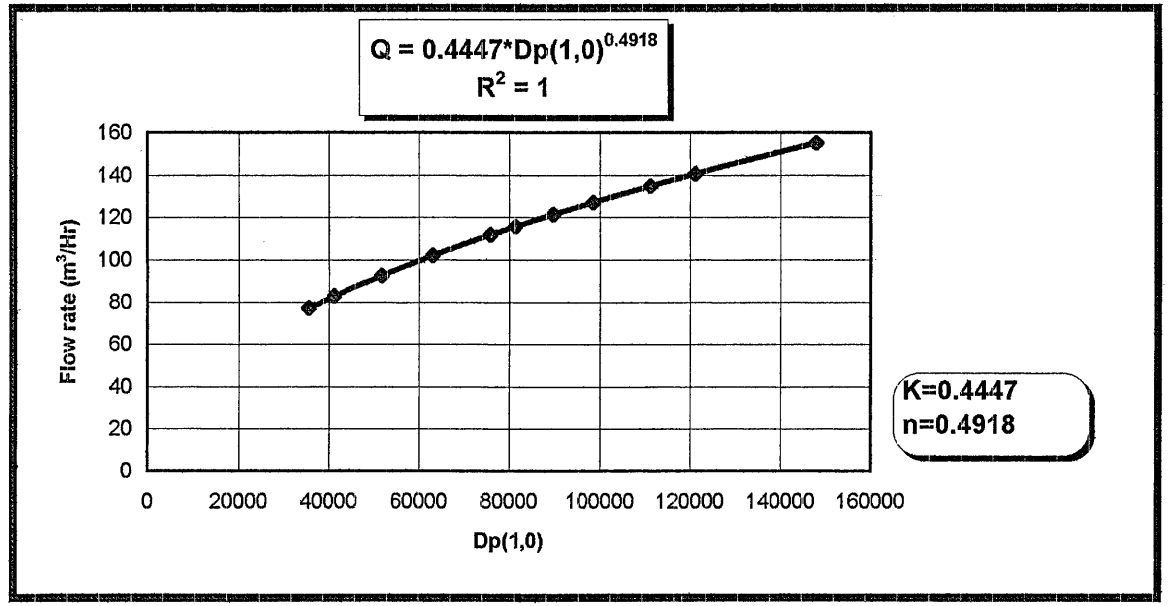

Figure 4.12b. Theoretical estimated K(1,0) factor.

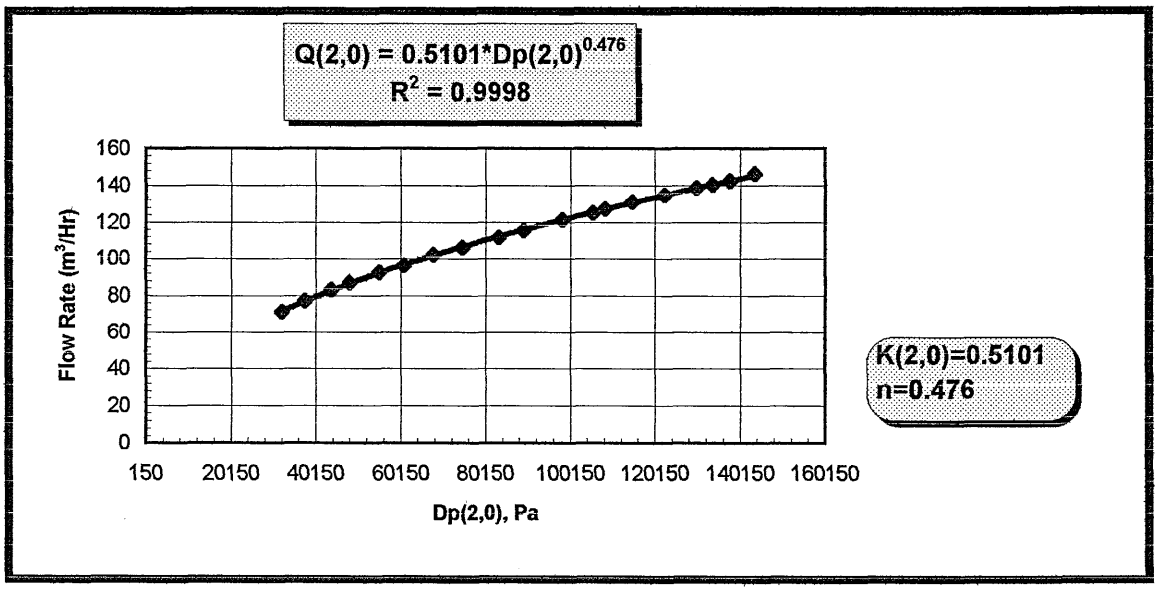

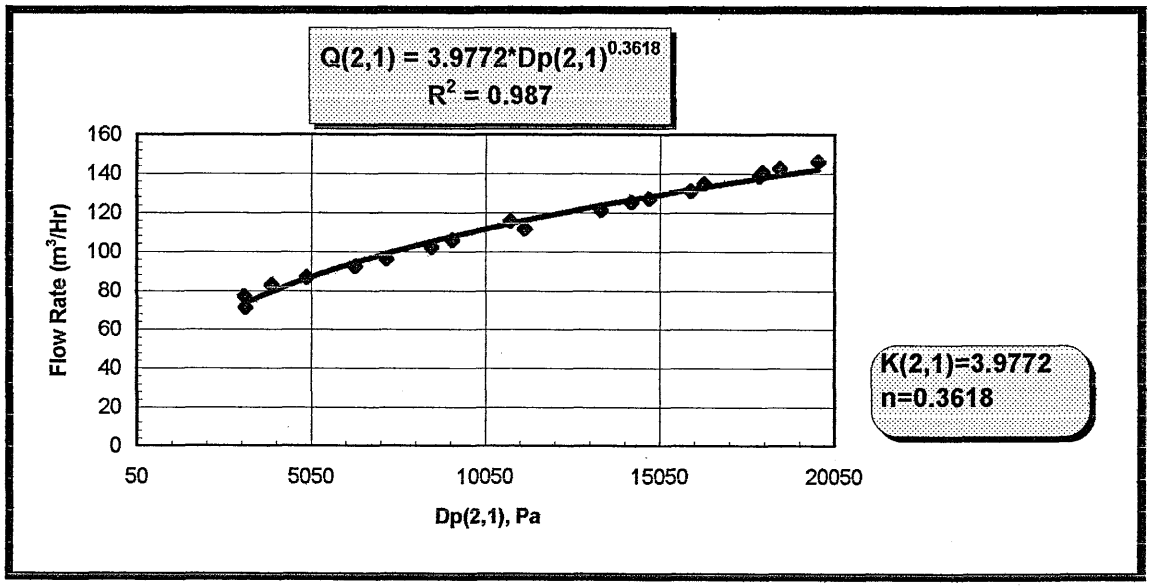

Figure 5.1 Flow rate and differential pressures in Test 1.

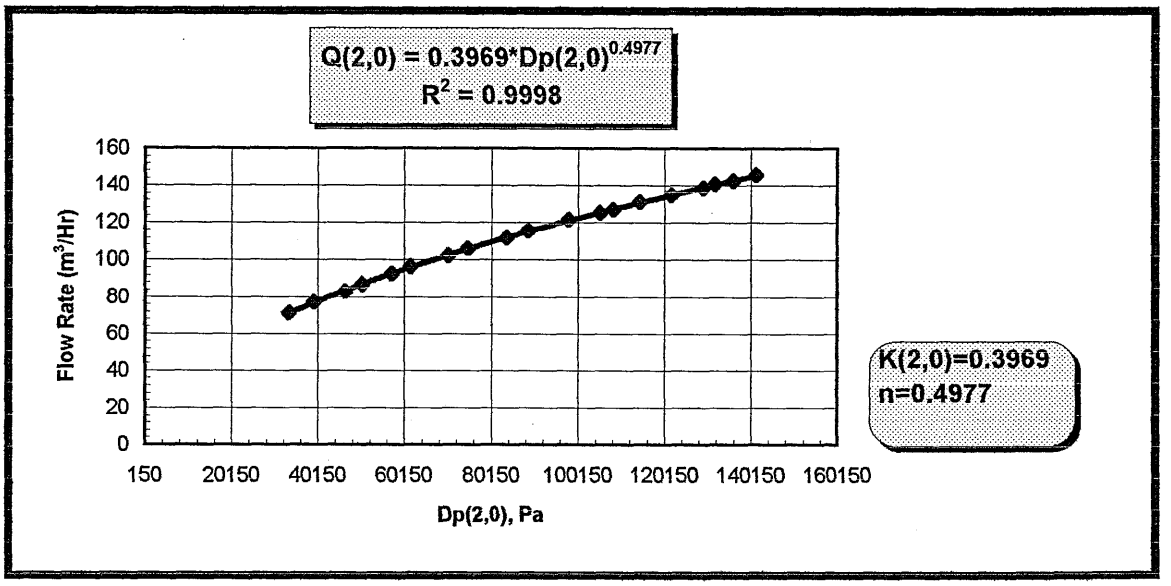

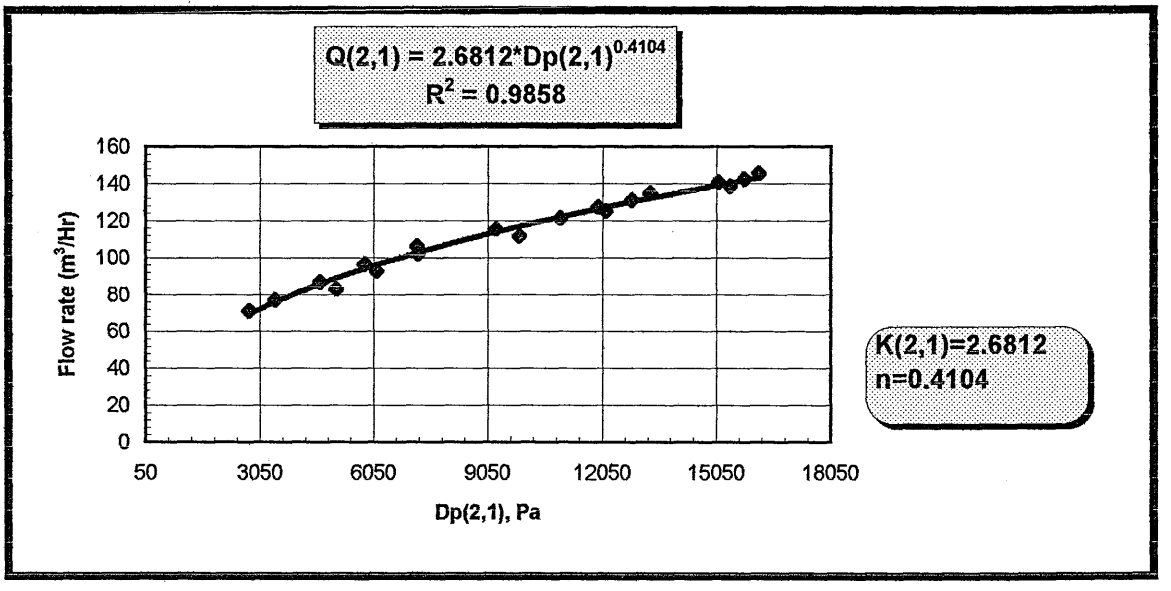

Figure 5.2 Flow rate and differential pressures in Test 4.

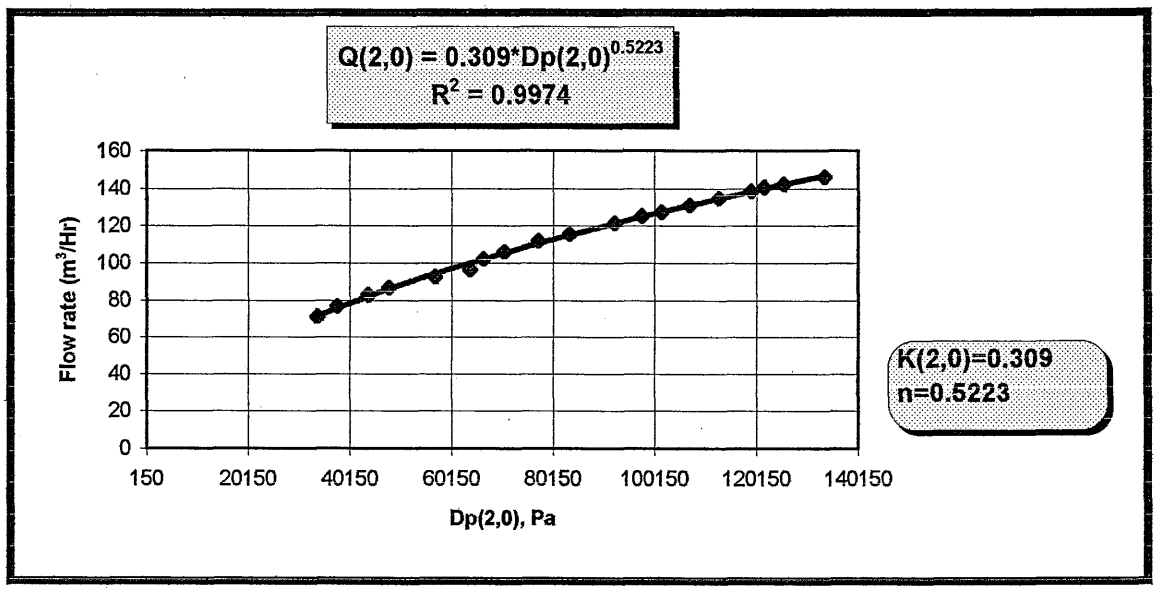

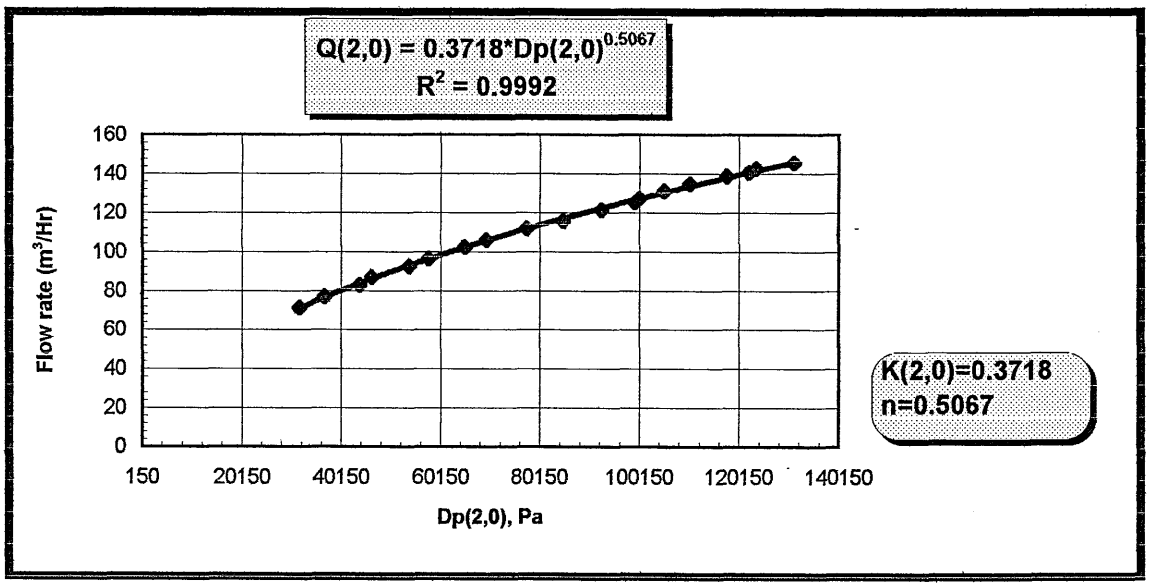

Figure 5.3 Flow rate and differential pressures in Test 2 and Test 3.

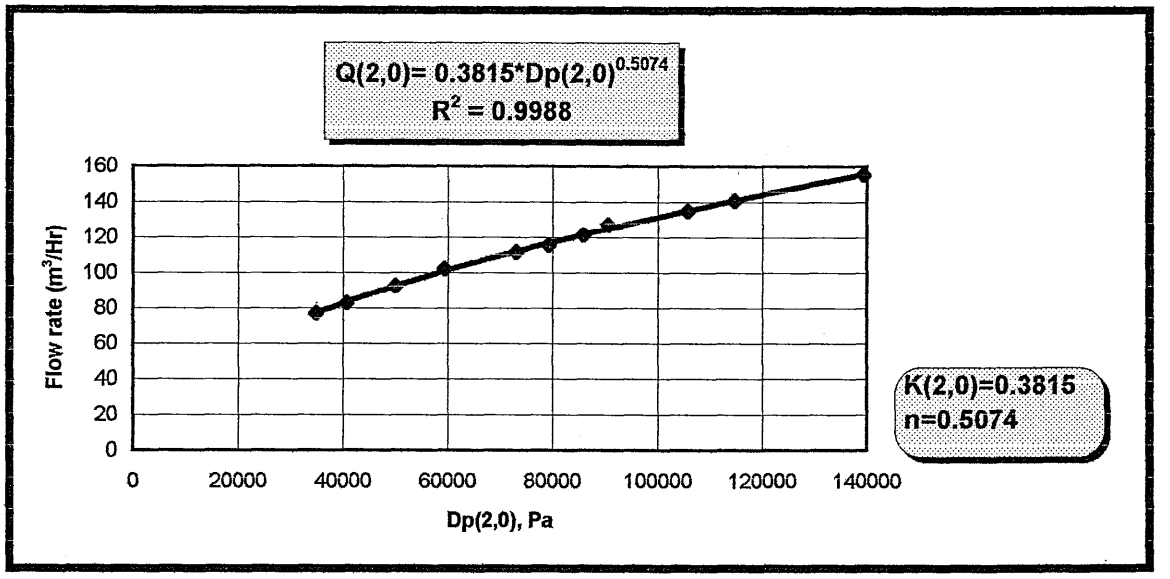

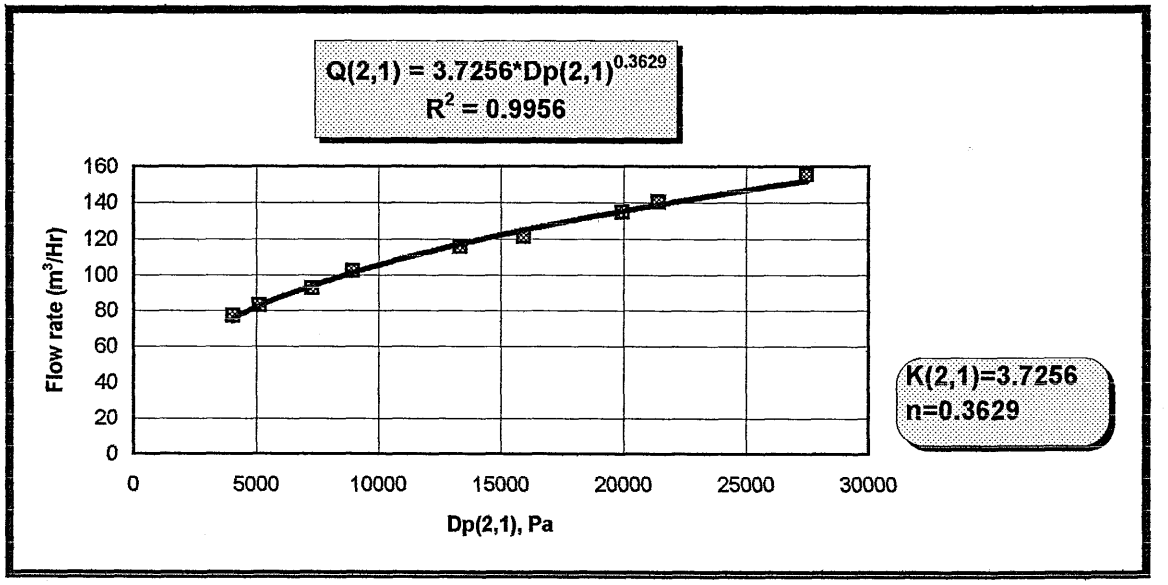

Figure 5.4 Flow rate and differential pressures in Test 6.

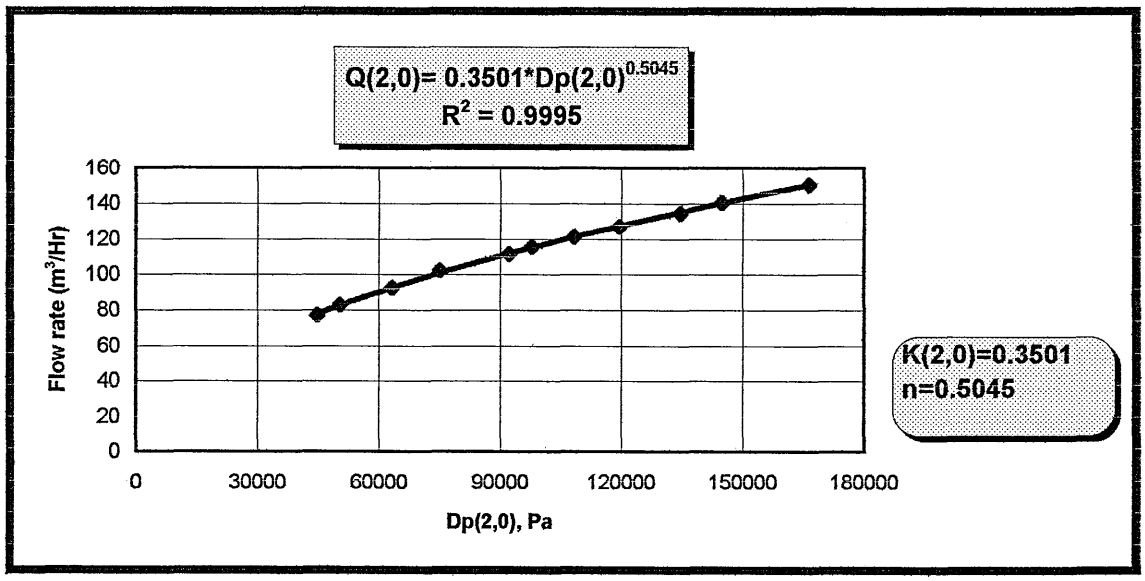

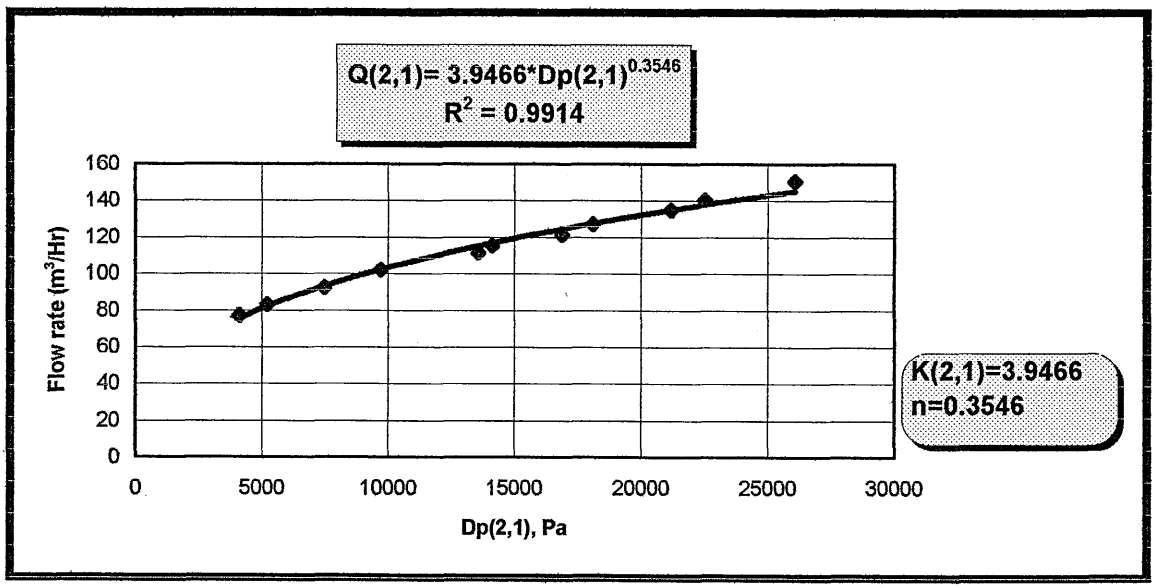

Figure 5.5 Flow rate and differential pressures in Test 7

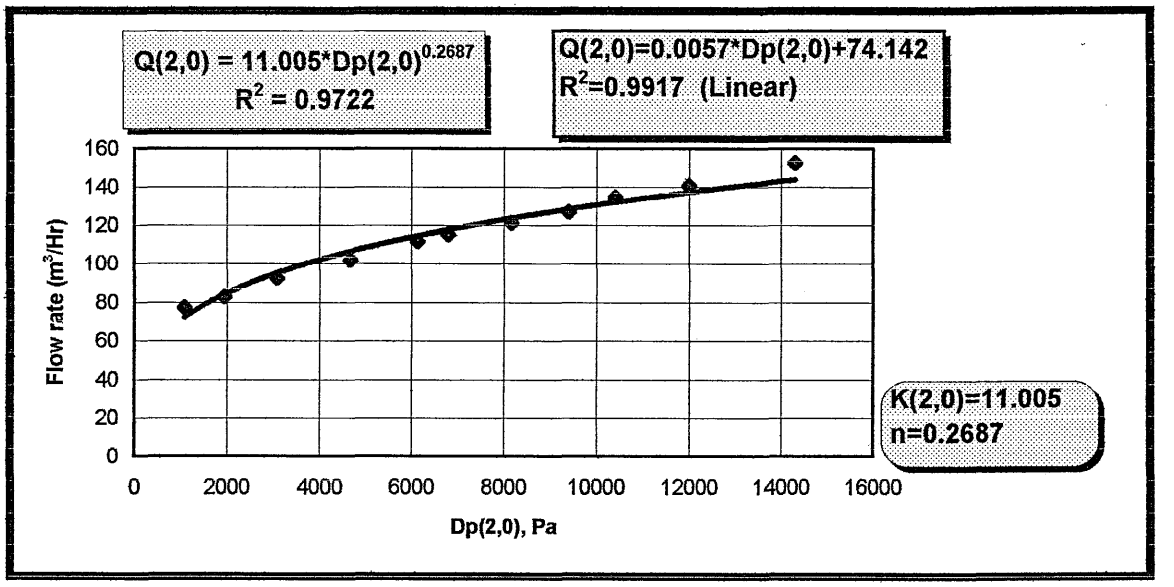

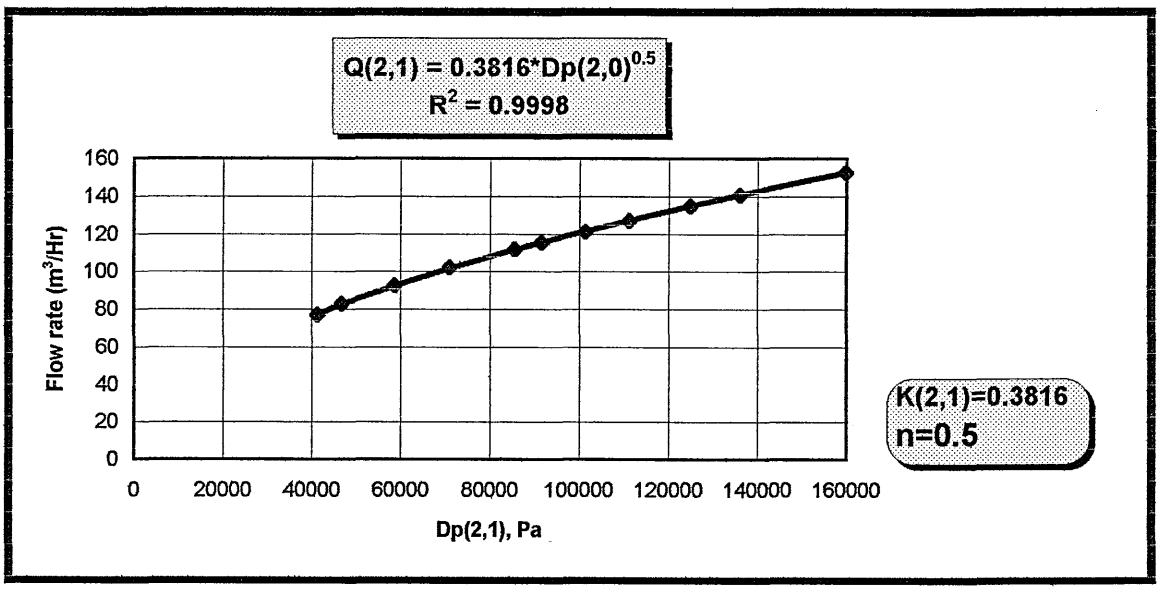

Figure 5.6 Flow rate and differential pressures in Test 8

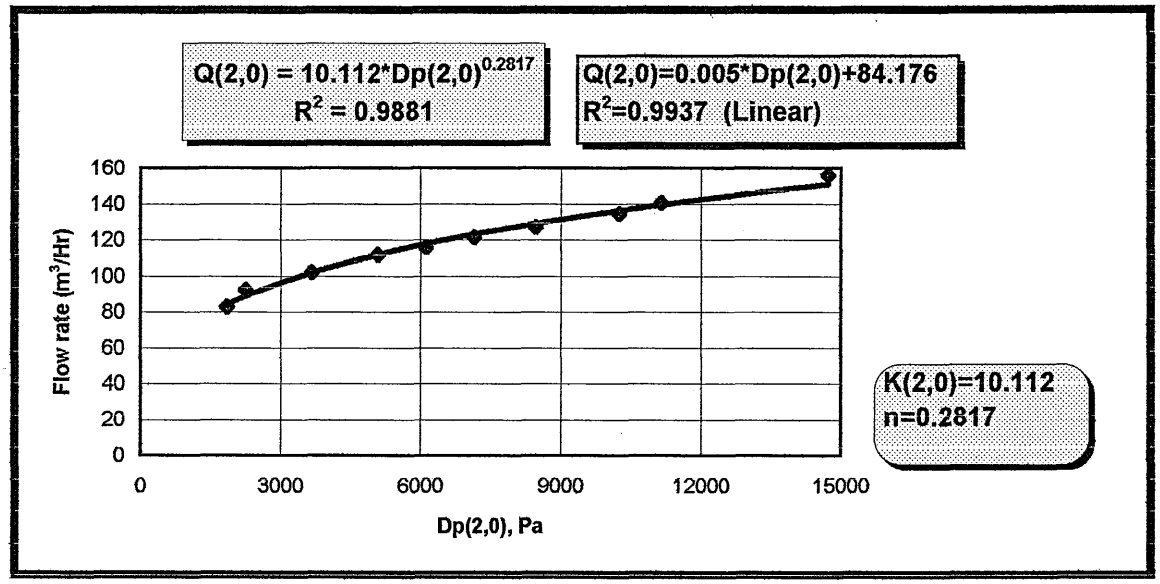

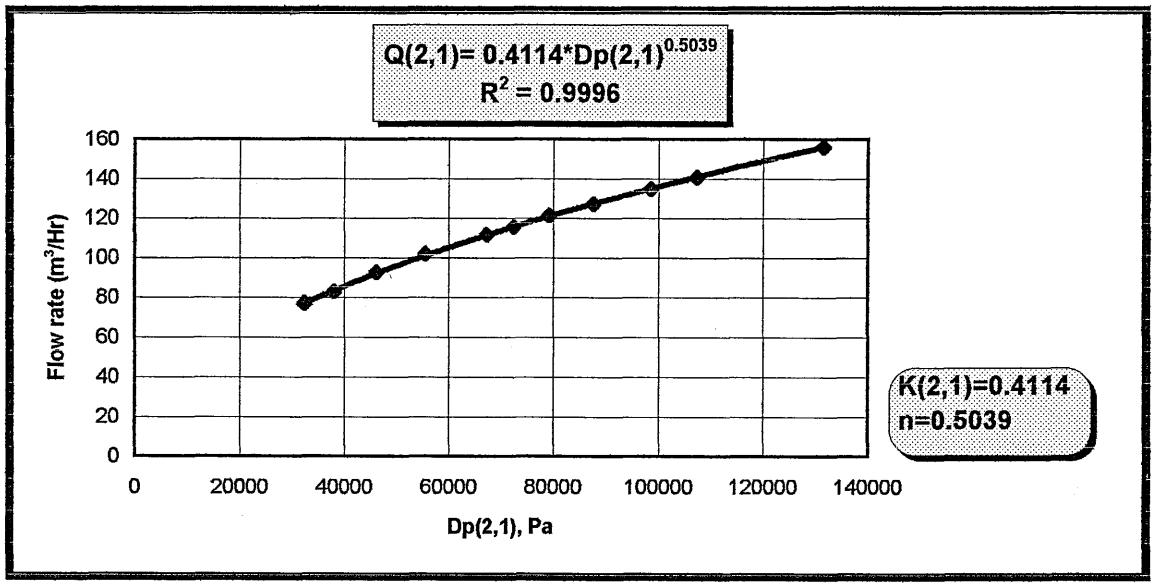

Figure 5.7 Flow rate and differential pressures in Test 9

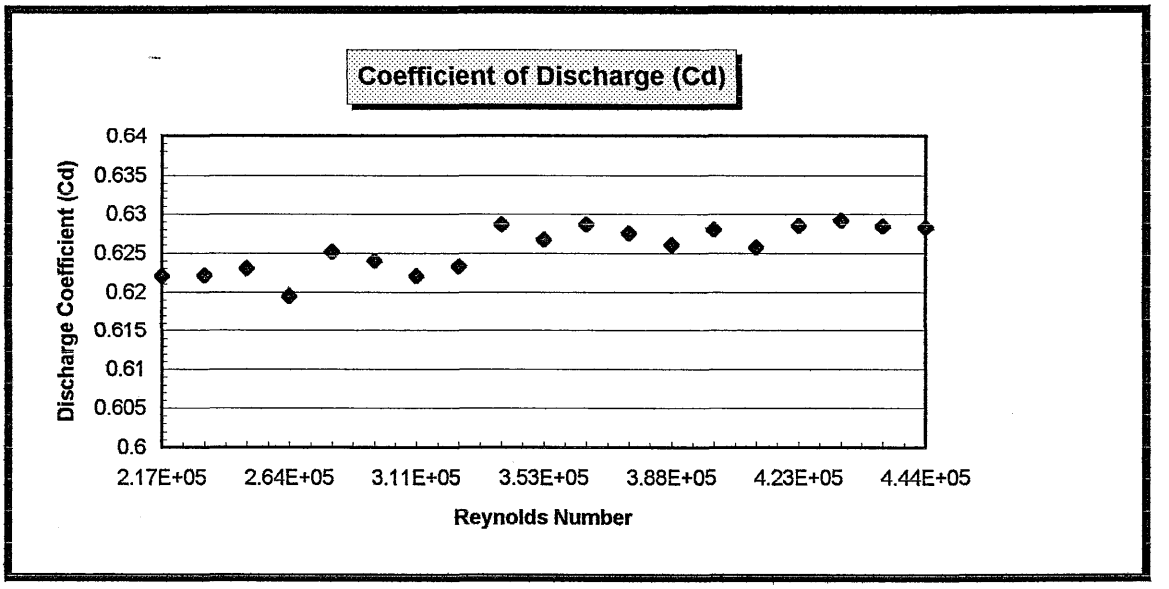

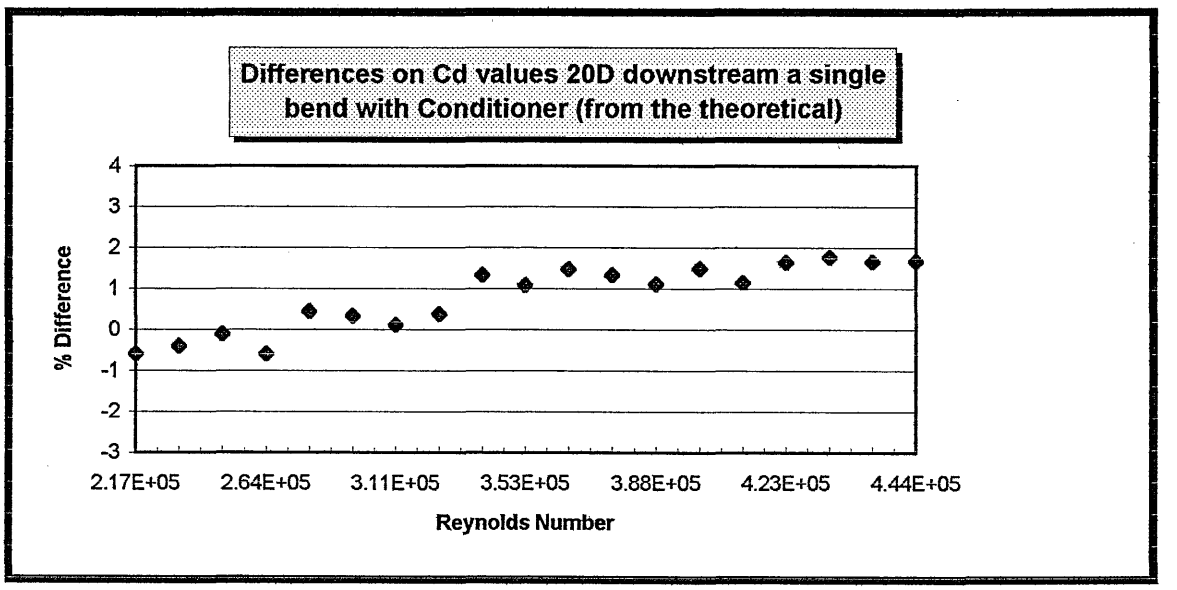

Figure 5.8 Coefficient of discharge (Cd) with the orifice and the Mitsubishi conditioner installed 20D and 6D respectively downstream a single 90^0 bend. (Test 4) - % difference from the theoretical.

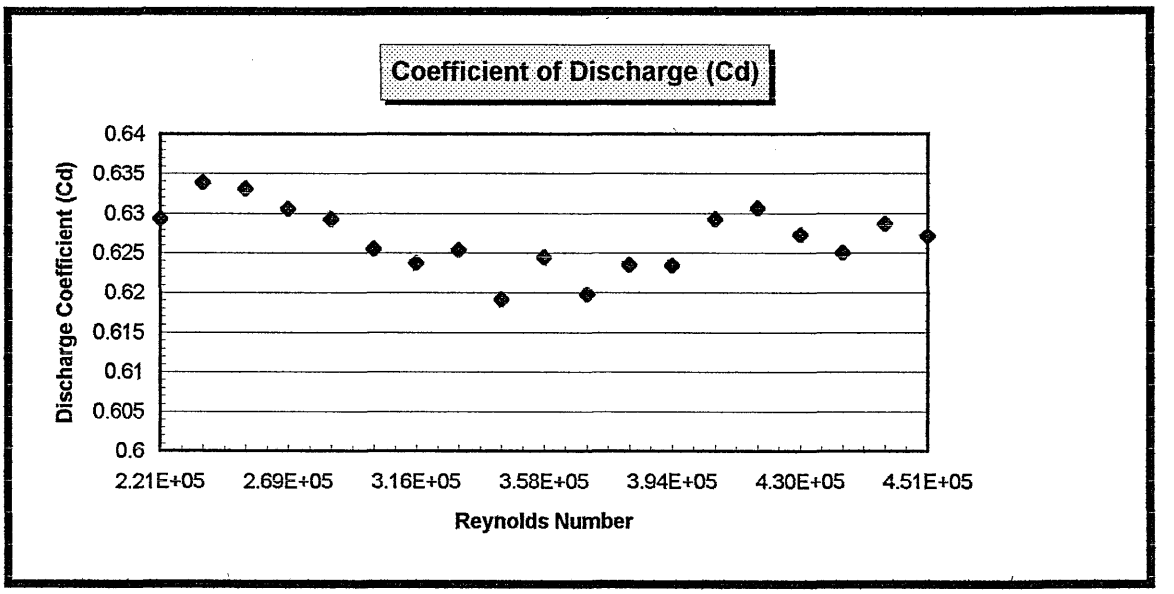

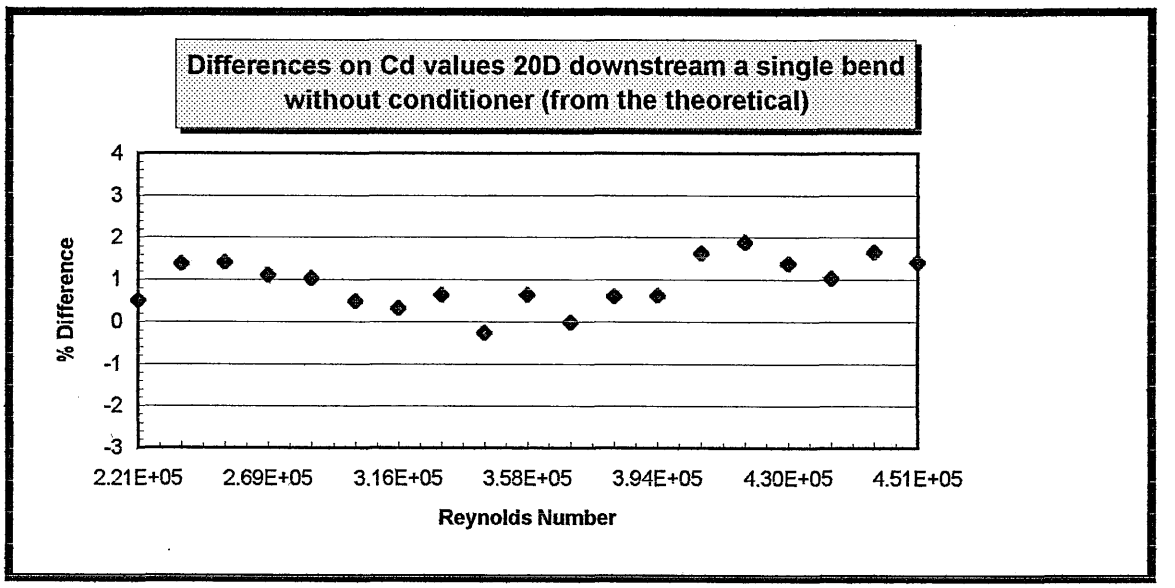

Figure 5.9 Coefficient of discharge with the orifice installed 20D downstream a single 90^0 bend, without conditioner. (Test 3). - % difference from the theoretical.

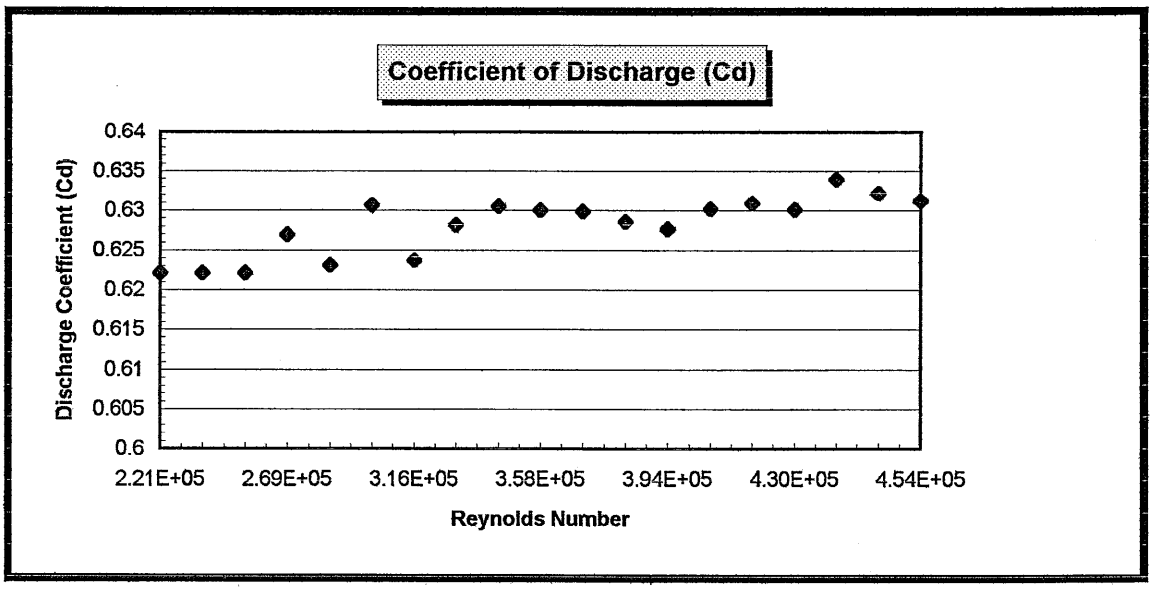

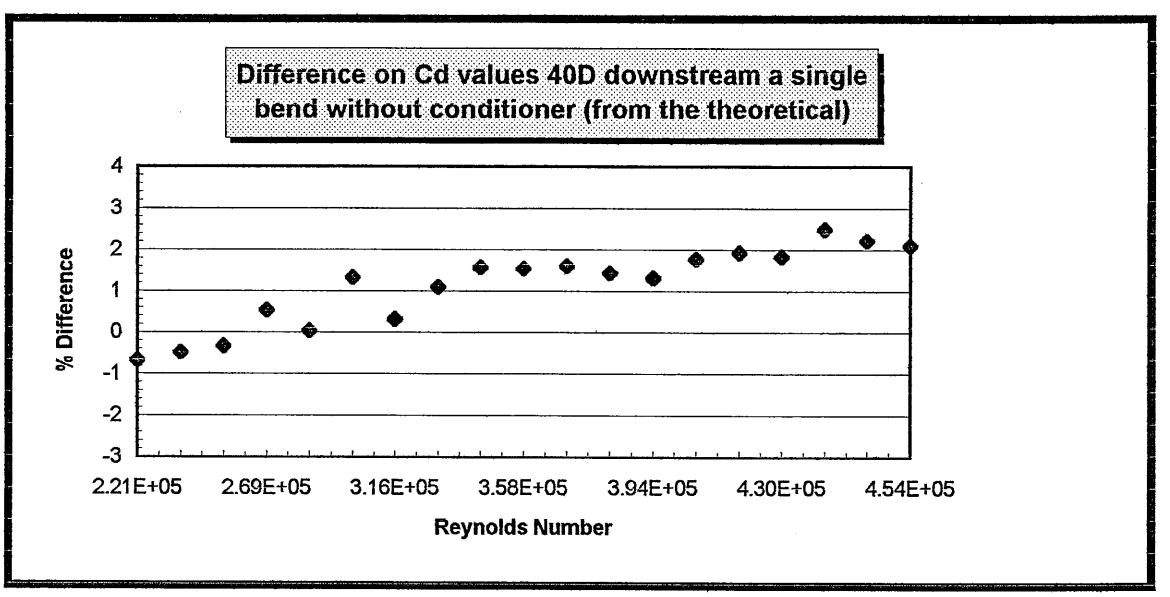

Figure 5.10 Coefficient of discharge with the orifice installed 40D downstream a single 90^0 bend, without conditioner. (Test 2). - % difference from the theoretical.

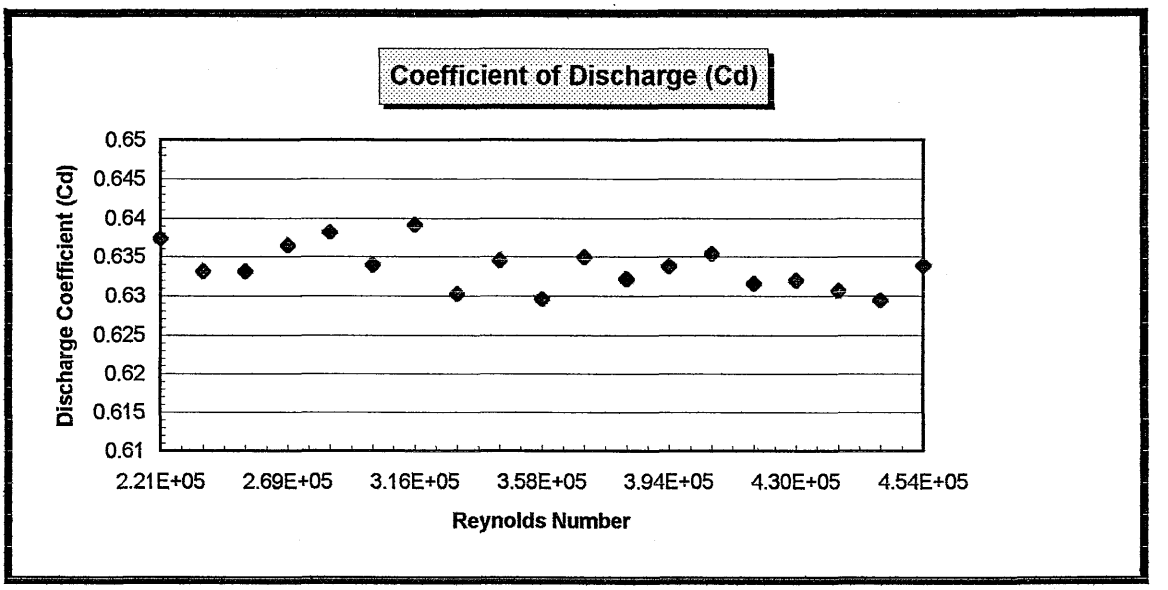

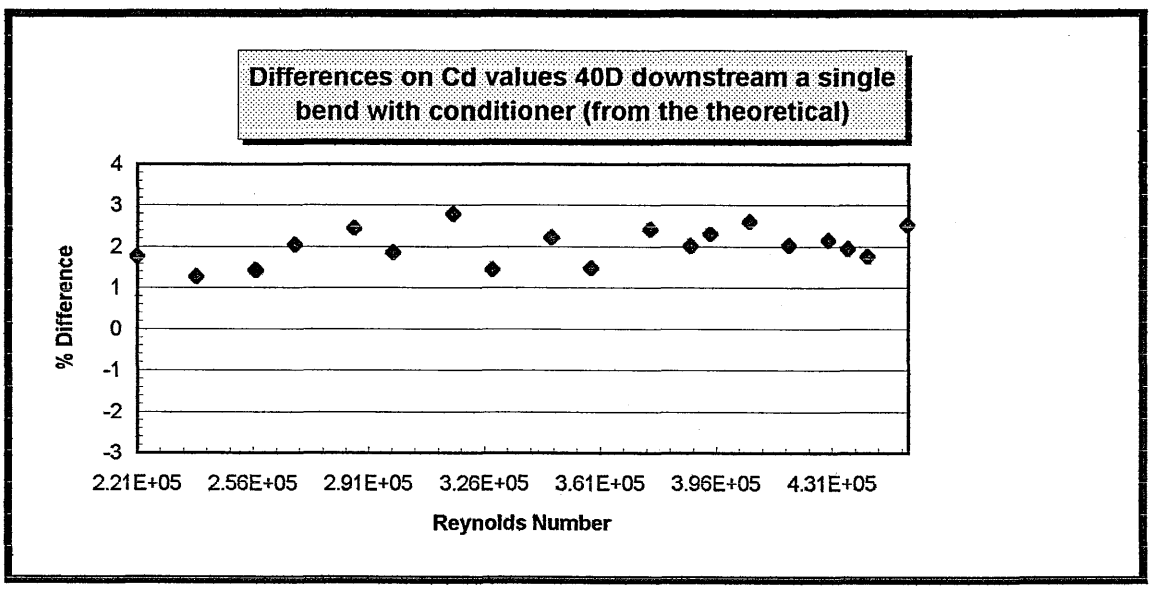

Figure 5.11 Coefficient of discharge with the orifice and the Mitsubishi flow conditioner installed 40D and 6D respectively downstream a single 90^0 bend. (Test 1). - % difference from the theoretical.

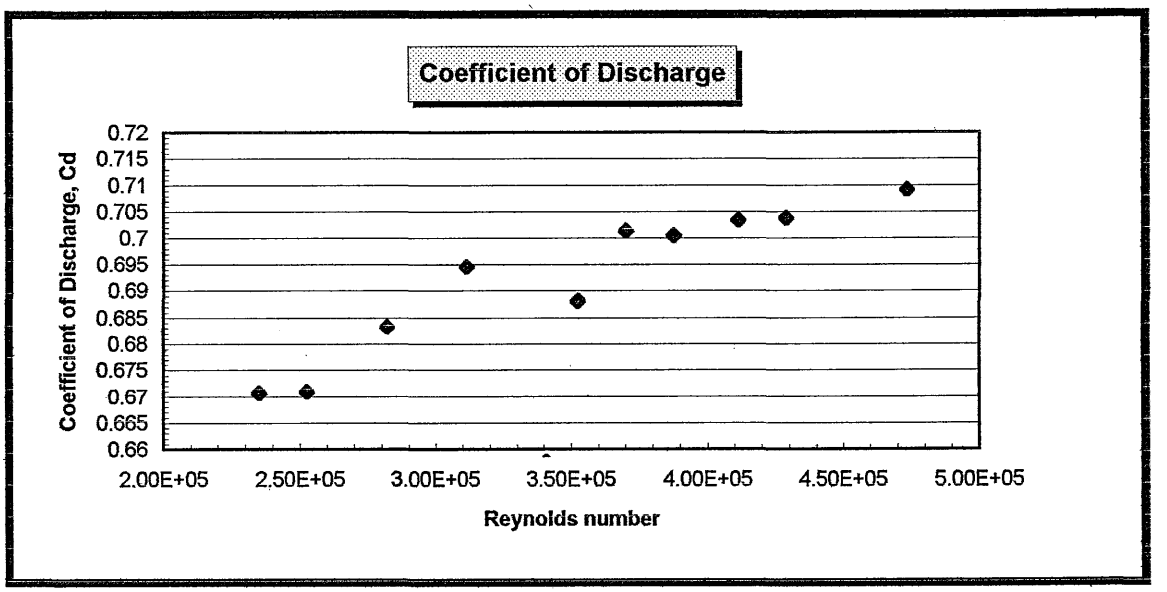

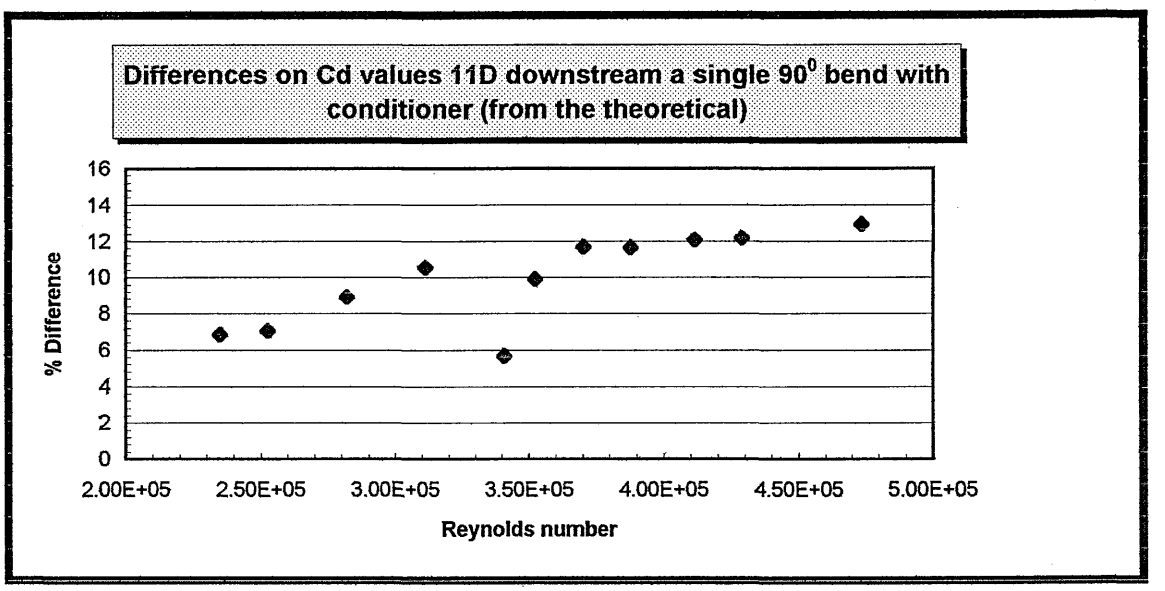

Figure 5.12 Coefficient of discharge with the orifice and the Mitsubishi conditioner installed 11D and 6D respectively downstream a single 90^0 bend. (Test 6). - % difference from the theoretical

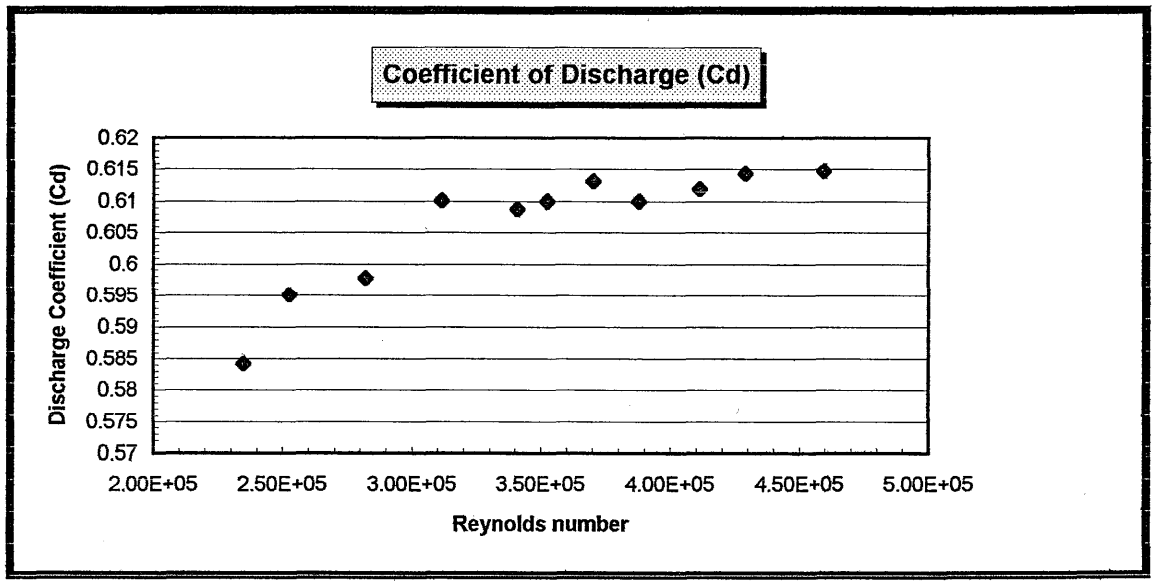

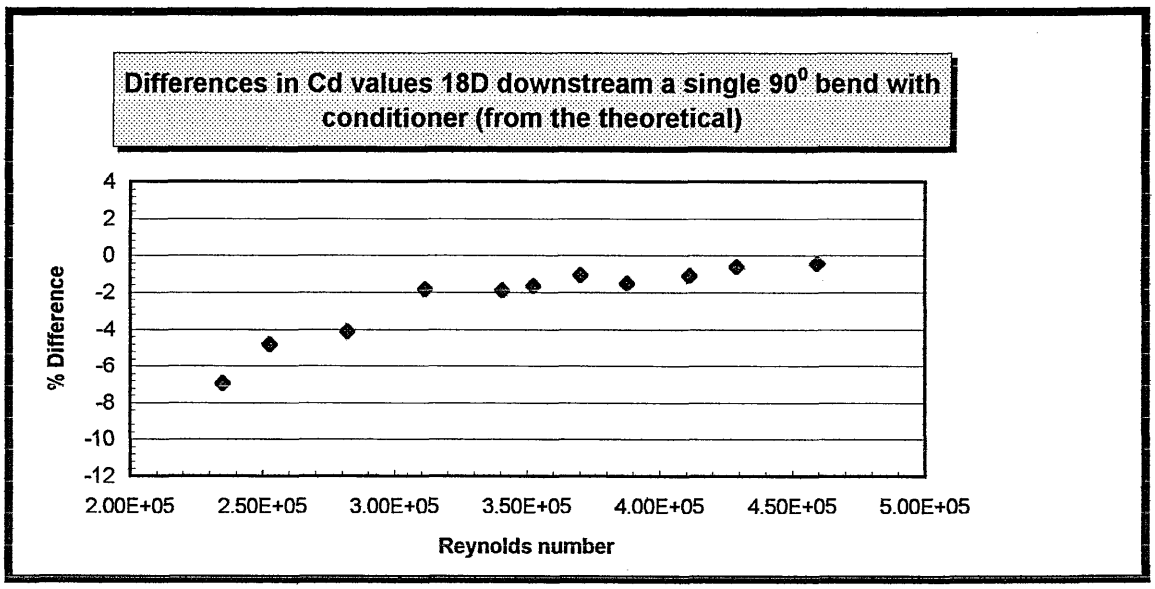

Figure 5.13 Coefficient of discharge with the orifice and the Mitsubishi flow conditioner installed 18D and 6D respectively downstream a single 90^0 bend. (Test 7). - % difference from the theoretical.

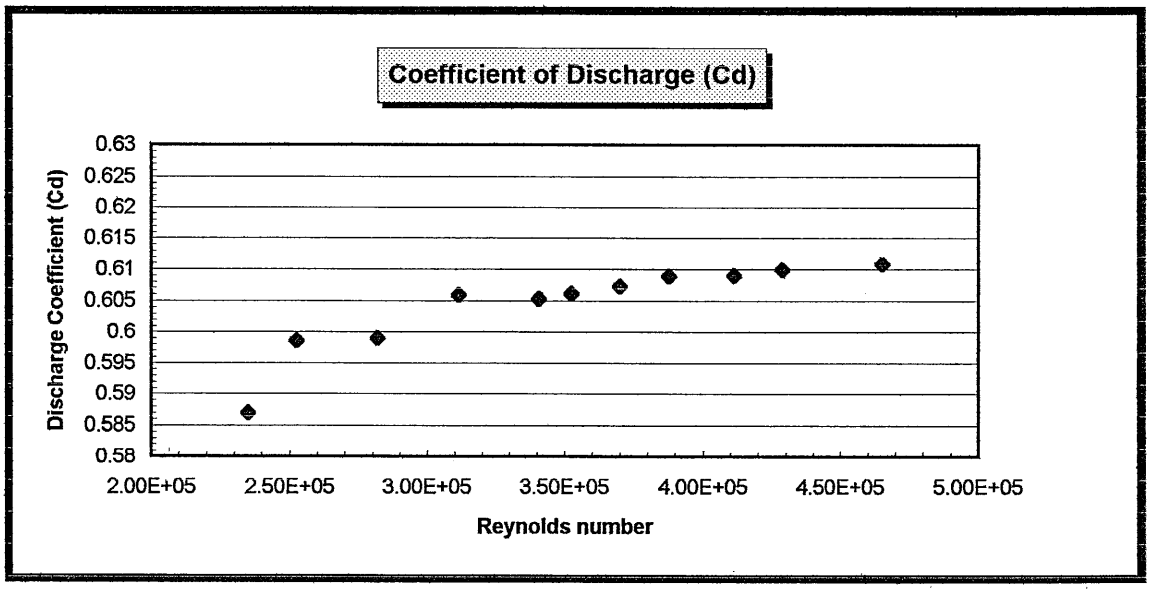

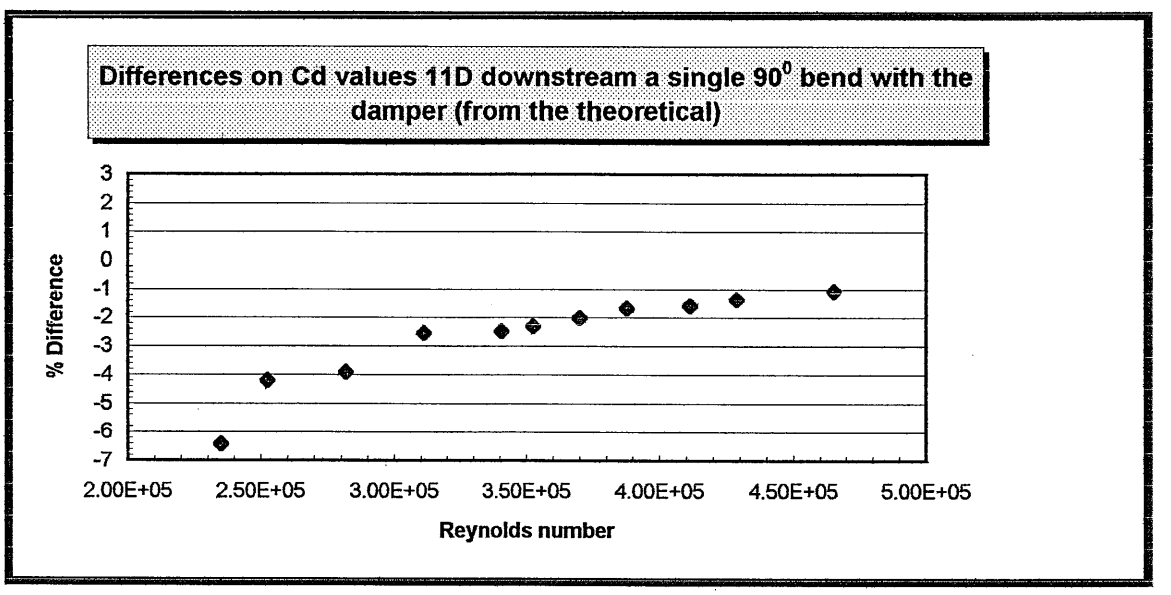

Figure 5.14 Coefficient of discharge with the orifice and the "damper" installed 11D and 5D respectively downstream a single 90^0 bend. (Test 8). - % difference from the theoretical.

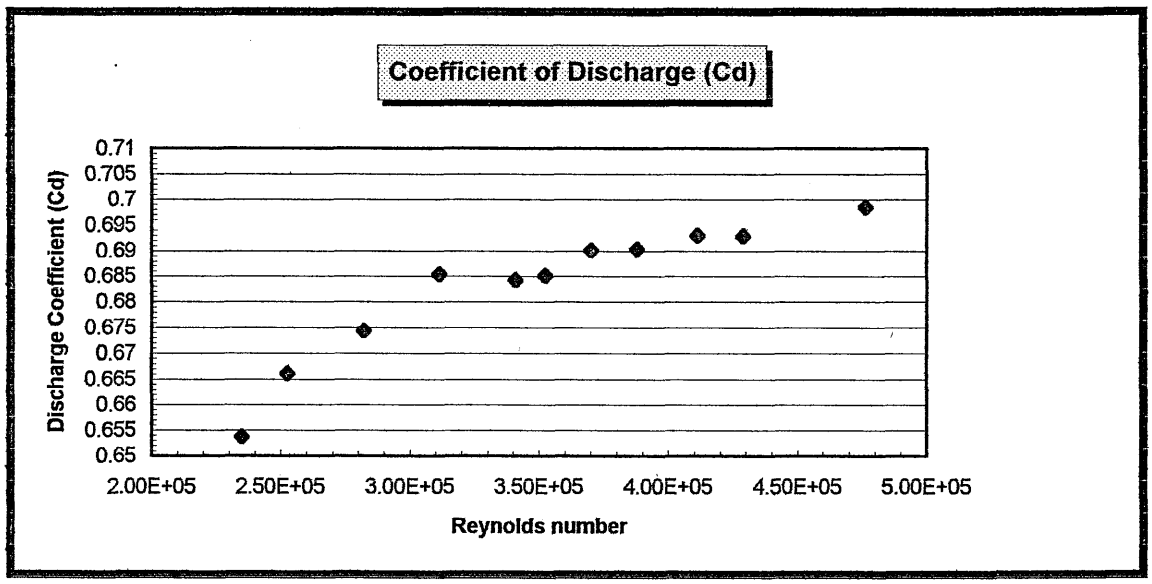

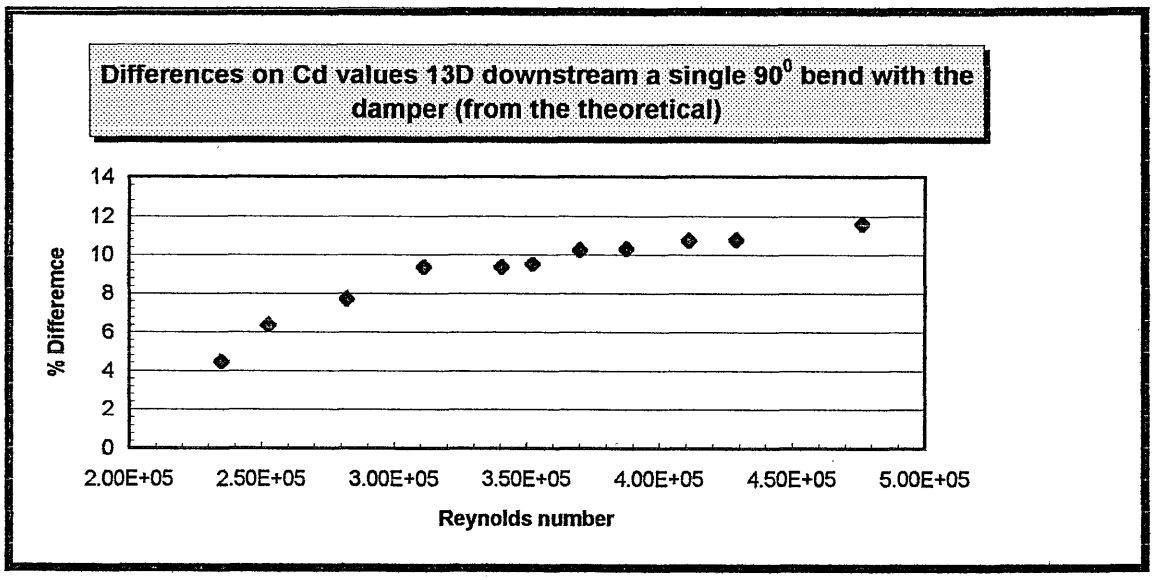

Figure 5.15 Coefficient of discharge with the orifice and the "damper" installed 13D and 5D respectively downstream a single 90^0 bend. (Test 9). - % difference from the theoretical.

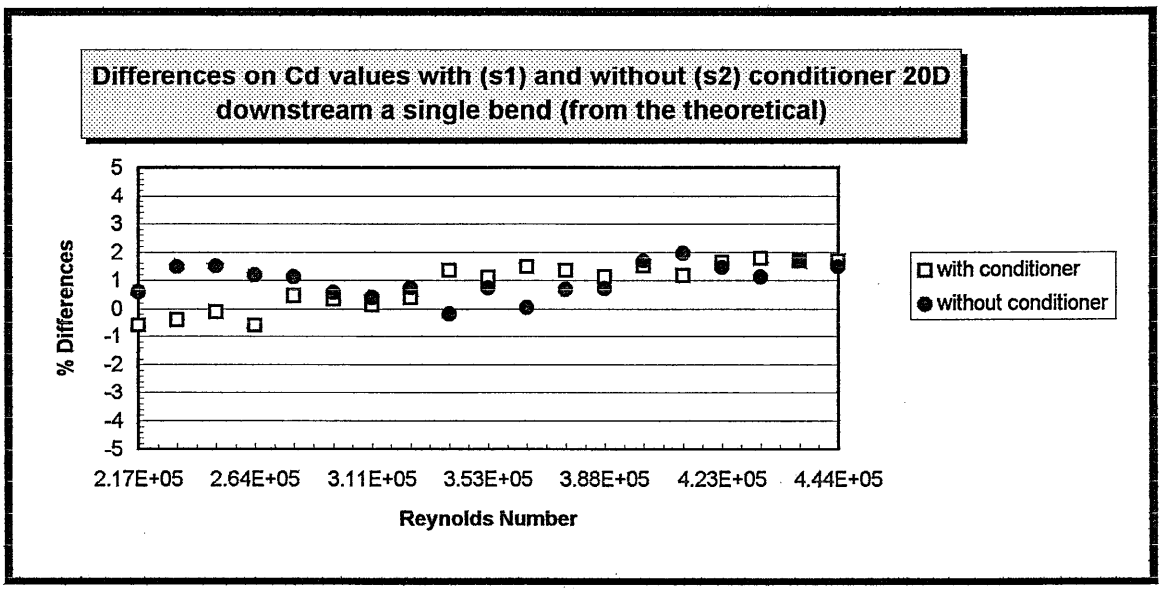

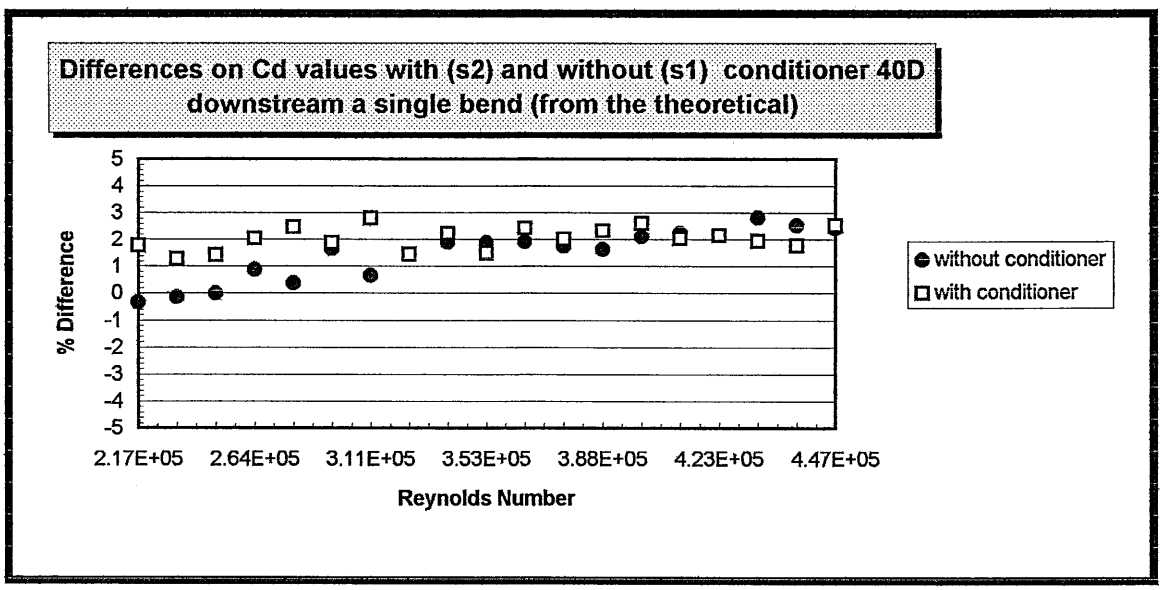

Figure 5.16 Comparative results of the orifice plate performance 40D and 20D downstream a single 90^0 bend with or without conditioner installed.

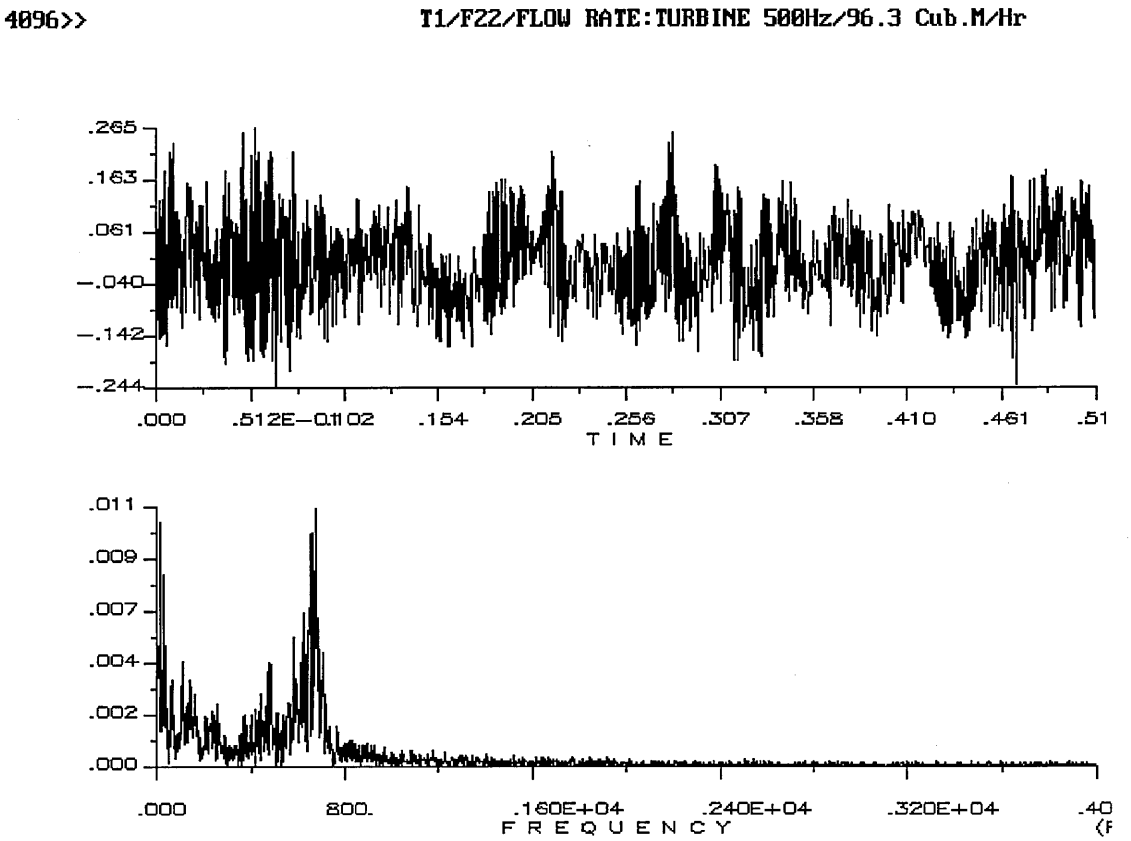

Figure 5.17 Voltage versus time and Amplitude spectrum in Test 1.

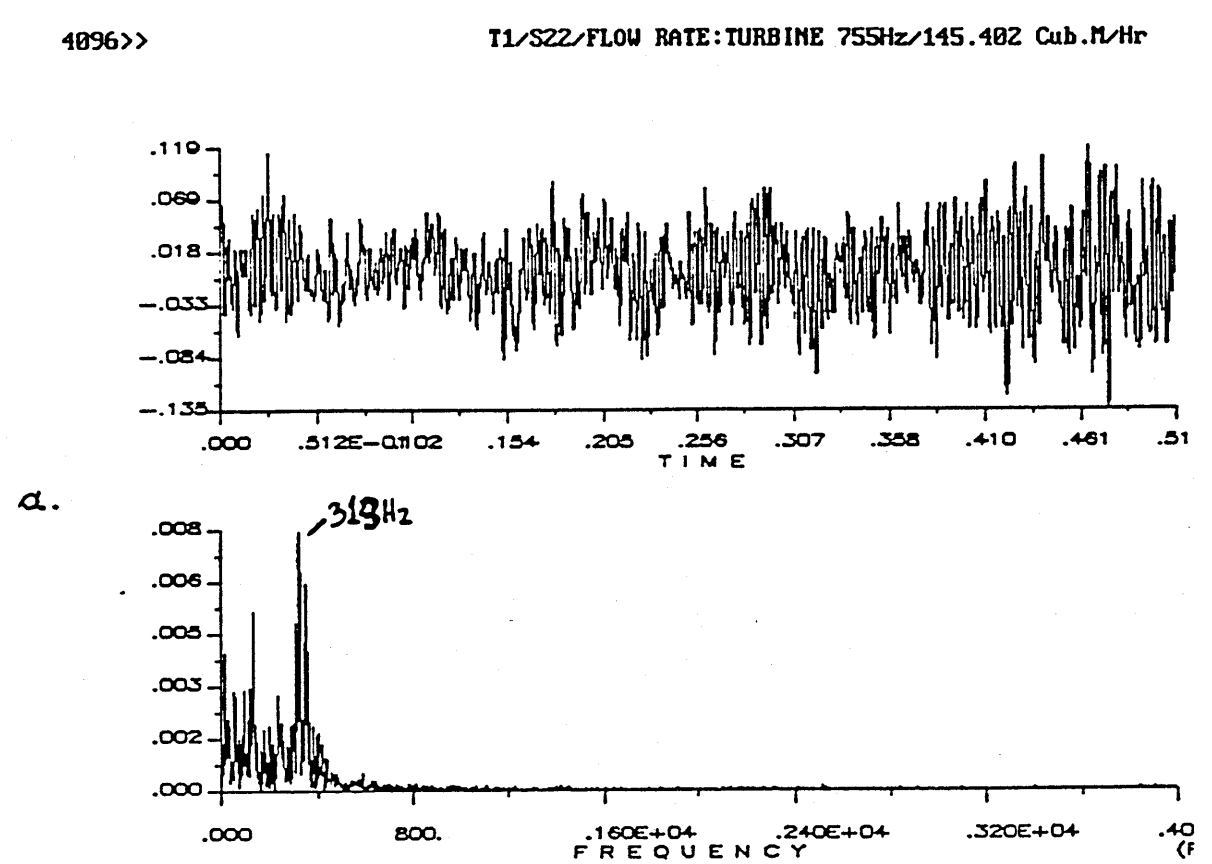

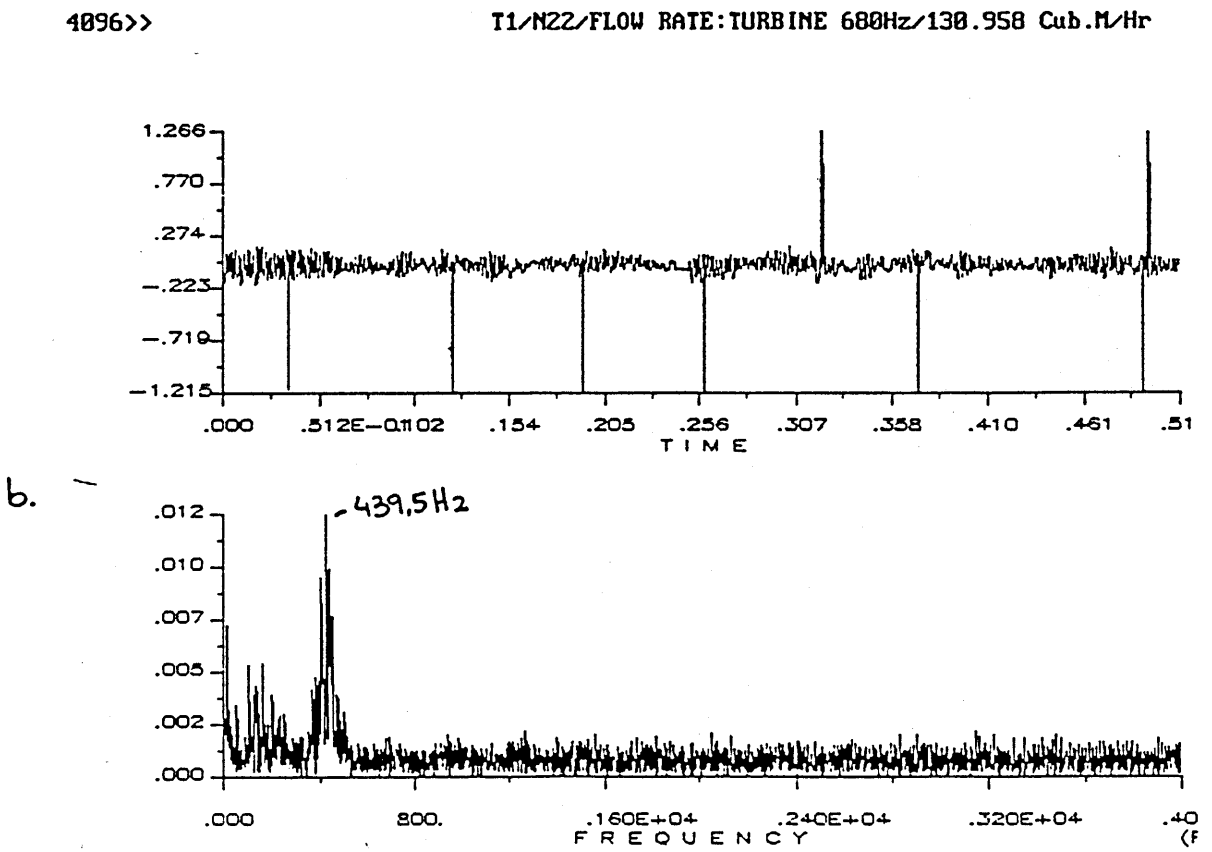

Figure 5.18 Pressure signal in the time domain and amplitude spectrum upstream the Mitsubishi conditioner in Test 1. a) Flow rate 145.4 m^3/Hr b) flow rate 131 m^3/Hr.

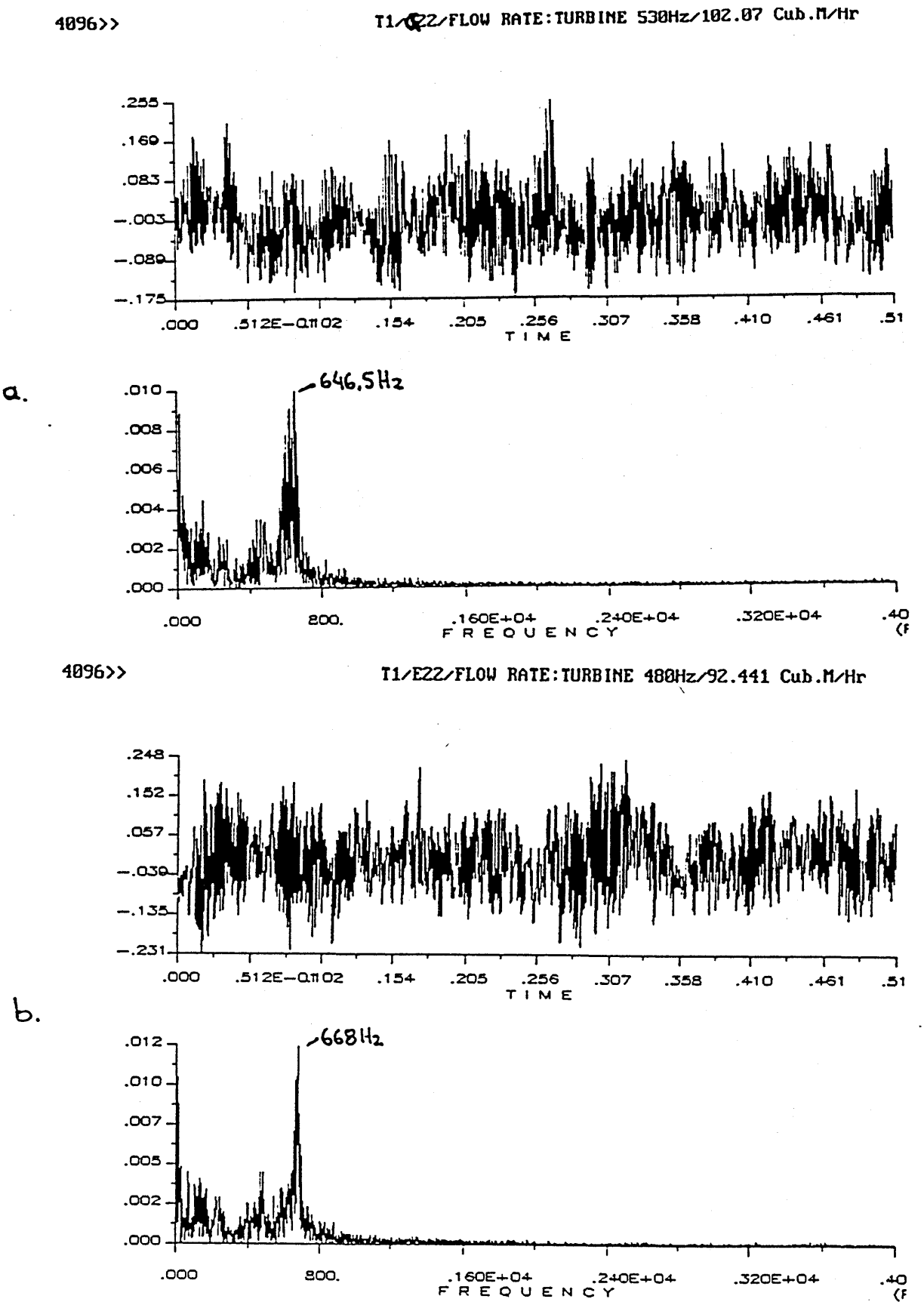

Figure 5.19 Pressure signal in the time domain and amplitude spectrum upstream the Mitsubishi conditioner in Test 1. a) Flow rate 102 m^3/Hr b) flow rate 92.4 m^3/Hr.

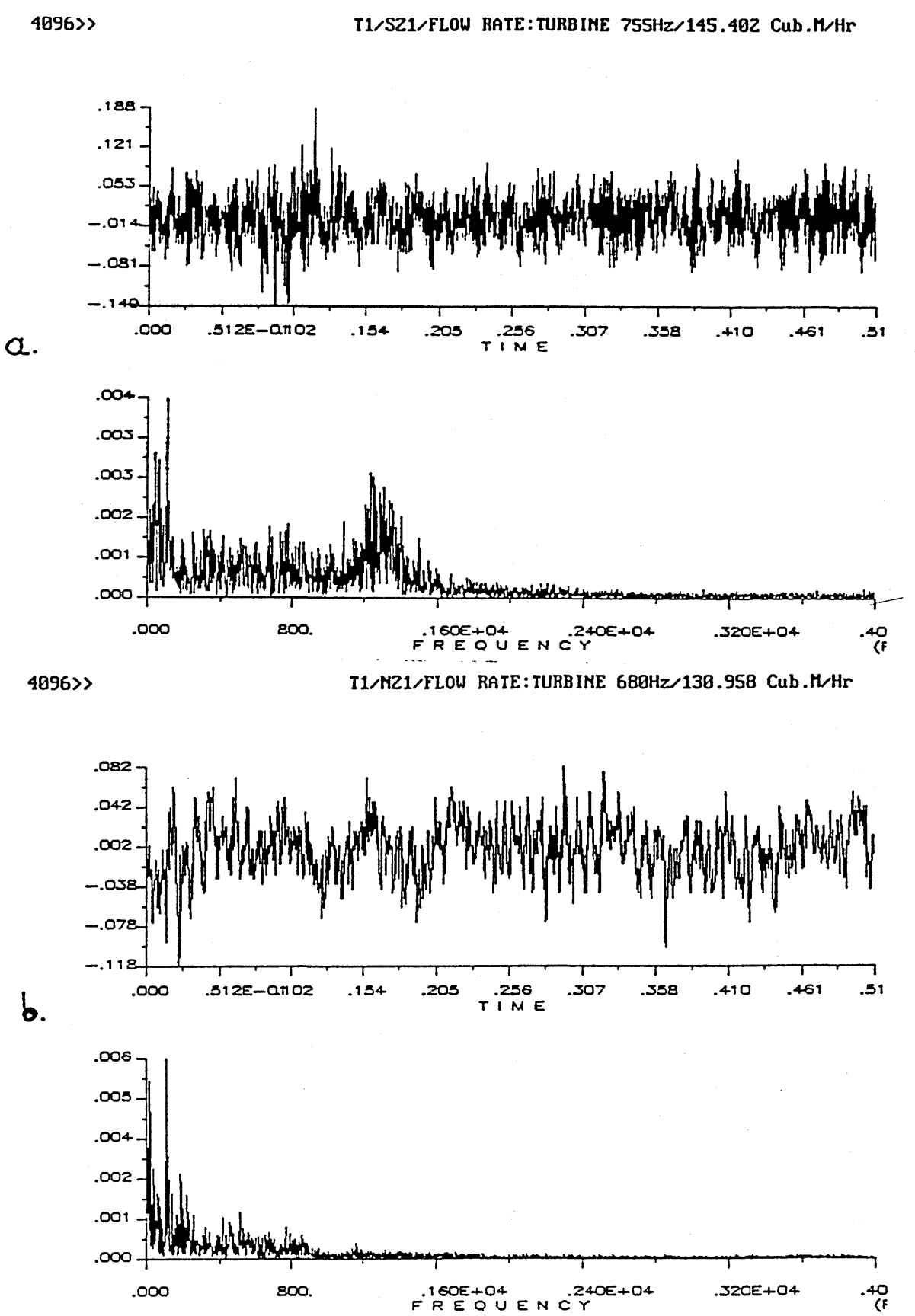

Figure 5.20 Pressure signal in the time domain and amplitude spectrum upstream the Orifice in Test 1. a) Flow rate 145.4 m^3/Hr b) flow rate 131 m^3/Hr.

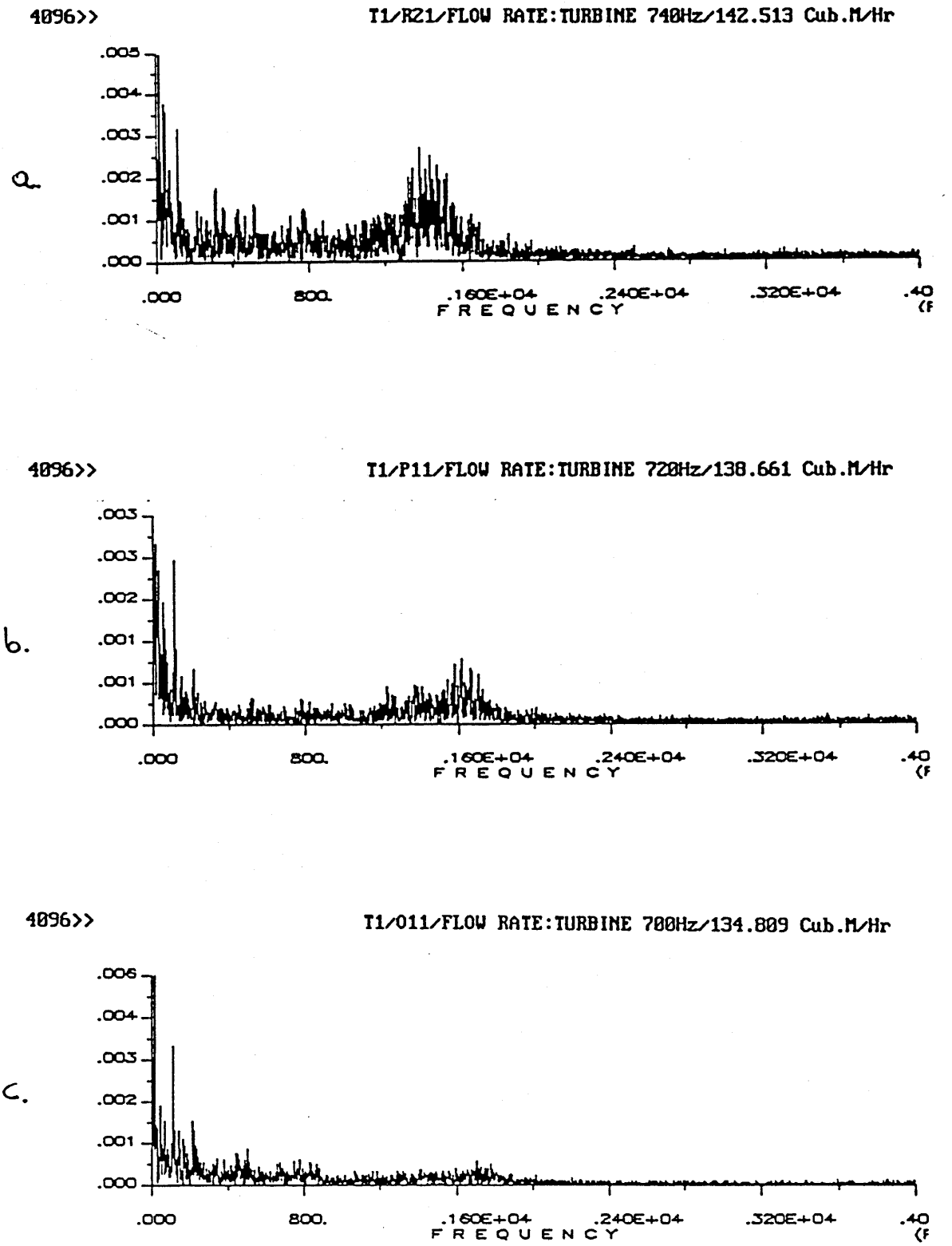

Figure 5.21 Evolution of the amplitude spectrum upstream the Orifice in Test 1. a) Flow rate 142.5 m^3/Hr b) flow rate 138.7 m^3/Hr c)flow rate 134.8 m^3/Hr.

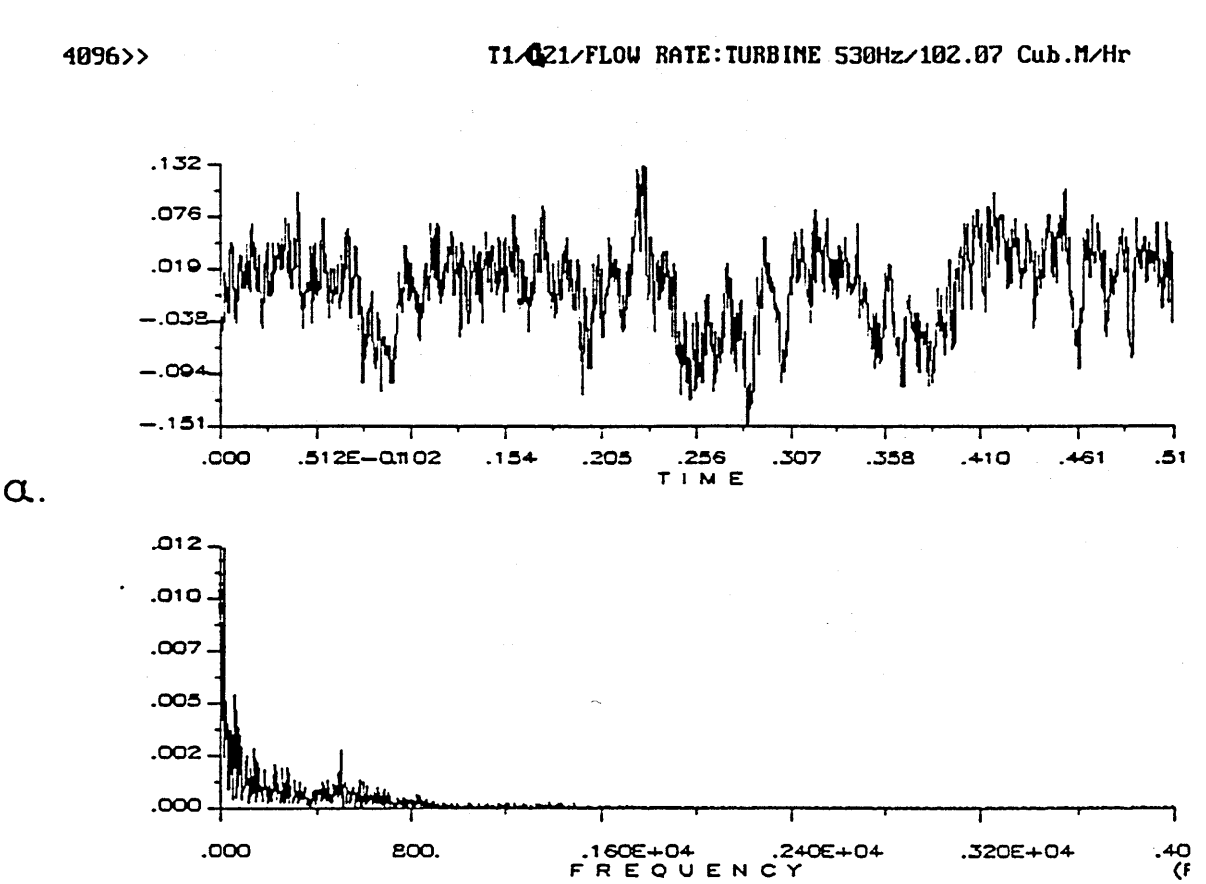

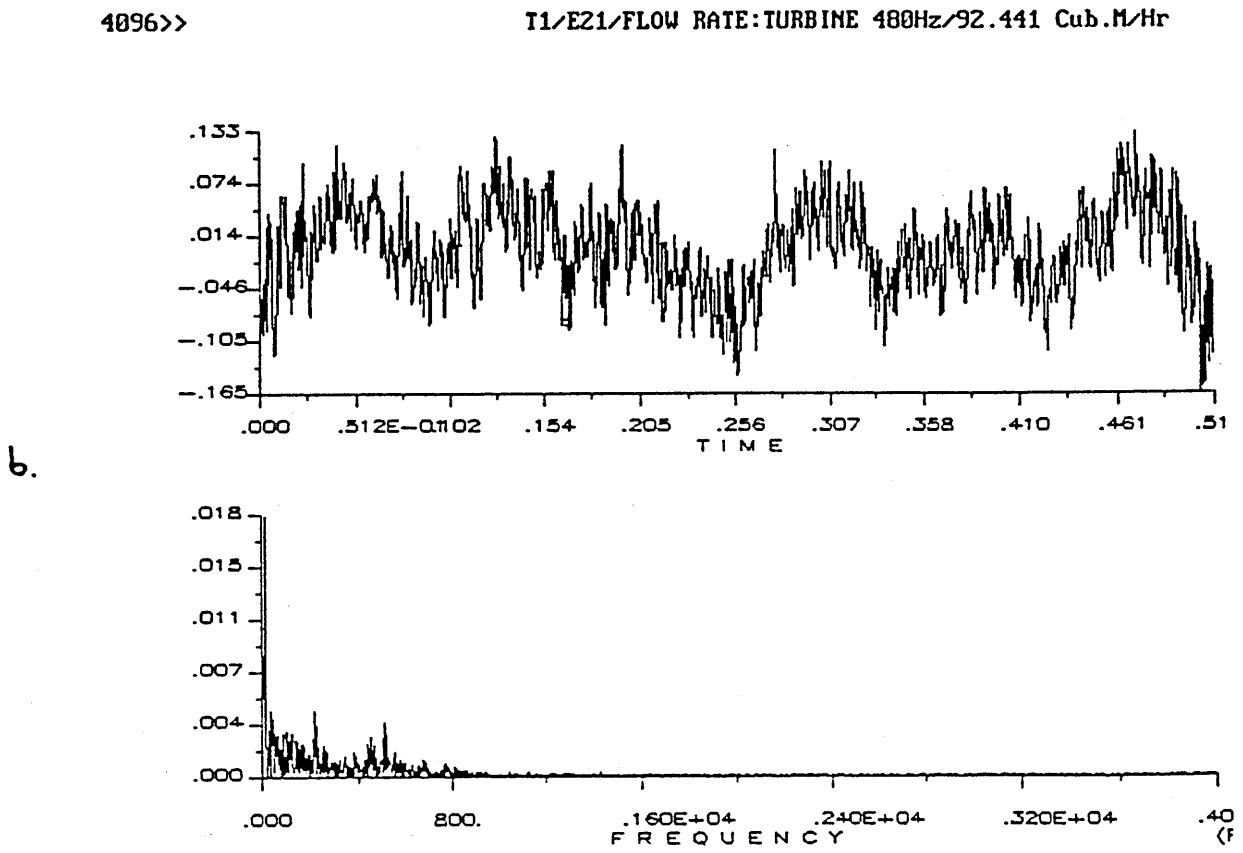

Figure 5.22 Pressure signals in the time domain and amplitude spectrum upstream the Orifice in Test 1. a) Flow rate 102 m^3/Hr b) flow rate 92.4 m^3/Hr.

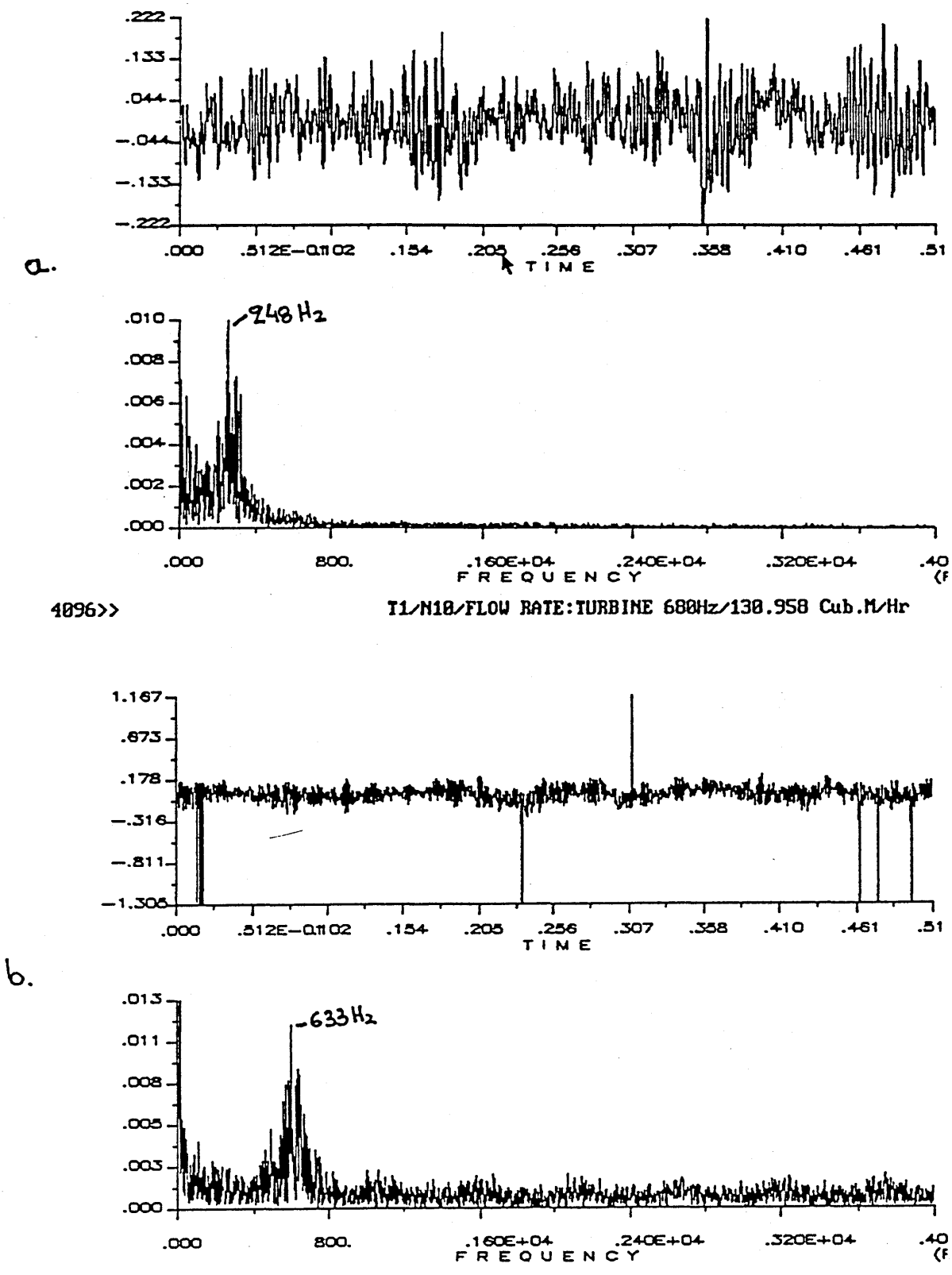

Figure 5.23 Pressure signals in the time domain and amplitude spectrum downstream the Orifice in Test 1. a) Flow rate 145.4m^3/Hr b) flow rate 131 m^3/Hr.

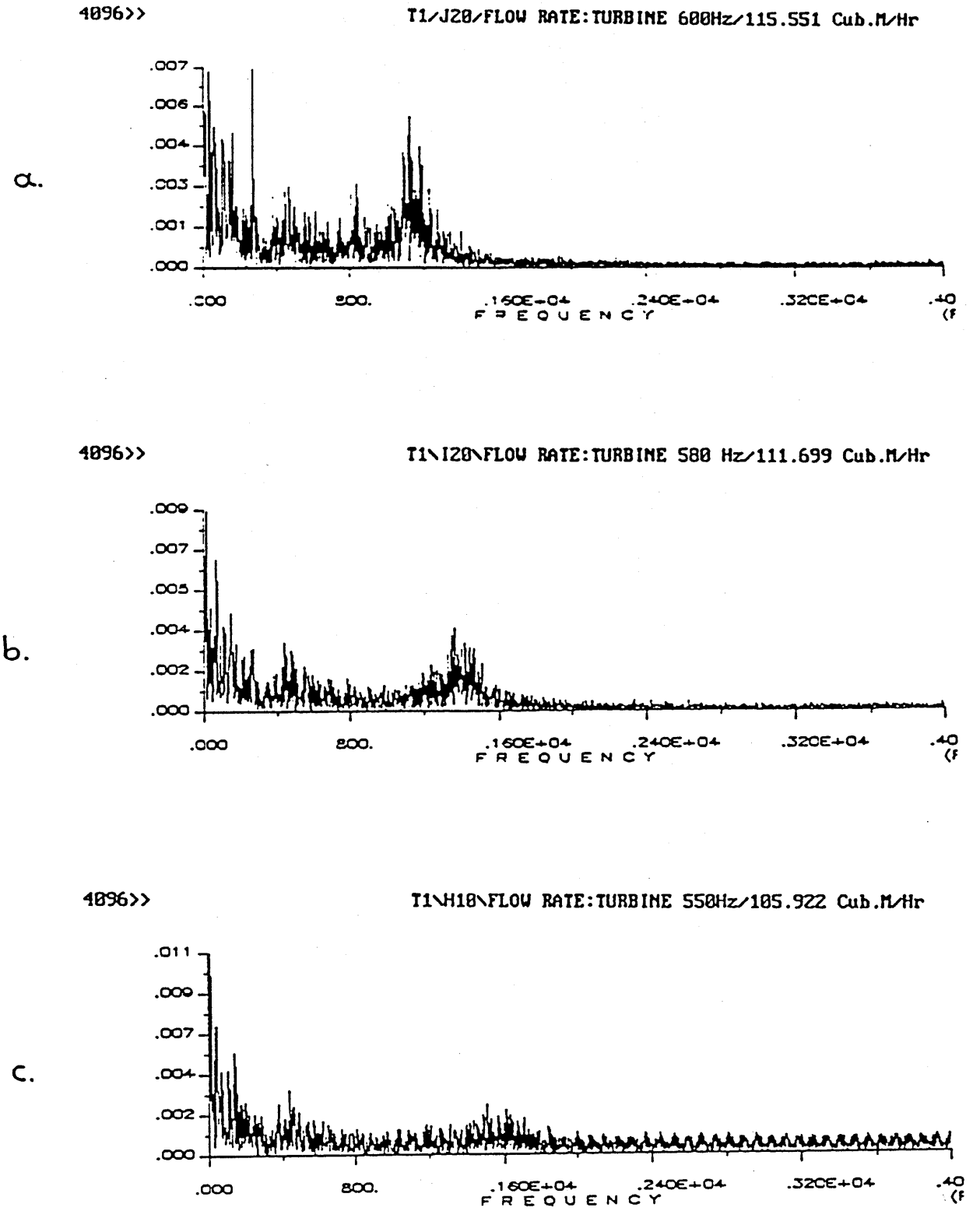

Figure 5.24 Evolution of the amplitude spectrum downstream the Orifice in Test 1. a) Flow rate 115.6 m^3/Hr b) flow rate 111.7 m^3/Hr c)flow rate 105.9 m^3/Hr.

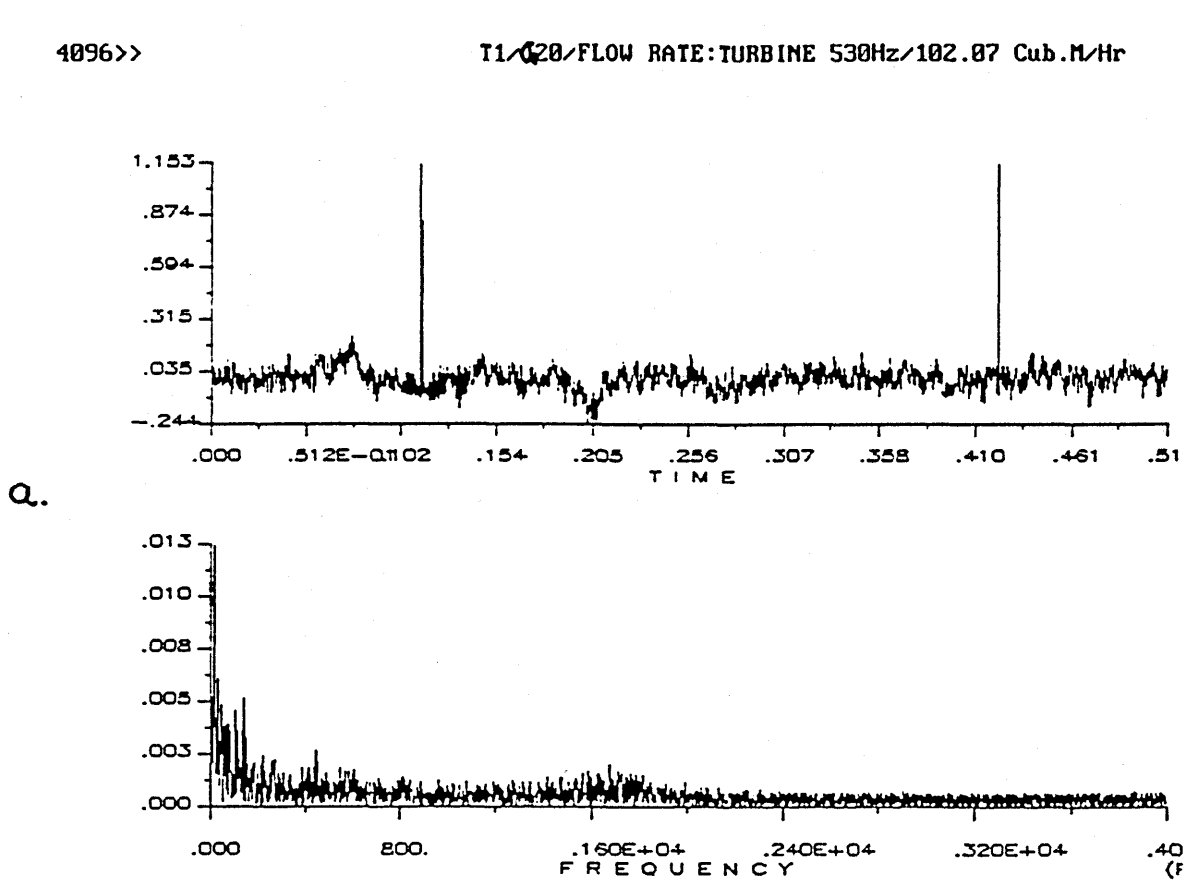

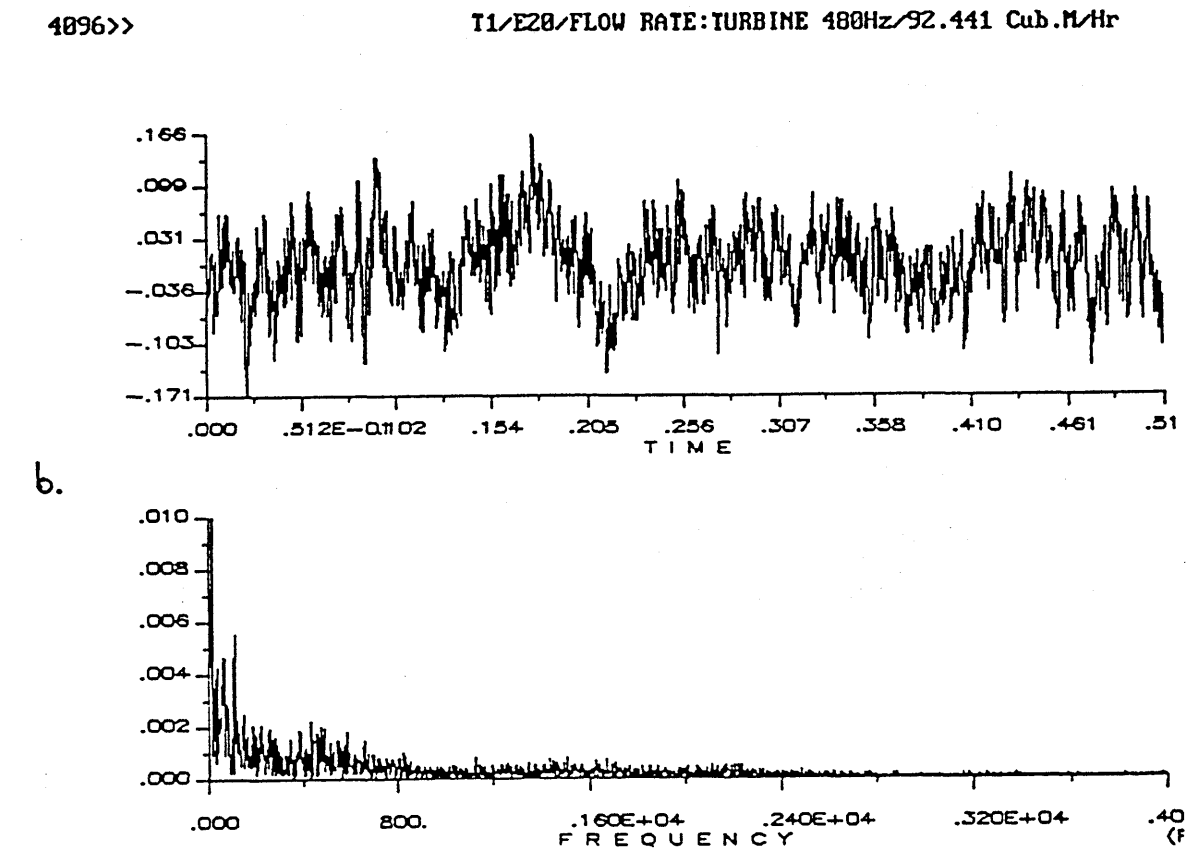

Figure 5.25 Pressure signals in the time domain and amplitude spectrum downstream the Orifice in Test 1. a) Flow rate 102m^3/Hr b) flow rate 92.4m^3/Hr.

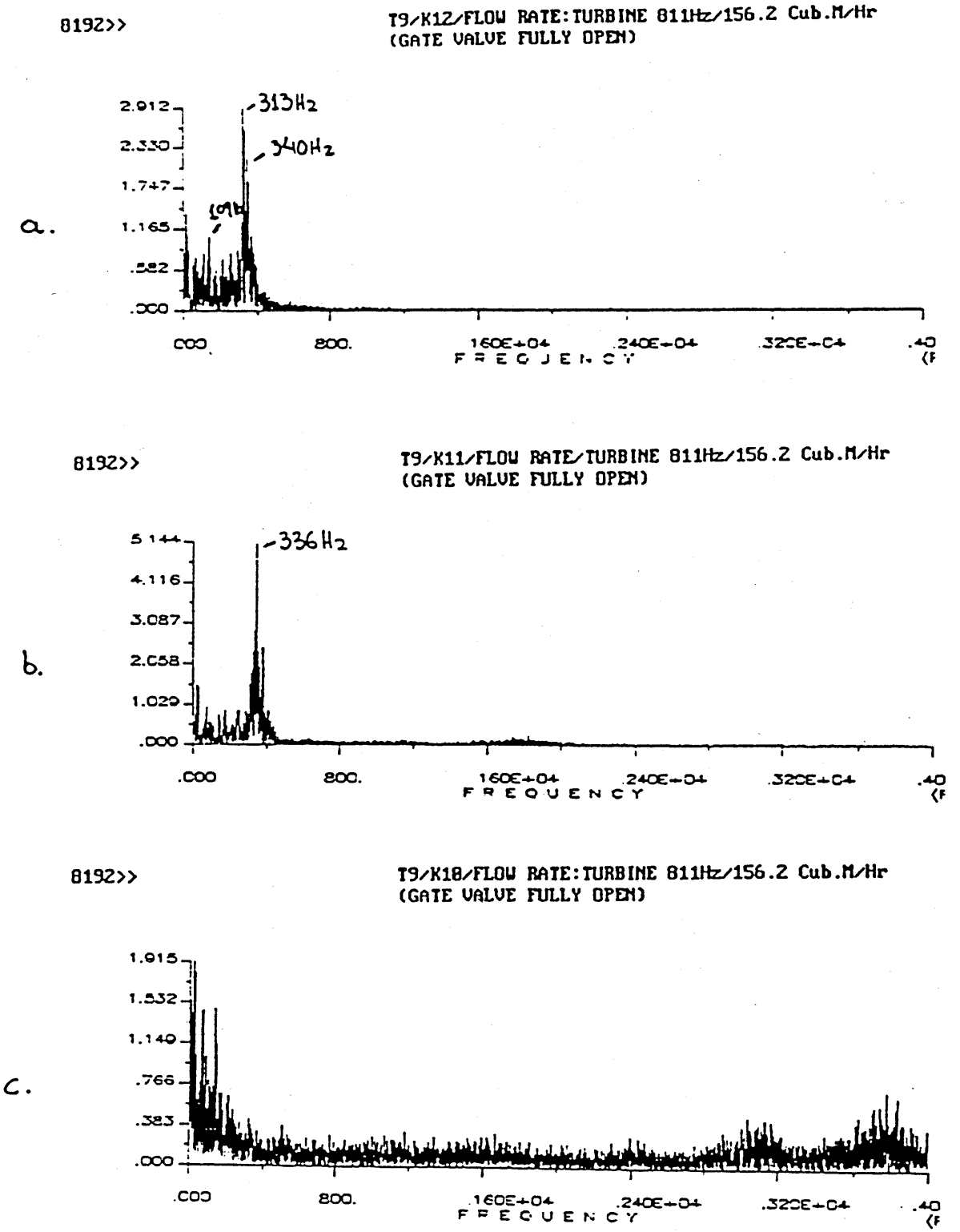

Figure 5.26 Evolution of the amplitude spectrum with a flow rate 155.2 m^3/Hr (Full flow) In Test 6 a) Upstream the conditioner b) Upstream the Orifice c) Downstream the Orifice.

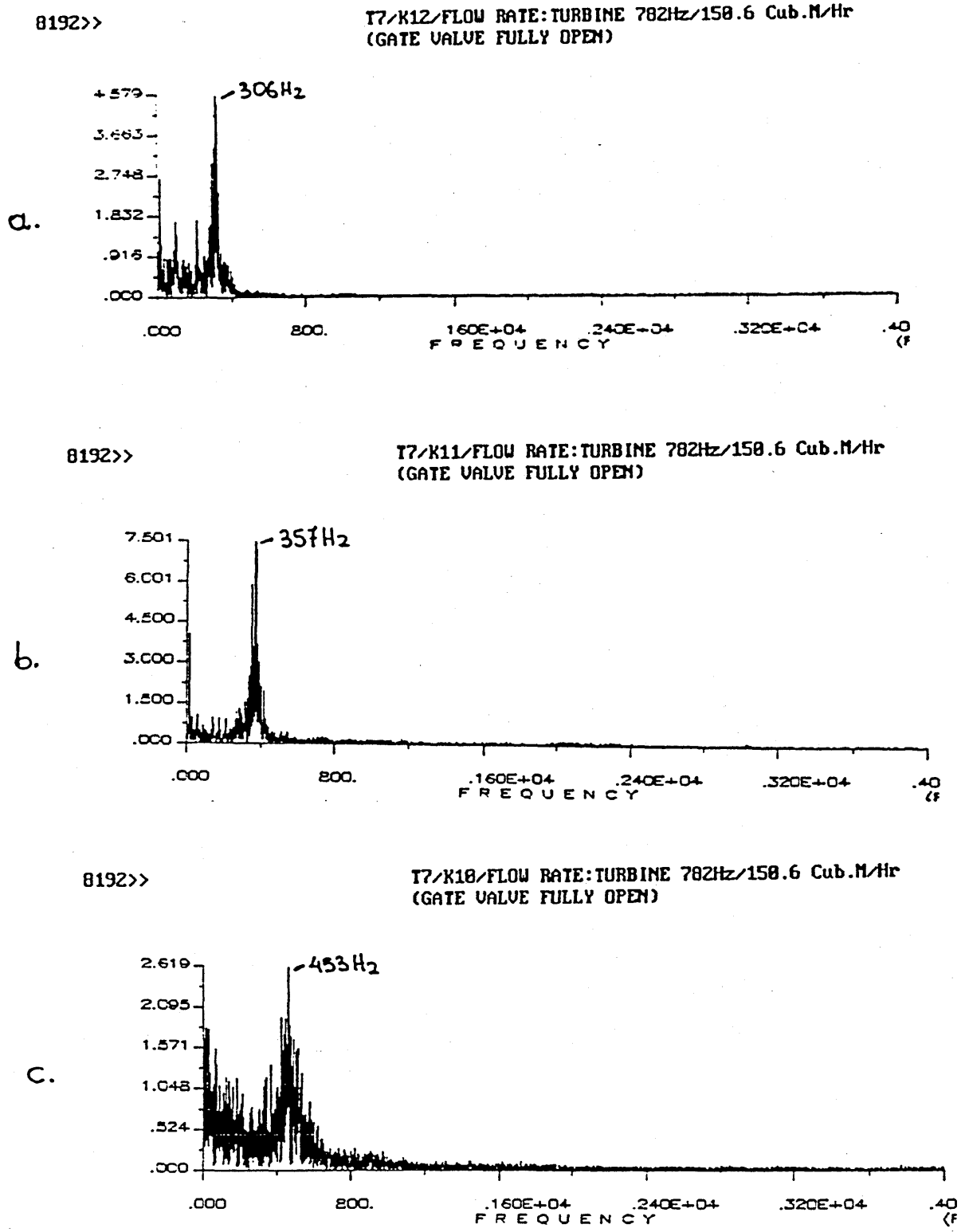

Figure 5.27 Evolution of the amplitude spectrum with a flow rate 150.6 m^3/Hr (Full flow) in Test 7 a) Upstream the conditioner b) Upstream the Orifice c) Downstream the Orifice.

8192>>

T8/K12/FLOW RATE:TURBINE 792Hz/152.5 Cub.M/Hr
(GATE VALVE FULLY OPEN)

a.

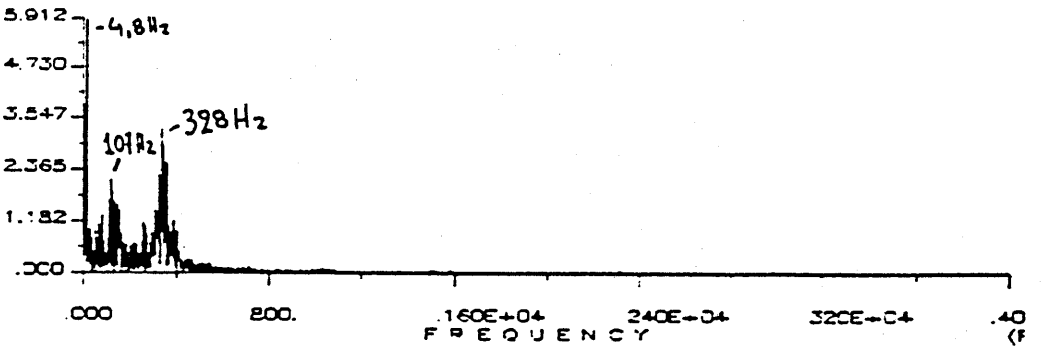

8192>>

T8/K11/FLOW RATE:TURBINE 792Hz/152.5 Cub.M/Hr
(GATE VALVE FULLY OPEN)

b.

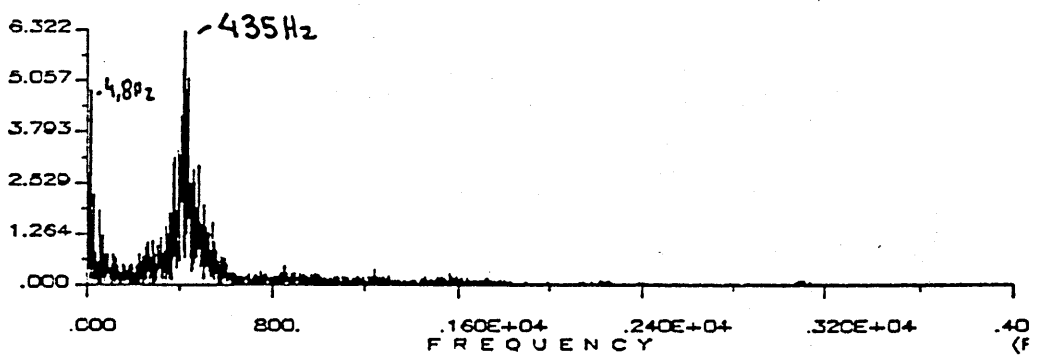

8192>>

T8/K10/FLOW RATE/TURBINE 792Hz/152.5 Cub.M/Hr
(GATE VALVE FULLY OPEN)

c.

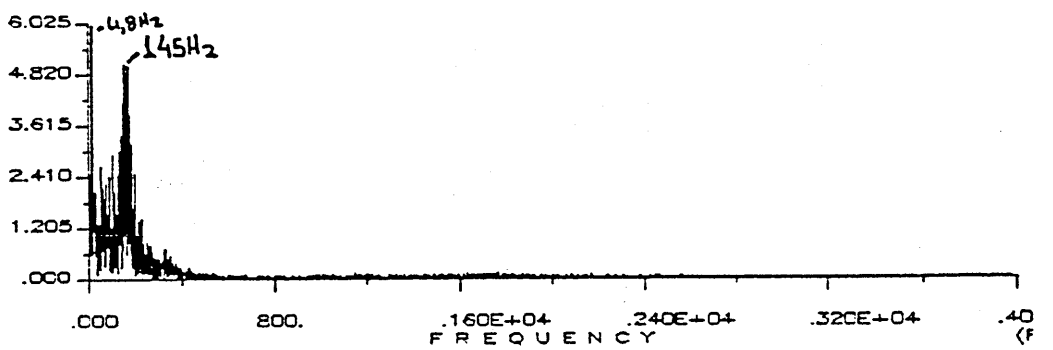

Figure 5.28 Evolution of the amplitude spectrum with a flow rate 152.5 m^3/Hr (Full flow) in Test 8 a) Upstream the conditioner b) Upstream the Orifice c) Downstream the Orifice.

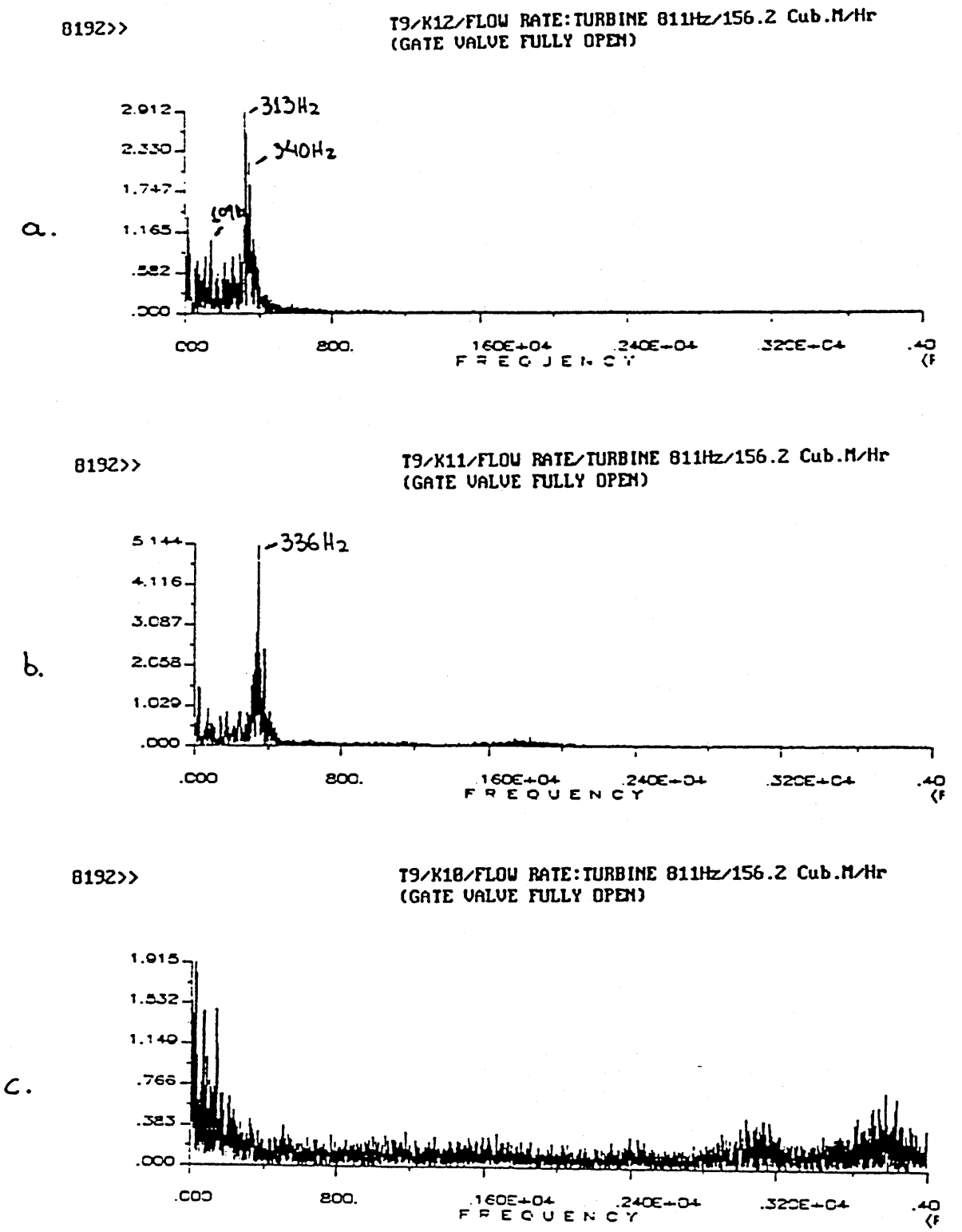

Figure 5.29 Evolution of the amplitude spectrum with a flow rate 156.2 m^3/Hr (Full flow) in Test 9 a) Upstream the conditioner b) Upstream the Orifice c) Downstream the Orifice.

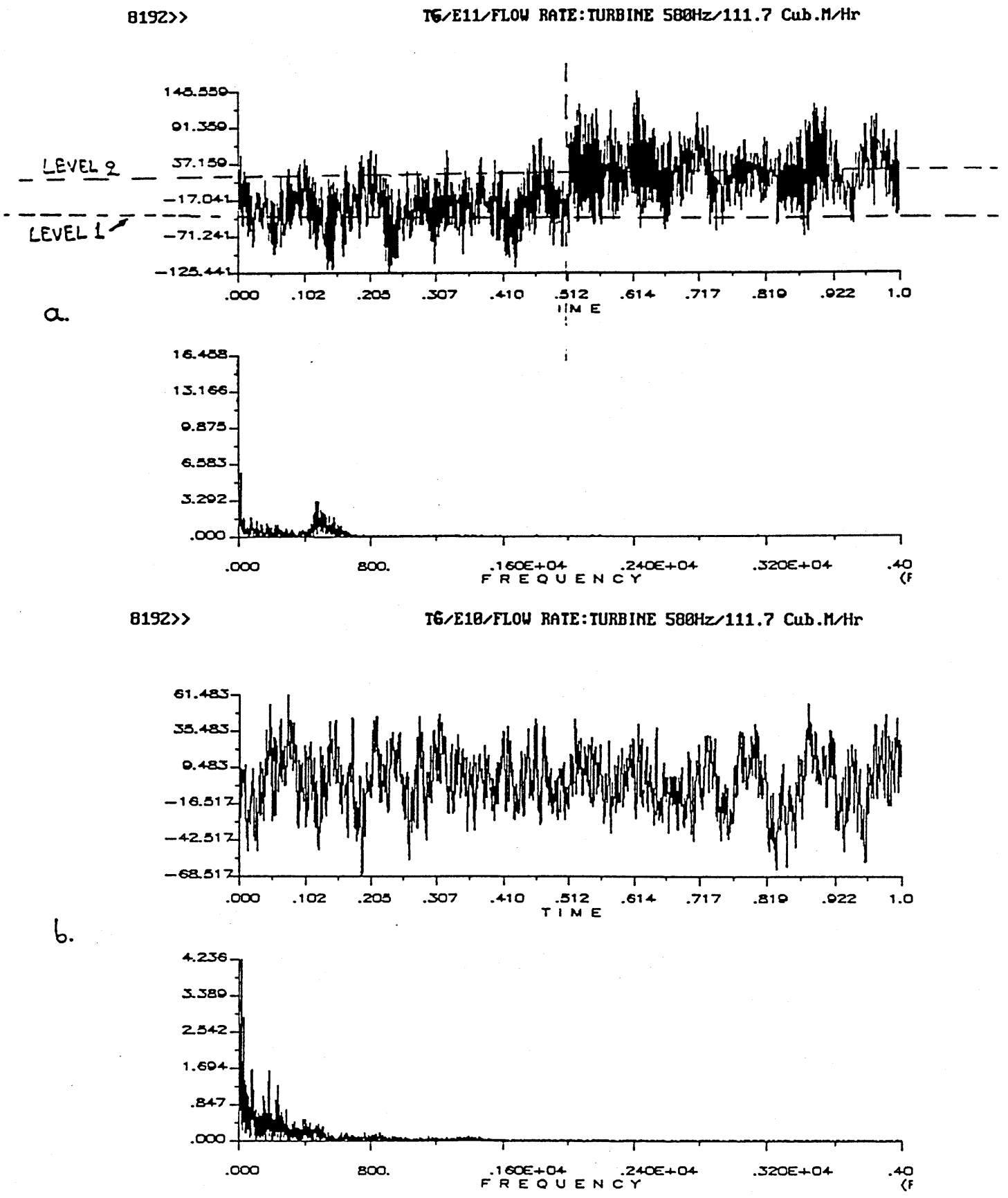

Figure 5.30 Pressure signals in the time domain and amplitude spectrum with a flow rate 111.7 m^3/Hr in Test 6 a) Upstream the Orifice (Discrenable sharp increase of dc level) b) Downstream the Orifice.

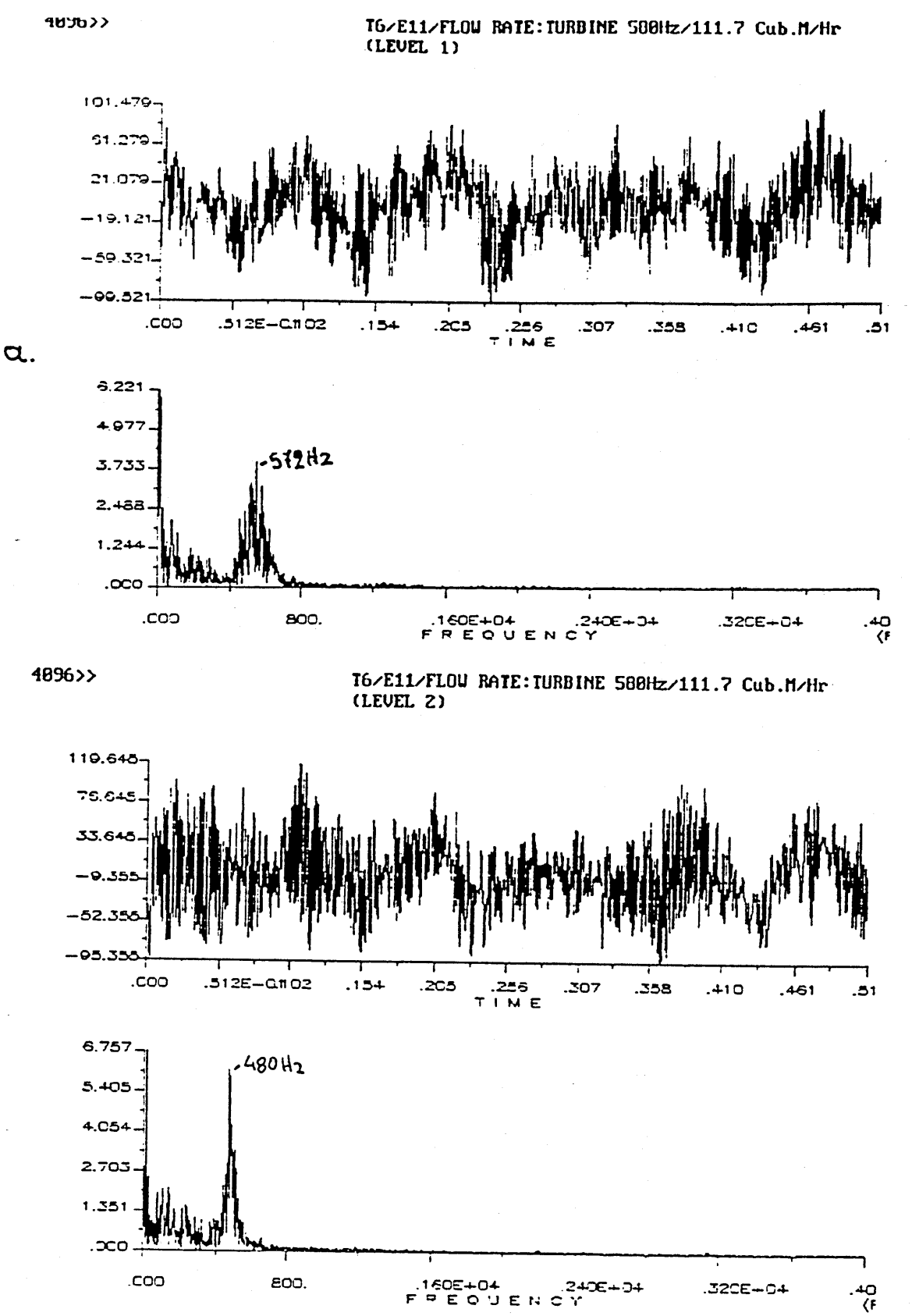

Figure 5.31 Separate analysis of the pressure signal shown in figure 5.30a in the time and frequency domain

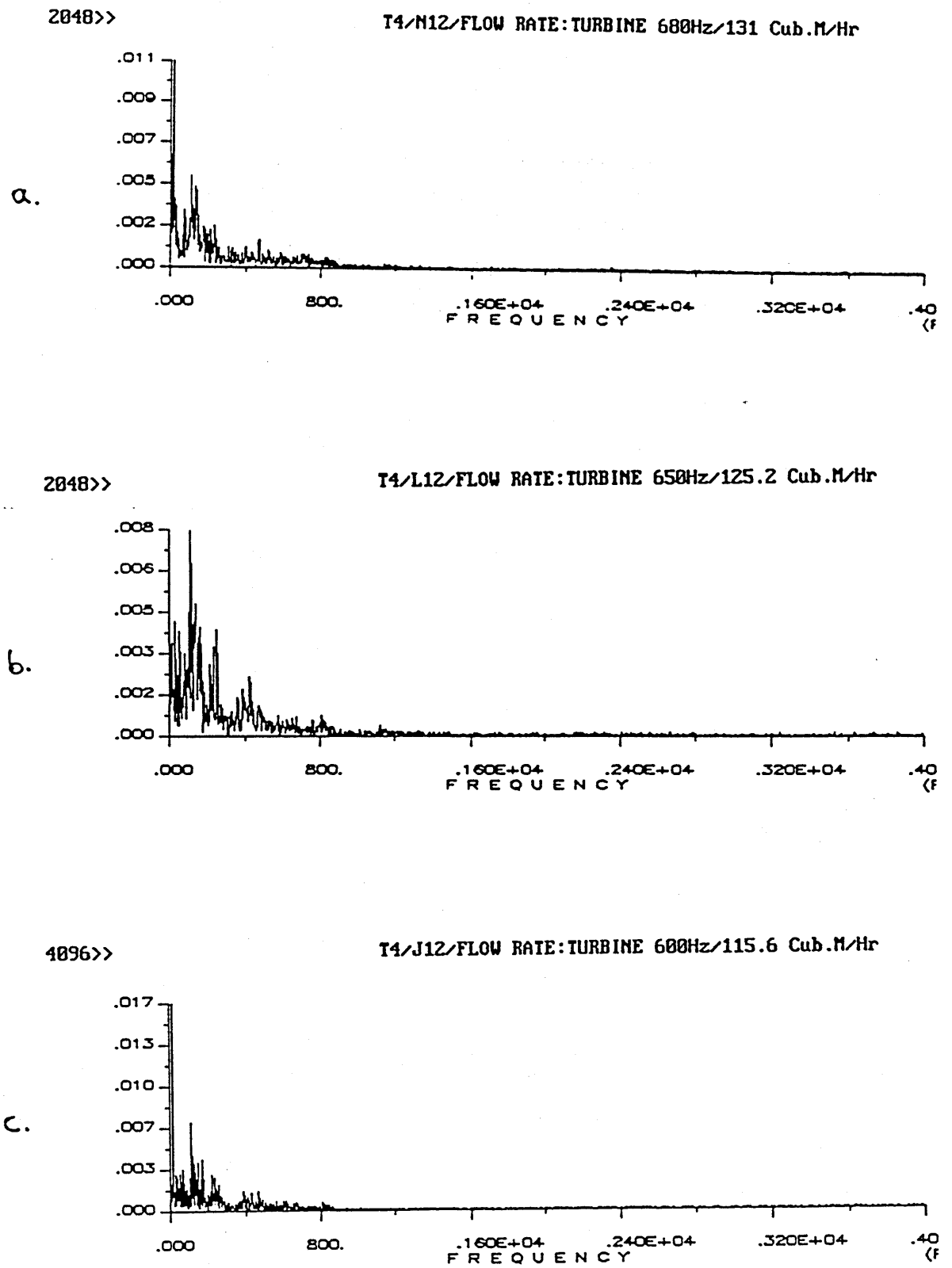

Figure 5.32 Evolution of the amplitude spectrum upstream the conditioner in Test 4 a) flow rate 131 m^3/Hr b) flow rate 125.2 m^3/Hr c) flow rate 115.6 m^3/Hr.

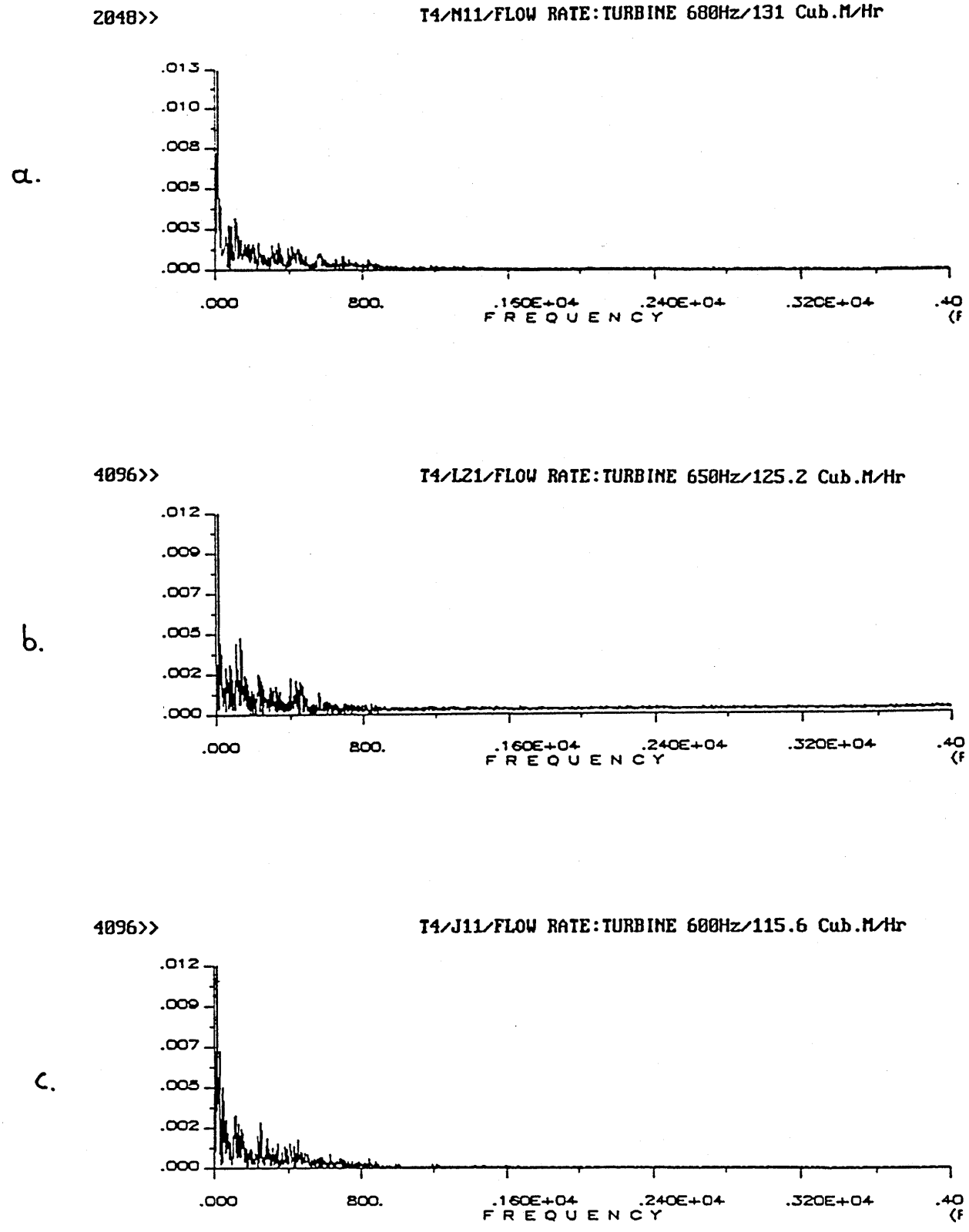

Figure 5.33 Evolution of the amplitude spectrum upstream the Orifice in Test 4 a) flow rate 131 m^3/Hr b) flow rate 125.2 m^3/Hr c) flow rate 115.6 m^3/Hr.

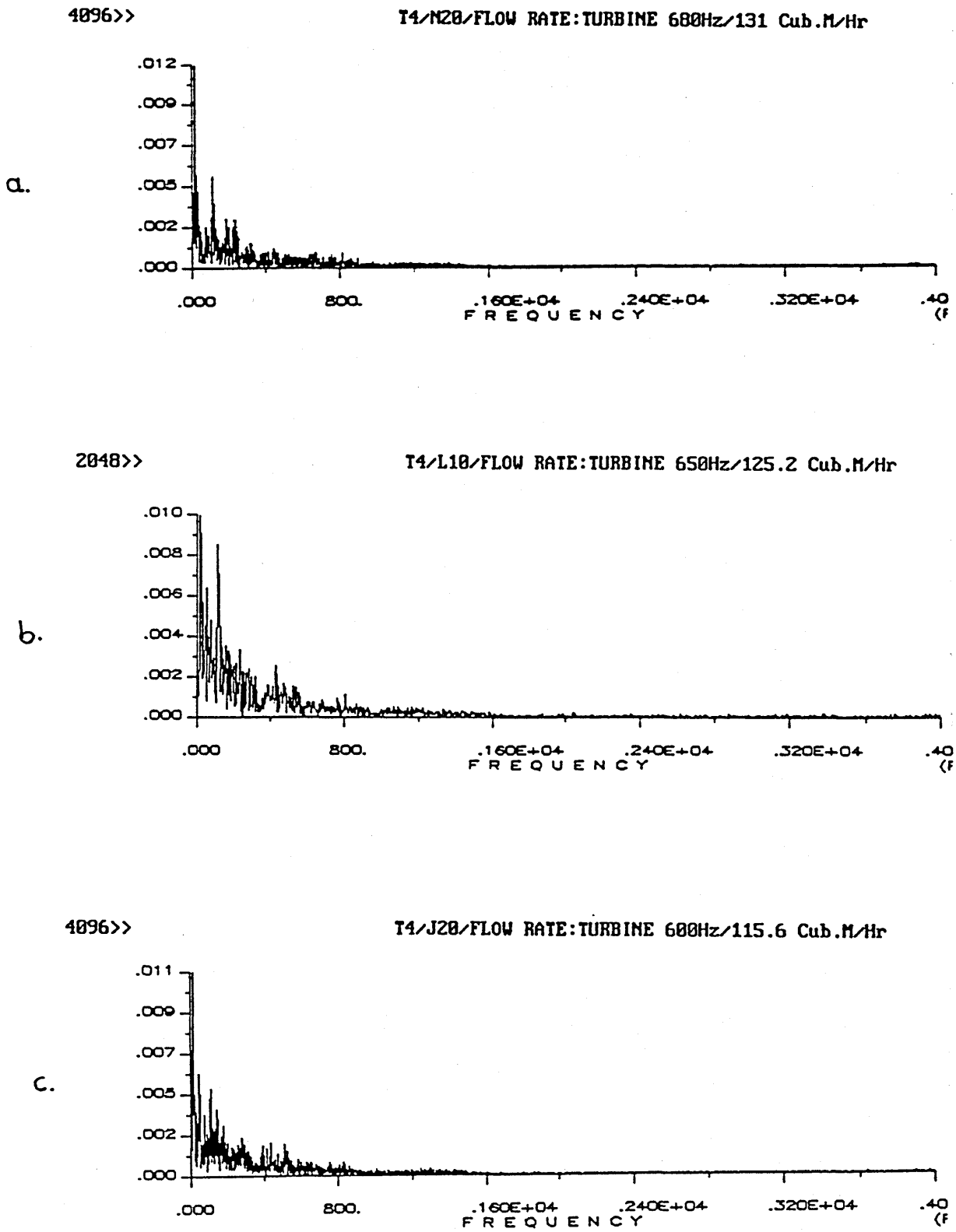

Figure 5.34 Evolution of the amplitude spectrum downstream the Orifice in Test 4 a) flow rate 131 m^3/Hr b) flow rate 125.2 m^3/Hr c) flow rate 115.6 m^3/Hr.

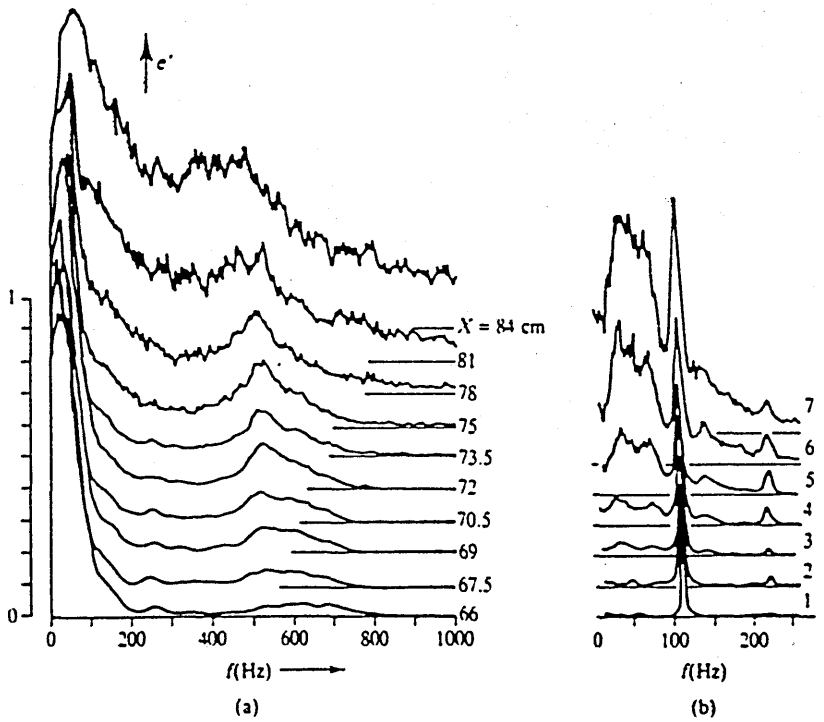

FIGURE 13.59
Evolution of u' spectra during transition. (a) Natural transition in wind tunnel with high level of low-frequency freestream disturbances. Dominant TS frequency ≈ 550 Hz. (Reproduced, by permission, from D. Arnal. AGARD Report 709, pp. 3–64, 1984.) (b) Transition in a very quiet environment, stimulated by ribbon vibrations at 110 Hz, dominant TS frequency. (Reproduced, by permission, from Y. S. Kachanov and V. Y. Levchenko, 1984.[66])

Figure 5.35 Evolution of the u spectrum during transition (Reproduced from Sherman F.S., - Viscous flow - 1990)

	TEST 1	TEST 2	TEST 3	TEST 4	TEST 6	TEST 7	TEST 8	TEST 9	TEST 6B	TEST 9B
Turbine	Upst.	Upst.	Upst.	Upst.	Upst.	Upst.	Upst.	Upst.	Upst.	Upst.
frequen	cond.	cond.	cond.	cond.	cond.	cond.	cond.	cond.	cond.	cond.
370	285877	290748	290949	289798						
400	275722	280105	282716	280548	284723	287702	286737	288408	276697	278421
430	265970	270566	273478	272304	275924	278492	277961	279177	266728	268589
450	259133	263437	263738	263255						
480	247169	255405	253396	252799	260054	262241	261460	262354	247441	249695
500	239126	250786	244360	243550						
530	227262	231708	230604	234501	238820	241890	242117	240769	223117	227238
550	216906	219157	217852	219018						
580	203032	204899	203795	205344	215234	218311	217499	216473	195316	199392
600	190565	194457	195461	193983	205560	209037	208612	207076	184550	188484
630	174478	178994	177688	178198	191878	195880	194759	193627	168551	172759
650	163519	167246	168852	167239						
660	157085	161924	161824	161308	172661	180266	179581	178500	149326	153542
680	145020	148670	147967	148640						
700	132050	134011	136119	135067	153433	156981	155899	154958	121808	127241
	TEST 1	TEST 2	TEST 3	TEST 4	TEST 6	TEST 7	TEST 8	TEST 9	TESt 6B	TEST 9B
Turbine	Upst.	Upst.	Upst.	Upst.	Upst.	Upst.	Upst.	Upst.	Upst.	Upst.
frequen	orif.	orif.	orif.	orif.	orif.	orif.	orif.	orif.	orif.	orif.
370	282716	287486	288994	287033						
400	272574	278135	280247	277093	280677	283593	285645	288432	272740	273996
430	262031	267981	269489	267253	270798	273262	276021	277326	260880	262708
450	254200	260038	261446	258618						
480	240845	249783	249783	246669	252781	254744	258371	260111	240044	244161
500	231909	241237	241840	237733						
530	218755	227664	227865	227290	229880	232177	237441	237104	213805	219787
550	207811	214795	215298	211827						
580	191846	200619	201926	195461	209571	204745	211355	211390	182596	191848
600	179797	189358	190364	184717	192203	194918	201809	200964	170786	180253
630	161121	173071	174378	167246	175932	178990	186599	186469	152760	164543
650	149273	161911	163419	155096						
660	142344	155778	158392	149373	158981	162164	170180	170021	131794	145511
680	129091	142104	143613	135818						
700	115736	127526	132151	121761	133500	135792	145491	144693	102384	115829
	TEST 1	TEST 2	TEST 3	TEST 4	TEST 6	TEST 7	TEST 8	TEST 9	TEST 6B	TEST 9B
Turbine	Downst.	Downst.	Downst.	Downst.	Downst.	Downst.	Downst.	Downst.	Downst.	Downst.
frequen	orif.	orif.	orif.	orif.	orif.	orif.	orif.	orif.	orif.	orif.
370	253629	256952	259166	256348						
400	238126	242455	245878	241247	249855	242966	245421	256002	236008	234833
430	222220	226750	229669	225945	235212	228026	231318	241219	219068	219102
450	211045	215575	217488	212857						
480	192018	198562	199569	195542	210025	198882	202746	216216	188582	188740
500	178226	186985	186683	182052						
530	159400	165340	165541	164333	179432	166784	171164	185306	150976	153745
550	142085	148629	148528	144300						
580	119736	127588	126179	121648	142187	126096	131834	149145	108137	111416
600	101413	111078	110675	105239	126346	111090	116930	134529	90811	95030
630	76145	86715	85205	80172	106016	87505	93377	114282	65625	70209
650	58024	69601	69601	62051						
660	48762	60339	61648	52990	82083	60730	68403	90846	35507	41322
680	30238	41614	42822	34165						
700	9701	21279	25809	13225	47700	22413	31044	56318	561	2270

Table 1. Summary table of the pressure measurements in the three positions for all the tests

Orifice plate - Theoretical estimations.								
Pipe diameter, D		101.6	mm	Density, rho		998	kg/m3	
Orifice diameter, d		68	mm	Kinematic visc,nu		1.14E-06	m2/s	
Diameter ratio, B		0.67						
Vel of approach, E		1.118						
Pipe area, A		0.008107	m2					
Orifice area, a		0.003632	m2					
Turbine	Actual	Actual	Actual	Differential	Discharge	Reynolds	Actual	Code
frequency	flow	flow	Flow	pressure	coefficient	number	velocity	letter
Hz	m^3/h	Kgr/sec	l/s	Pa	Cd	Re	m/sec	
370	71.3	19.76	19.79	30373	0.626	2.17E+05	2.443	A
400	77.0	21.36	21.40	35620	0.625	2.35E+05	2.641	B
430	82.8	22.96	23.00	41286	0.624	2.53E+05	2.839	C
450	86.7	24.03	24.07	45298	0.624	2.64E+05	2.971	D
480	92.4	25.63	25.68	51666	0.623	2.82E+05	3.169	E
500	96.3	26.70	26.75	56145	0.622	2.94E+05	3.301	F
530	102.1	28.30	28.35	63215	0.622	3.11E+05	3.499	G
550	105.9	29.37	29.42	68162	0.621	3.23E+05	3.631	H
580	111.7	30.97	31.03	75934	0.621	3.41E+05	3.829	I
600	115.6	32.04	32.10	81349	0.620	3.53E+05	3.961	G
630	121.3	33.64	33.70	89823	0.620	3.70E+05	4.159	K
650	125.2	34.71	34.77	95707	0.620	3.82E+05	4.291	L
660	127.1	35.24	35.31	98719	0.619	3.88E+05	4.357	M
680	131.0	36.31	36.38	104884	0.619	4.00E+05	4.489	N
700	134.8	37.38	37.45	111236	0.619	4.11E+05	4.621	O
720	138.7	38.45	38.52	117776	0.619	4.23E+05	4.753	P
730	140.6	38.98	39.05	121116	0.619	4.29E+05	4.819	Q
740	142.5	39.52	39.59	124503	0.618	4.35E+05	4.885	R
760	146.4	40.58	40.66	131418	0.618	4.47E+05	5.017	S

Table 2. Theoretical estimations of the orifice plate - Cd

TEST 1 (RESULTS) DIFFERENTIAL PRESSURES AND COEFFICIENT OF DISCHARGE						
Turbine frequency Hz	Reynolds number Re	Model flow m^3/h	Differentia pressure (2,1) Pa	Differentia pressure (2,0) Pa	Differentia pressure (1,0) Pa	Discharge coefficient Cd
370	2,17E+05	71,26	3161	32248	29086	0,639
400	2,35E+05	77,03	3148	37597	34449	0,635
430	2,53E+05	82,81	3938	43750	39812	0,635
450	2,64E+05	86,66	4934	48088	43154	0,638
480	2,82E+05	92,44	6324	55151	48827	0,640
500	2,94E+05	96,29	7217	60900	53683	0,635
530	3,11E+05	102,07	8507	67862	59355	0,641
550	3,23E+05	105,92	9095	74821	65726	0,632
580	3,41E+05	111,70	11186	83296	72110	0,636
600	3,53E+05	115,55	10768	89151	78383	0,631
630	3,70E+05	121,33	13357	98334	84976	0,636
650	3,82E+05	125,18	14247	105496	91249	0,634
660	3,88E+05	127,11	14740	108323	93583	0,635
680	4,00E+05	130,96	15930	114782	98852	0,637
700	4,11E+05	134,81	16314	122349	106035	0,633
720	4,23E+05	138,66	17905	129915	112011	0,633
730	4,29E+05	140,59	17997	133648	115651	0,632
740	4,35E+05	142,51	18489	137786	119298	0,631
760	4,47E+05	146,36	19580	143638	124058	0,635

Differential pressure (2,1): Differential pressure upstream the conditioner and upstream the orifice.
Differential pressure (2,0): Differential pressure upstream the conditioner and downstream the orifice.
Differential pressure (1,0): Differential pressure across the orifice.

Table 3. Differential pressures and Coefficient of Discharge (Cd) in Test 1

TEST 2 (RESULTS)						
DIFFERENTIAL PRESSURES AND COEFFICIENT OF DISCHARGE						
Turbine frequency Hz	Reynolds number Re	Model flow m^3/h	Differentia pressure (2,1) Pa	Differentia pressure (2,0) Pa	Differentia pressure (1,0) Pa	Discharge coefficient Cd
370	2,17E+05	71,26	3263	33797	30534	0,624
400	2,35E+05	77,03	1970	37650	35681	0,624
430	2,53E+05	82,81	2585	43816	41231	0,624
450	2,64E+05	86,66	3399	47862	44463	0,629
480	2,82E+05	92,44	5622	56843	51221	0,625
500	2,94E+05	96,29	9549	63801	54253	0,632
530	3,11E+05	102,07	4044	66368	62324	0,625
550	3,23E+05	105,92	4362	70529	66166	0,630
580	3,41E+05	111,70	4280	77311	73031	0,632
600	3,53E+05	115,55	5098	83379	78280	0,632
630	3,70E+05	121,33	5923	92278	86356	0,631
650	3,82E+05	125,18	5335	97645	92310	0,630
660	3,88E+05	127,11	6146	101585	95439	0,629
680	4,00E+05	130,96	6566	107056	100490	0,632
700	4,11E+05	134,81	6485	112732	106248	0,633
720	4,23E+05	138,66	6500	119205	112706	0,632
730	4,29E+05	140,59	7213	121640	114427	0,636
740	4,35E+05	142,51	7221	125482	118261	0,634
760	4,47E+05	146,36	8444	133568	125125	0,633

Differential pressure (2,1): Differential pressure upstream the conditioner and upstream the orifice.
Differential pressure (2,0): Differential pressure upstream the conditioner and downstream the orifice.
Differential pressure (1,0): Differential pressure across the orifice.

Table 4. Differential pressures and Coefficient of discharge (Cd) in test 2

TEST 3 (RESULTS)						
DIFFERENTIAL PRESSURES AND COEFFICIENT OF DISCHARGE						
Turbine frequency Hz	Reynolds number Re	Model flow m^3/h	Differentia pressure (2,1) Pa	Differentia pressure (2,0) Pa	Differentia pressure (1,0) Pa	Discharge coefficient Cd
370	2,17E+05	71,26	1955	31783	29827	0,631
400	2,35E+05	77,03	2469	36838	34369	0,635
430	2,53E+05	82,81	3989	43809	39819	0,635
450	2,64E+05	86,66	2293	46250	43958	0,632
480	2,82E+05	92,44	3613	53828	50214	0,631
500	2,94E+05	96,29	2519	57677	55158	0,627
530	3,11E+05	102,07	2738	65062	62324	0,625
550	3,23E+05	105,92	2554	69324	66770	0,627
580	3,41E+05	111,70	1869	77616	75747	0,621
600	3,53E+05	115,55	5097	84785	79689	0,626
630	3,70E+05	121,33	3310	92483	89173	0,621
650	3,82E+05	125,18	5433	99251	93818	0,625
660	3,88E+05	127,11	3432	100176	96744	0,625
680	4,00E+05	130,96	4355	105145	100790	0,631
700	4,11E+05	134,81	3968	110310	106342	0,632
720	4,23E+05	138,66	3985	117693	113708	0,629
730	4,29E+05	140,59	4393	122134	117741	0,626
740	4,35E+05	142,51	4002	123565	119563	0,630
755	4,44E+05	145,40	5921	131033	125112	0,629

Differential pressure (2,1): Differential pressure upstream the conditioner and upstream the orifice.
Differential pressure (2,0): Differential pressure upstream the conditioner and downstream the orifice.
Differential pressure (1,0): Differential pressure across the orifice.

Table 5. Differential pressures and Coefficient of discharge (Cd) in Test 3.

TEST 4 (RESULTS)						
DIFFERENTIAL PRESSURES AND COEFFICIENT OF DISCHARGE						
Turbine frequency Hz	Reynolds number Re	Model flow m^3/h	Differentia pressure (2,1) Pa	Differentia pressure (2,0) Pa	Differentia pressure (1,0) Pa	Discharge coefficient Cd
370	2,17E+05	71,26	2765	33451	30686	0,622
400	2,35E+05	77,03	3456	39302	35846	0,622
430	2,53E+05	82,81	5051	46359	41308	0,623
450	2,64E+05	86,66	4638	50398	45760	0,619
480	2,82E+05	92,44	6130	57258	51127	0,625
500	2,94E+05	96,29	5817	61498	55681	0,624
530	3,11E+05	102,07	7211	70168	62957	0,622
550	3,23E+05	105,92	7190	74718	67528	0,623
580	3,41E+05	111,70	9884	83696	73812	0,629
600	3,53E+05	115,55	9266	88744	79478	0,627
630	3,70E+05	121,33	10953	98027	87074	0,629
650	3,82E+05	125,18	12143	105189	93046	0,627
660	3,88E+05	127,11	11934	108317	96383	0,626
680	4,00E+05	130,96	12822	114475	101653	0,628
700	4,11E+05	134,81	13306	121842	108536	0,626
720	4,23E+05	138,66	15399	129206	113807	0,628
730	4,29E+05	140,59	15089	131833	116744	0,629
740	4,35E+05	142,51	15779	136023	120244	0,628
755	4,44E+05	145,40	16170	141389	125219	0,628

Differential pressure (2,1): Differential pressure upstream the conditioner and upstream the orifice.
Differential pressure (2,0): Differential pressure upstream the conditioner and downstream the orifice.
Differential pressure (1,0): Differential pressure across the orifice.

Table 6. Differential pressures and Coefficient of discharge (Cd) in Test 4.

TEST 6 (RESULTS)						
DIFFERENTIAL PRESSURES AND COEFFICIENT OF DISCHARGE						
Turbine frequency Hz	Reynolds number Re	Model flow m^3/h	Differentia pressure (2,1) Pa	Differentia pressure (2,0) Pa	Differentia pressure (1,0) Pa	Discharge coefficient Cd
400	2,35E+05	77,03	4046	34867	30822	0,671
430	2,53E+05	82,81	5126	40713	35587	0,671
480	2,82E+05	92,44	7273	50029	42756	0,683
530	3,11E+05	102,07	8940	59389	50449	0,695
580	3,41E+05	111,70	5663	73047	67384	0,658
600	3,53E+05	115,55	13357	79214	65857	0,688
630	3,70E+05	121,33	15945	85861	69916	0,701
660	3,88E+05	127,11	13680	90577	76898	0,701
700	4,11E+05	134,81	19933	105733	85801	0,703
730	4,29E+05	140,59	21426	114655	93228	0,704
806	4,74E+05	155,22	27456	139348	111892	0,709

Differential pressure (2,1): Differential pressure upstream the conditioner and upstream the orifice.
Differential pressure (2,0): Differential pressure upstream the conditioner and downstream the orifice.
Differential pressure (1,0): Differential pressure across the orifice.

Table 7. Differential pressures and Coefficient of discharge (Cd) in Test 6

TEST 7 (RESULTS)						
DIFFERENTIAL PRESSURES AND COEFFICIENT OF DISCHARGE						
Turbine frequency Hz	Reynolds number Re	Model flow m^3/h	Differentia pressure (2,1) Pa	Differentia pressure (2,0) Pa	Differentia pressure (1,0) Pa	Discharge coefficient Cd
400	2,35E+05	77,03	4109	44736	40627	0,584
430	2,53E+05	82,81	5230	50466	45236	0,595
480	2,82E+05	92,44	7498	63360	55862	0,598
530	3,11E+05	102,07	9713	75107	65394	0,610
580	3,41E+05	111,70	13565	92215	78650	0,609
600	3,53E+05	115,55	14119	97947	83828	0,610
630	3,70E+05	121,33	16890	108374	91484	0,613
660	3,88E+05	127,11	18102	119536	101434	0,610
700	4,11E+05	134,81	21189	134568	113379	0,612
730	4,29E+05	140,59	22500	144812	122311	0,614
782	4,59E+05	150,60	26088	166295	140207	0,615

Differential pressure (2,1): Differential pressure upstream the conditioner and upstream the orifice.
Differential pressure (2,0): Differential pressure upstream the conditioner and downstream the orifice.
Differential pressure (1,0): Differential pressure across the orifice.

Table 8. Differential pressures and Coefficient of discharge (Cd) in Test 7.

TEST 8 (RESULTS)						
DIFFERENTIAL PRESSURES AND COEFFICIENT OF DISCHARGE						
Turbine frequency Hz	Reynolds number Re	Model flow m^3/h	Differentia pressure (2,1) Pa	Differentia pressure (2,0) Pa	Differentia pressure (1,0) Pa	Discharge coefficient Cd
400	2,35E+05	77,03	1092	41316	40224	0,587
430	2,53E+05	82,81	1940	46643	44704	0,599
480	2,82E+05	92,44	3090	58714	55625	0,599
530	3,11E+05	102,07	4676	70953	66278	0,606
580	3,41E+05	111,70	6143	85664	79521	0,605
600	3,53E+05	115,55	6803	91682	84879	0,606
630	3,70E+05	121,33	8160	101382	93222	0,607
660	3,88E+05	127,11	9401	111178	101777	0,609
700	4,11E+05	134,81	10407	124855	114448	0,609
730	4,29E+05	140,59	12002	136081	124079	0,610
792	4,65E+05	152,53	14303	159893	145590	0,611

Differential pressure (2,1): Differential pressure upstream the conditioner and upstream the orifice.
Differential pressure (2,0): Differential pressure upstream the conditioner and downstream the orifice.
Differential pressure (1,0): Differential pressure across the orifice.

Table 9. Differential pressures and coefficient of discharge (Cd) in Test 8.

TEST 9 (RESULTS)						
DIFFERENTIAL PRESSURES AND COEFFICIENT OF DISCHARGE						
Turbine frequency Hz	Reynolds number Re	Model flow m^3/h	Differentia pressure (2,1) Pa	Differentia pressure (2,0) Pa	Differentia pressure (1,0) Pa	Discharge coefficient Cd
400	2,35E+05	77,03	-25	32406	32431	0,654
430	2,53E+05	82,81	1851	37958	36107	0,666
480	2,82E+05	92,44	2242	46138	43896	0,674
530	3,11E+05	102,07	3665	55463	51798	0,685
580	3,41E+05	111,70	5082	67327	62245	0,684
600	3,53E+05	115,55	6113	72547	66434	0,685
630	3,70E+05	121,33	7158	79344	72187	0,690
660	3,88E+05	127,11	8479	87654	79176	0,690
700	4,11E+05	134,81	10265	98641	88375	0,693
730	4,29E+05	140,59	11161	107326	96165	0,693
811	4,77E+05	156,19	14729	131516	116787	0,699

Differential pressure (2,1): Differential pressure upstream the conditioner and upstream the orifice.
Differential pressure (2,0): Differential pressure upstream the conditioner and downstream the orifice.
Differential pressure (1,0): Differential pressure across the orifice.

Table 10. Differential pressures and Coefficient of discharge (Cd) in Test 9.

Upstream Conditions	Meter	b	Conditioner	t/D	d/D	a	C'	C	Change %
Straight	Orifice	0,8	Mitsubishi	1	0,13	0,59	2	6	2
pipe	plate							10	0,8
Single 90^0	Orifice	0,8	Mitsubishi	1	0,13	0,59	2	6	2
bend	plate							10	0,1
Two 90^0	Orifice	0,8	Mitsubishi	1	0,13	0,59	2	6	-0,5
bends	plate							10	-0,1

C: Distance between conditioner and the meter
C': Distance between the disturbance and the conditioner
t: Plate thickness
a: Porosity (area of holes divided by the total area)

Table 11. Percentage changes in the calibration of an Orifice plate (Presented by Reader-Harris, Hutton and Laws, 1989)

Test Conditions	Reynolds Number					
	2.53E+05	3.11E+05	3.53E+05	3.88E+05	4.29E+05	Average
Orifice 40D (T1) Conditioner 6D	0.635 (+1.7%)	0.641 (+3%)	0.631 (+1.7%)	0.635 (+2.5%)	0.632 (+2%)	0.635 (+2.2%)
Orifice 40D (T2) No conditioner	0.624 (0%)	0.625 (+0.5%)	0.632 (+1.9%)	0.629 (+1.6%)	0.636 (+2.7%)	0.629 (+1.3%)
Orifice 20D (T3) No conditioner	0.635 (+1.7%)	0.625 (+0.5%)	0.626 (+1%)	0.625 (+1%)	0.626 (+1.1%)	0.627 (+1%)
Orifice 20D (T4) Conditioner 6D	0.623 (-0.2%)	0.622 (0%)	0.627 (+1.1%)	0.626 (+1.1%)	0.629 (+1.6%)	0.625 (+0.6%)
Orifice 11D (T6) Conditioner 6D	0.671 (+7%)	0.695 (+10.5%)	0.688 (+9.9%)	0.701 (+11.7%)	0.704 (+12%)	0.692 (+10.3%)
Orifice 18D (T7) Conditioner 6D	0.595 (-4.9%)	0.610 (-2%)	0.610 (-1.6%)	0.610 (-1.5%)	0.614 (-0.8%)	0.608 (-2.1%)
Orifice 11D (T8) Damper	0.599 (-10.8%)	0.606 (-2.6%)	0.606 (-2.3%)	0.609 (-1.6%)	0.610 (-1.5%)	0.606 (-2.5%)
Orifice 13D (T9) Damper	0.666 (+6.3%)	0.685 (+9.2%)	0.685 (+9.5%)	0.690 (+10.3%)	0.693 (+10.7%)	0.684 (10.1%)
Theoretical values	0.624	0.622	0.620	0.619	0.619	0.621

Table 12. Summary table of discharge Coefficient (Cd) for all the tests and percentage differences from the theoretical values.

APPENDIX A

- **Table A1 - Calibration curves and data of pressure transducers No 0 and No 1**
- **Table A2 - Calibration curves and data of pressure transducer No 2**
- **Table A3 - Characteristic results of SIMAN for the data file T3/J12**
- **Table A4 - Codification of the measurements.**

DVM (Volts)	Calibrator (Bars)
1.007	0.0028
1.119	0.1134
1.241	0.2332
1.551	0.542
1.85	0.838
1.851	0.8388
2.141	1.128
2.399	1.3843
2.55	1.535
2.837	1.8213
2.927	1.9097

Power Supply: 15V
Ambient Temp: 24 ^{0}C
Bar. Press:742mmHg

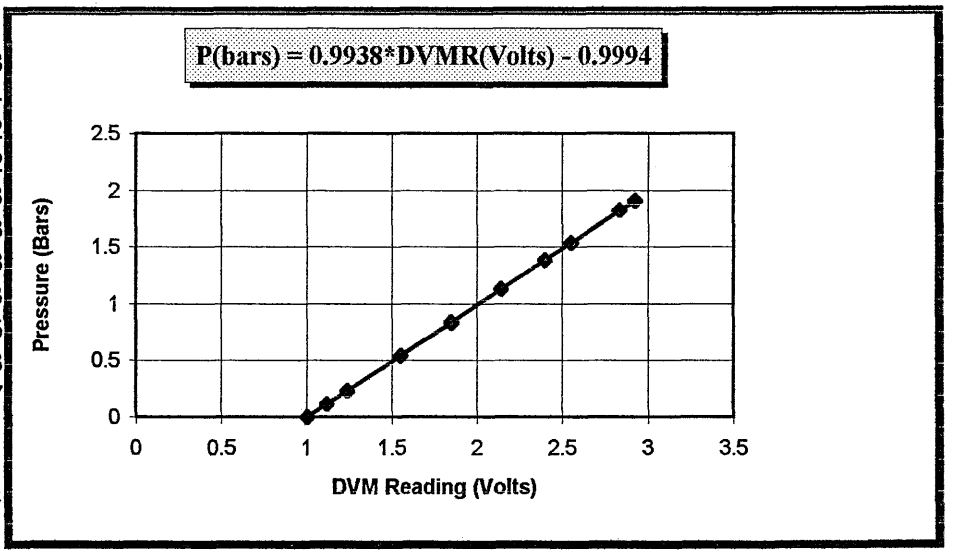

Transducer No: 0

Volts DVM	Pressure Bars
1.068	0.0628
1.337	0.3295
1.354	0.3454
1.647	0.636
1.816	0.8027
1.823	0.8096
2.153	1.1368
2.505	1.4864
2.676	1.656
2.881	1.86

Power Supply: 15V
Ambient Temp: 23 ^{0}C
Bar. Press:738mmHg

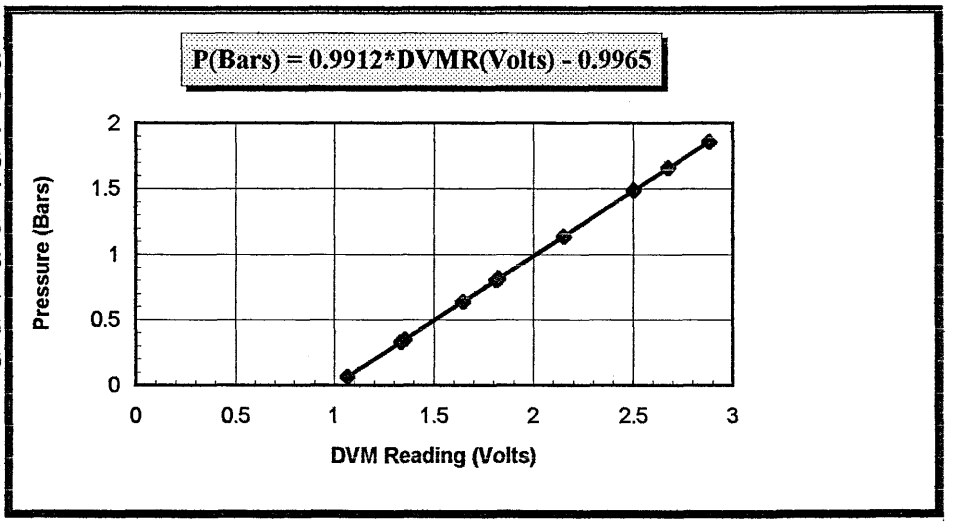

Transducer No: 1

Table A1 Calibration curves and data of pressure transducers No 0 and No 1.

DVM (Volts)	Calibrator (Bars)
1.022	0.0028
1.08	0.0538
1.177	0.1481
1.3	0.2708
1.88	0.8446
1.909	0.8763
2.177	1.1425
2.275	1.239
2.642	1.604
2.781	1.744
3.154	2.114

Power Supply: 15V
Ambient Temp: 23 ^{0}C
Bar. Press:740mmHg

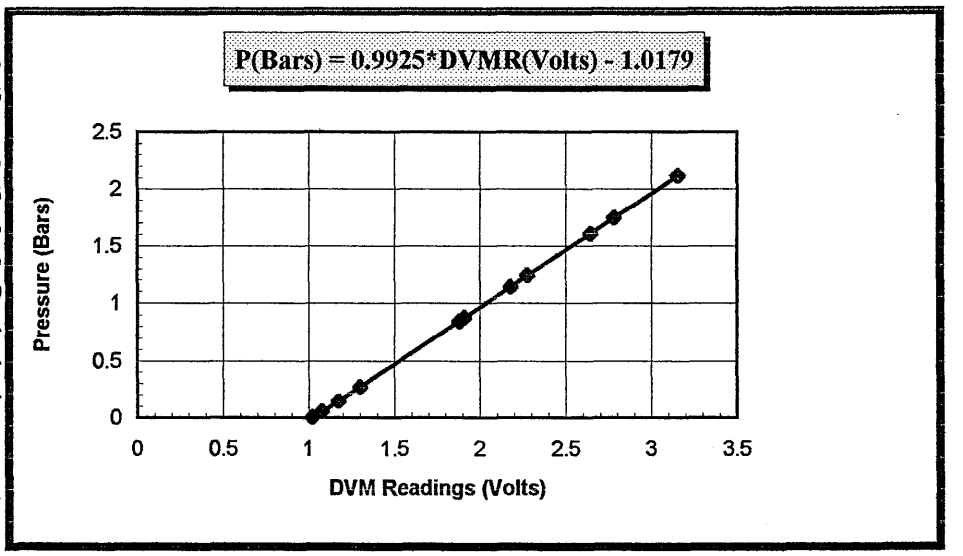

The pressure transducers were calibrated using a DECKER calibrator, Model: CNR4. The pres-sure was increased at intervals during a calibration up to a maximum and then decreased, to check for any hysterisis or non-linearity.Calibration curves were plotted for all the transducers.
To convert the voltages registered by the digital voltmeter or the data acquisition board were used the equations that are shown in the plots. These equations are only applicable under 15V power supply. Calibration checks on the transducers were made frequently throughout the test programm.-(DVMR: Digital Voltmeter Reading.)

Table A2 Calibration curve and data of pressure transducer No 2.

Table A3. Characteristic results of SIMAN for the data file T3/J12.

==========

==========

Data File: J12.DAT

Histogram Range: 2.64 to 3.23

No. of Data Points = 4096
No. of Intervals = 20

Min Data Value = 2.69
Max Data Value = 3.18

Sample Mean = 2.94
Sample Std Dev = 0.0673

Distribution Function: Normal

==========

SIMAN USAGE: NORM(2.94, 0.0673)

Sq Error = 0.000576

Chi Square Test:
No. of intervals = 14
Degrees of freedom = 11
Test Statistic = 33.9
Corresponding p-value = < 0.005

Kolmogorov-Smirnov Test:
Test Statistic = 0.0199
Corresponding p-value = 0.0804

==========

Table A3 (Continued)

Int. No.	No. of Data Pts.	x	Probability Density		Cumulative Distribution	
		Data		Function	Data	Function
1	0	2.670e+00	0.000	0.000	0.000	0.000
2	1	2.699e+00	0.000	0.000	0.000	0.000
3	0	2.729e+00	0.000	0.001	0.000	0.001
4	5	2.758e+00	0.001	0.002	0.001	0.003
5	17	2.788e+00	0.004	0.007	0.006	0.010
6	79	2.817e+00	0.019	0.020	0.025	0.030
7	206	2.847e+00	0.050	0.045	0.075	0.075
8	385	2.876e+00	0.094	0.084	0.169	0.159
9	479	2.906e+00	0.117	0.129	0.286	0.288
10	620	2.935e+00	0.151	0.164	0.438	0.451
11	731	2.965e+00	0.178	0.173	0.616	0.624
12	630	2.994e+00	0.154	0.151	0.770	0.775
13	418	3.024e+00	0.102	0.109	0.872	0.883
14	285	3.053e+00	0.070	0.065	0.941	0.948
15	151	3.083e+00	0.037	0.032	0.978	0.981
16	64	3.112e+00	0.016	0.013	0.994	0.994
17	20	3.142e+00	0.005	0.004	0.999	0.998
18	4	3.171e+00	0.001	0.001	1.000	1.000
19	1	3.201e+00	0.000	0.000	1.000	1.000
20	0	3.230e+00	0.000	0.000	1.000	1.000

	Turbine	Flow	TESTS 1 TO 4					TESTS 6 TO 9				
a/a	frequenc	rate	Code	Test No	Test No	Test No	Test No	Code	Test No	Test No	Test No	Test No
	Hz	m/hr	letter	1	2	3	4	letter	6	7	8	9
1	370	71,3	A	T1/Ax0,1,2	T2/Ax0,1,2	T3/Ax0,1,2	"					
2	400	77,0	B	T1/Bx0,1,2	T2/Bx0,1,2	"	"	A	T6/Ax0,1,2	T7/Ax0,1,2	T8/Ax0,1,	"
3	430	82,8	C	T1/Cx0,1,2		"	"	B	T6/Bx0,1,2	T7/Bx0,1,2	"	"
4	450	86,7	D	"	"	"	"					
5	480	92,4	E	"	"	"	"	C	T6/Cx0,1,2	"	"	"
6	500	96,3	F	"	"	"	"					
7	530	102,1	G	"	"	"	"	D	"	"	"	"
8	550	105,9	H	"	"	"	"					
9	580	111,7	I	"	"	"	"	E	"	"	"	"
10	600	115,6	J	"	"	"	"	F	"	"	"	"
11	630	121,3	K	"	"	"	"	G	"	"	"	"
12	650	125,2	L	"	"	"	"					
13	660	127,1	M	"	"	"	"	H	"	"	"	"
14	680	131,0	N	"	"	"	"					
15	700	134,8	O	"	"	"	"	I	"	"	"	"
16	720	138,7	P	"	"	"	"					
17	730	140,6	Q	"	"	"	"	J	"	"	"	"
18	740	142,5	R	"	"	"	"					
19	Variable*	Variable*	S	760Hz*	760Hz*	755Hz*	755Hz*	K(full flow)*	806Hz*	782Hz*	792Hz*	811Hz*

1) **x** is the number of measurement among the total 9 (see section 4.1)
2) 0,1,2 means:
 a) 0 is the pressure transducer D/2 downstream the orifice
 b) 1 is the pressure transducer D upstream the orifice
 c) 2 is the pressure transducer D upstream the conditioner or the damper

Table A4: Codification of the tests

APPENDIX B

- **Figure B1 - Discharge Coefficient in Test 6B after repeatable measurements**
- **Figure B2 - Maximum percentage difference on Cd values from the theoretical in Test 6B**
- **Figure B3 - Discharge Coefficient and percentage difference from the theoretical values in Test 9B**

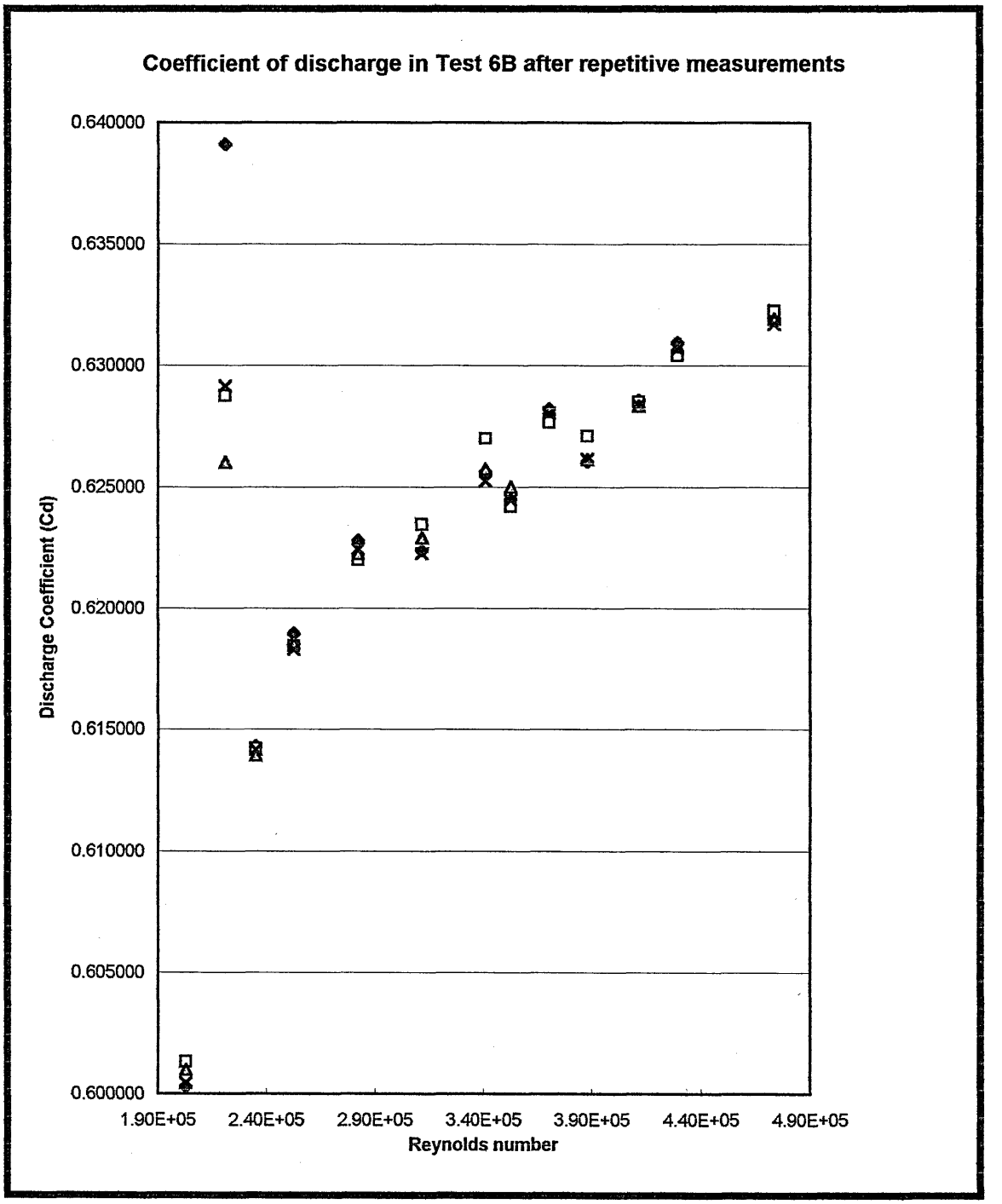

Figure B1 Discharge Coefficient in Test 6B

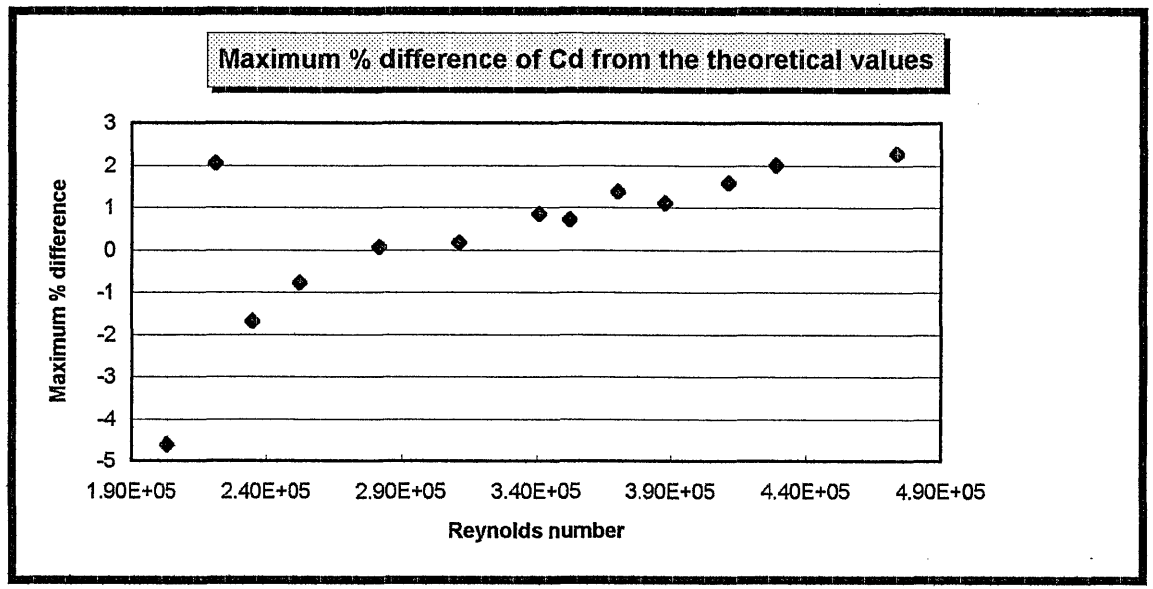

Figure B2 Maximum % difference on Cd values from the theoretical in Test 6B (Orifice 11D from the bend with the conditioner at 6D).

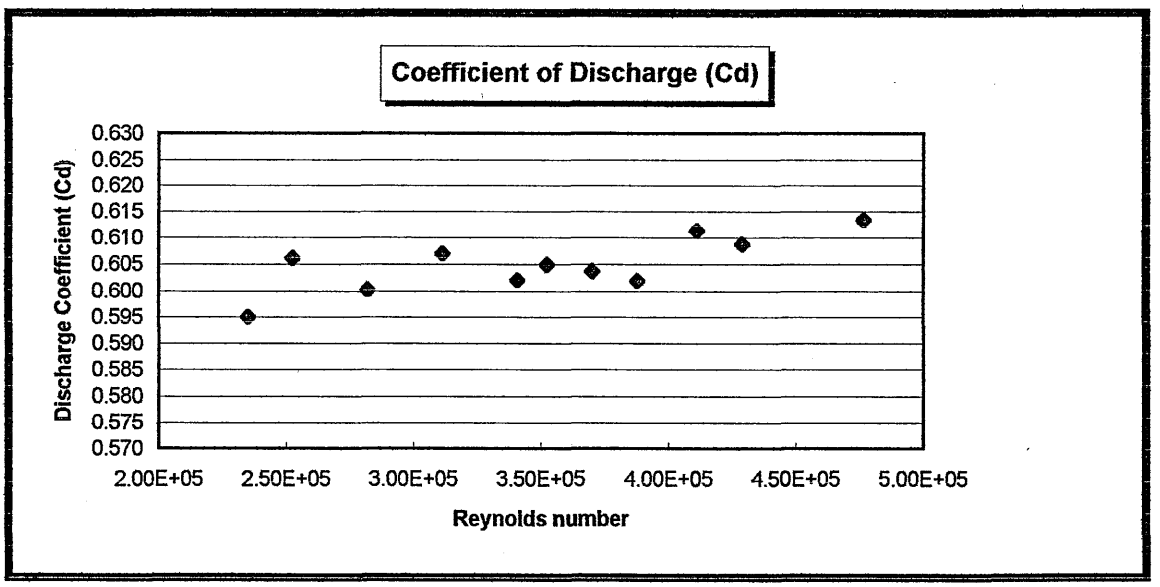

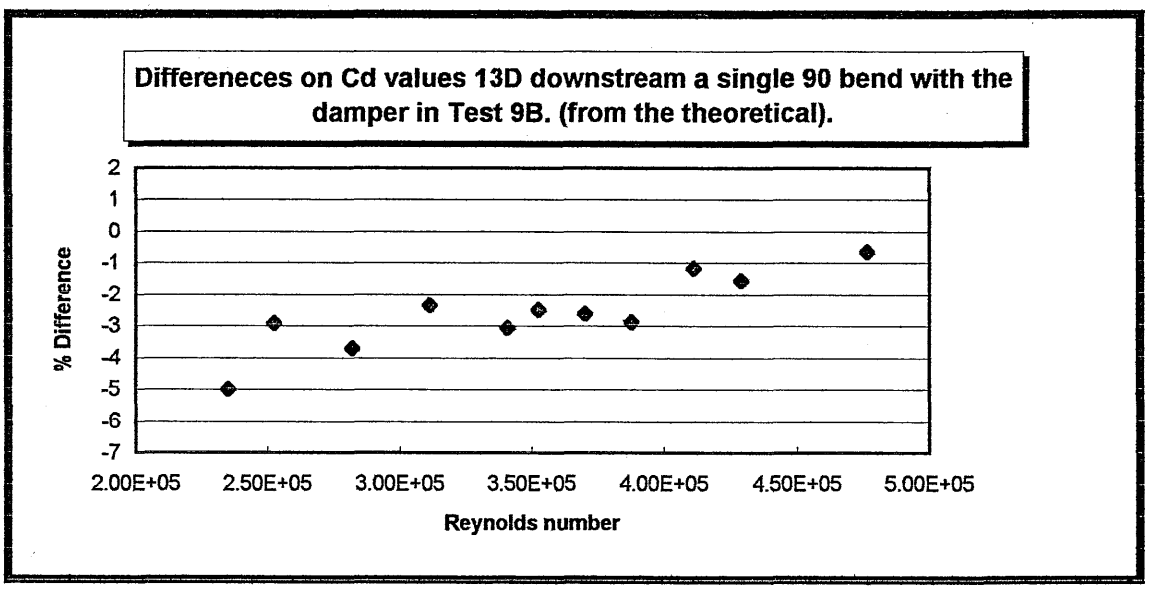

Figure B3 Coefficient of discharge with the orifice and the damper installed 13D and 5D respectively downstream a single 90 bend. (Test 9B). - % difference from the theoretical

APPENDIX C

In the next pages are present some plots that have been obtained at the latest stages of this project and they revealed some very interesting features. On the y-axis have been placed the ratios of the pressures at the three measurement positions to the differential pressure across the orifice plate ($\frac{Pi}{\Delta P(1,0)}$) and x-axis is just a normal scale. This ratio could be regarded as a pressure coefficient.

The inverse of this factor could be found in **B.S. 1042, (ISO 5167-1:1991)** in the empirical formula used to compute the expansibility factor (Ex) for the flow measurement of gases and it is as follows:

$$Ex = 1 - \left(0.41 + 0.35\beta^4\right)\frac{\Delta P}{\kappa P_1}$$

where P_1 is the static pressure at the upstream tapping. It has to be stated as well that the uncertainty of expansibility factor is expressed as a function of this ratio and is equal in per cent to $4\frac{\Delta P}{P_1}$. Thus, this is reason that it was called as expansion's uncertainty factor. A sample of the plots that have been drawn for all the Tests is present in the next pages. However the case is similar to all of them and possibly this discontinuity of the plots at a specifice Reynolds number could be the only common factor that has been found among all the Tests carried out in this project.

So far, it is not possible to do any statement about their importance since further research is regarded necessary.

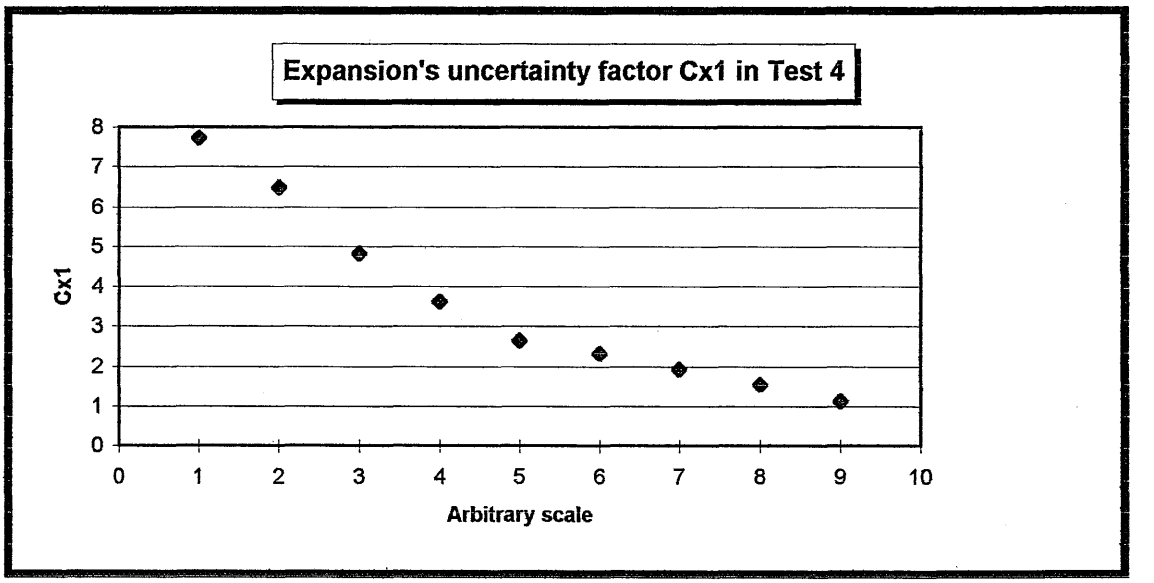

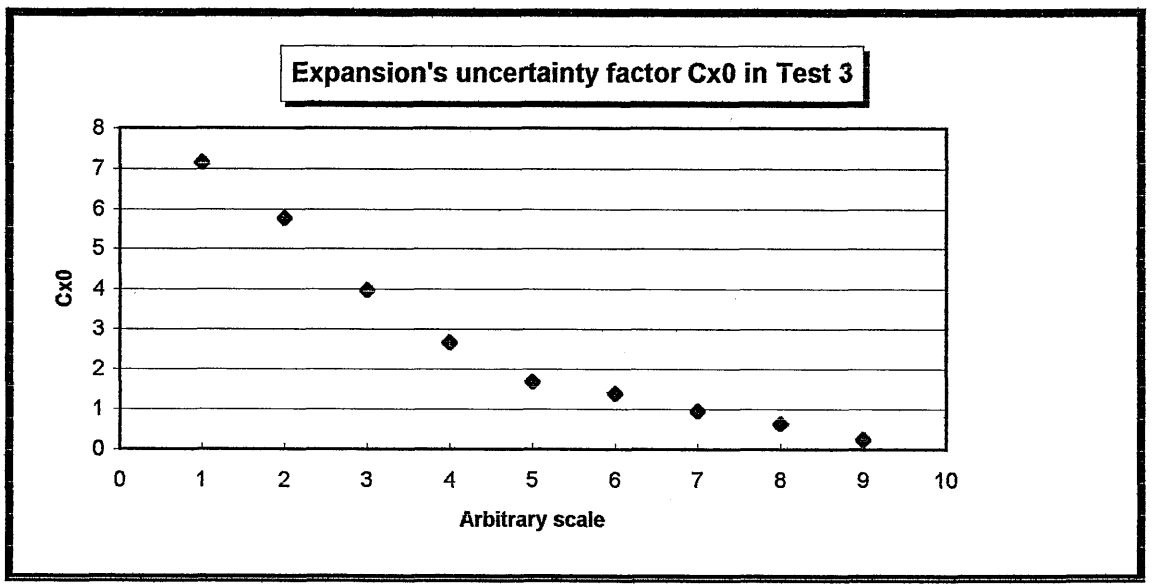

Figure C1 Expansion's uncertainty factor (Cx) in Tests 3 and 4.

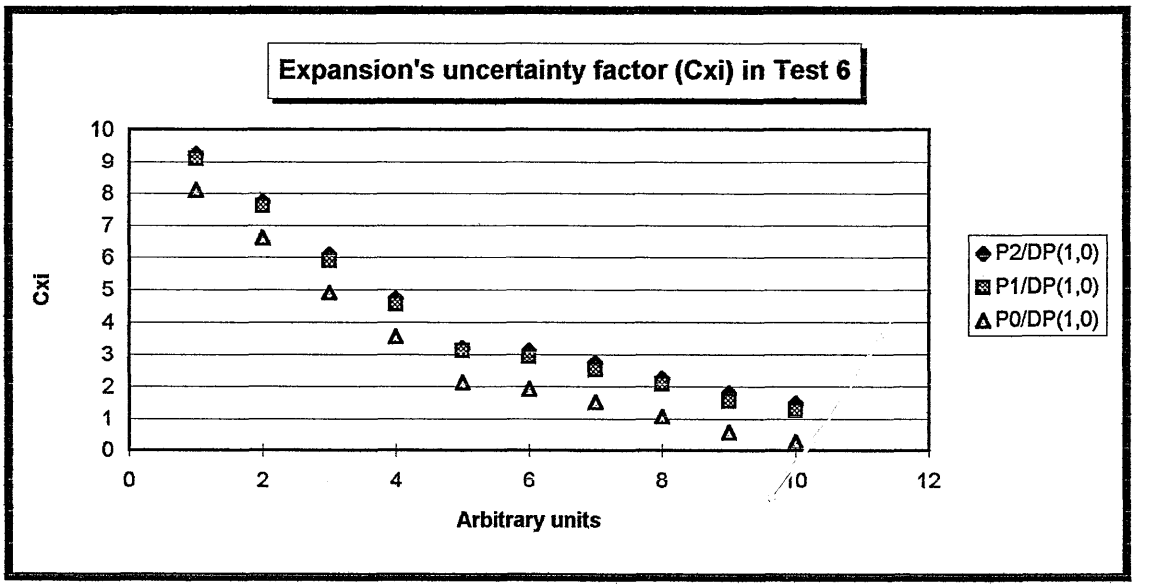

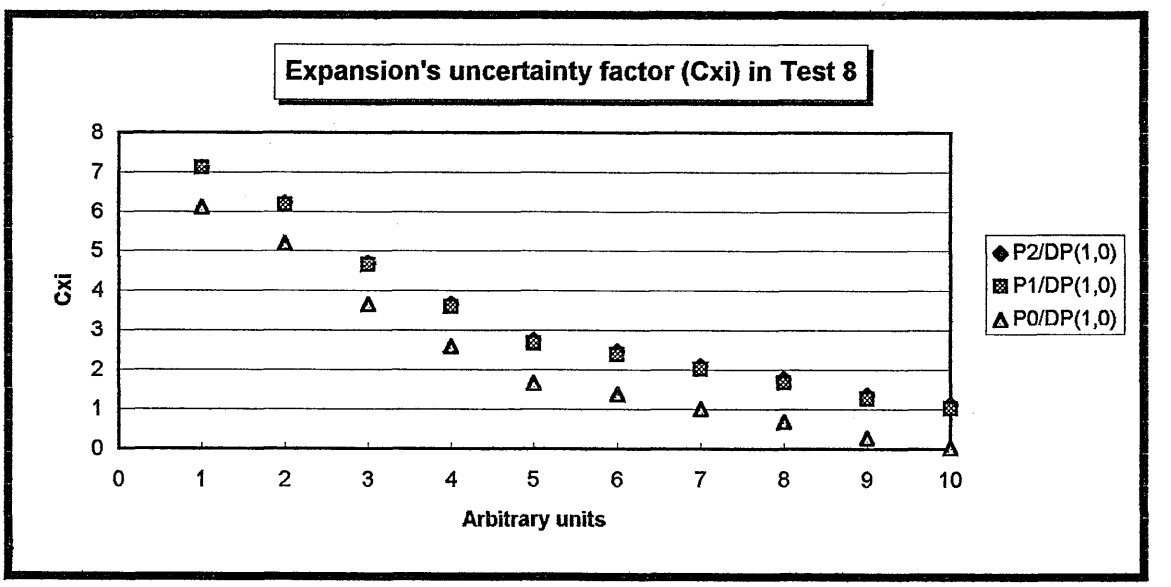

Figure C2 Expansion's uncertainty factor (Cx) in Tests 6 and 8.

BIBLIOGRAPHY

1.- **Al-Rafai W.N., Tridimas Y.D., Wooley N.H., (1990)** - *A Study Of Turbulent Flows In Pipe Bends.* - School Of Engineering And Technology Management, Liverpool Polytechnic.

2.- **Ariman T., Turk M.A., Sylvester N.D., (Mar. 1974)** - *On Steady And Pulsitile Flow Of Blood.* -ASME Applied Mechanics Division, Paper No 73-WA/APM-7.

3.- **Basseville , M., (1988)** - *Detecting Changes In Signals And Systems - A Survey* - Automatica, Vol 24, No3.

4.- **Bajura, R.A., Pellegrin, M.T., (1977)** - *Studies Of Pulsating Incompressible Flow Through Orifice Meters* - Proc. Symposium On Flow Measurement In Open Channels And Closed Conduits - Gaithersburg, Pp 523 To 548.

5.- **Bingham E.O., (1988)** - *The Fast Fourier Transformation And Its Application* - Prentice Hall.

6.- **Blake K.A.** - *The Development Of Velocity Profiles Downstream Of Swept And Simple Mitre Bends* - NEL Flow Measurement Memo No 107.

7.- **Bosch M., Hebrard P., (1984)** - *Experimental And Theoretical Studies Of A New Flow Conditioner* - Conference On The Metering Of Natural Gas And Liquified Hydrocarbon Gases - Oyer Scientific And Technical Services L.T.D.

8.- **Campbell J.M.S., (1960)** - *Development Of A Pipe Bend Having A Good Outlet Velocity Distribution And The Effect Of Subsequent Contractions* - BHRA, RR658.

9.- **Dinkelacker A.** - *Relations Between Wall Pressure Fluctuations And Velocity Fluctuations In Turbulent Pipe Flow* - Max Planck Institute - 1988 Zoran Zaric Memorial Conference.

10.- **Eckelmann Helmut** - *A Review Of Knowledge On Pressure Fluctuations* - Max Planck Institute - 1988 Zoran Zaric Memorial Conference.

11.- **ESDU 81/039** - *Pressure Losses Across Orifice Plates, Perforated Plates And Thick Orifice Plates In Ducts.*

12.- **Haalman, A. (1964)** - *Pulsation Errors In Turbine Flowmeter* - Control Eng., Vol 12, No 5, P 89.

13.- **Hebrard, P., Et Al, (1985)** - *An Investigation Of The Behaviour Of Orifice Meter In Pulsating Flow Conditions* - Proc. International Conference Of Flow Measurement : Flomeko 85.

14.- **Henry M.P., (2 - 3 May, 1990)** - *Intelligent Behaviour For Self Validating Sensors* - Proc. Conf., Advances In Mesurement, NEC, Birmingham.

15.- **Herbert T., (1988)** - *Secondary Instability Of Boundary Layers* - Annual Rev. Fluid Mech. 20, Pp 487 - 526.

16.- **Herron K.H., Webb D.R.B., (Oct., 1966)** - *Flight Measurements Of Pressure Fluctuations In A Turbulent Subsonic Boundary Layer And The Relation With Wall Shear Stress.* - Royal Aircraft Establishment, Technical Repost 66338.

17.- **Kwing-So-Choi** - *On Physical Mechanisms Of Turbulent Drag Reduction Using Riblets.* - Applied Fluid Mechanics Division, British Mritime Technology Ltd. -1988 Zoran Zaric Memorial Conference.

18.- **Laws E.M., Lim E.H., Livesey J.L. (London, 1979)** - *Turbulent Pipe Flow In Development And Decay* - 2nd Symposium On Turbulent Shear Flows, Imperial College.

19.- **Ljung, L., (1987)** - *System Identification - Theory For The User* - Prentice Hall, Englewood Cliffs.

20.- **McHugh A., Kinghorn F.C., Dyet W.D. (August 1984)** - *Efficiency Of An Etoile Flow Straightener In Non-Symmetric Swirling Flow Upstream Of Orifice Plates* - NEL Report No 692.

21.- **Mosely, D.S. (1966)** - *Measurement Error In The Orifice Meter On Pulsating Water Flow* - ASME Flow Measurement Symposium, Pittsburg, USA.

22.- **Mottram, R.C., (1981)** - *Measuring Pulsating Flow With A Differential Pressure Meter* - Proc, Conference At St Lois, Vol 2, Pp347 To 361.

23.- **Mottram, R.C., Mohammad, W.A. (1984)** - *Frequency Limits For Gas Flow Pulsation Criteria* - Trans. Inst. Measurement And Control, Vol 6, No2.

24.- **Serafini S.J., (Apr., 1963)** - *Wall - Pressure Fluctuations And Pressure - Velocity Correlations In Turbulent Boundary Layers* - Advisory Group For Aeronautical Research And Development, Report No 453.

25.- **Sherman F.S., (1990)** - *Viscous Flow* - University Of California At Berkeley, Mcgraw-Hill.

26.- **Sparks, C.R., Mckee, R.J., (1986)** - *Certifying Flow Conditions At Gas Pipe Line Metering Installations* - Proc. International Conference On Fluid Flow Measurement - AGA, Washington D.C.

27.- **Spencer E.A., Calame H., Singer S.,** - *Edge Sharpness And Pipe Roughness Effects On Orifice Plate Discharge Coefficients* - NEL Rep. No 427.

28.- **Stein, K., Et Al (1974)** - *Pressure Pulsations In Gas Pressure Contol And Metering Systems* - Inst. Mech. Eng. - Conference Paer C42/74.

29.- **Stipanovits J., (Jul - Sep., 1989)** - *Inteligent Instruments* - Measurement, Vol 7, No3, Pp98 -108.

30.- **Stower, M. A., (1987)** - *Analysis Of Unsteady Flows In Natural Gas Piping Systems* - Trans ASME, Vol 91, Series D.N., J.Basic Engineering, Paper 68-WA/FE-7, Netherlands.

31.- **Taub H., Schilling D.L.(1986)** - *Principles Of Communications Systems* - Mcgraw-Hill.

32.- **Thomson W.T., (1993)** - *Theory Of Vibrations With Applications* - Department Of Mechanical And Enviromental Engineering, University Of California - Fourth Edition.

33.- **William K. George (1988)** - *The Decay Of Homogeneous Isotropic Turbulence.* - International Synposia On Transport Phenomena - Turbulence Research Laboratory, State University Of New York .